Title
Mechanism of transgenerational inheritance of reproductive dysfunction stemming from environmental BPA exposure in C. elegans

Author
Camacho, Jessica Aimee

Publication Date
2019

Peer reviewed|Thesis/dissertation

UNIVERSITY OF CALIFORNIA

Los Angeles

Mechanism of transgenerational inheritance of reproductive dysfunction stemming from environmental BPA exposure in *C. elegans*

A dissertation submitted in partial satisfaction of the

requirements for the degree Doctor of Philosophy

in Molecular Toxicology

by

Jessica Aimee Camacho

2019

ABSTRACT OF THE DISSERTATION

Mechanism of transgenerational inheritance of reproductive dysfunction stemming from environmental BPA exposure in *C. elegans*

by

Jessica Aimee Camacho

Doctor of Philosophy in Molecular Toxicology

University of California, Los Angeles, 2019

Professor Patrick Allard, Chair

The transfer of environmental information from one generation to the next has been observed following exposure to natural stimuli in a variety of model systems. Mechanisms behind the transfer of information from natural cues have highlighted the central role played by the epigenome, including DNA methylation-based pathways as well as through the regulation of histone modifications. This transfer can induce specific phenotypes across generations that can result from multigenerational exposures (from a pregnant mother to her offspring) or transgenerational exposures (transmitted through the germ line in the absence of direct exposure). Interestingly, effects from man-made environmental chemicals remain controversial as studies in mammalian settings have not been consistently repeated, have not provided a clear mechanism of inheritance, and have solely focused on DNA methylation ignoring the potential involvement of other epigenetic marks.

The work presented here focuses on the development and validation of a *C. elegans* epigenetic reporter to address the need for a quick and efficient method to test chemicals in our environment for their effects on the germline epigenome. We characterize the epigenetic

maintenance of a *C. elegans* strain carrying a repetitive transgene that can be manipulated by chemical exposure and allows for easy visualization of GFP expression. With an epigenetic reporter, we then characterize the mechanisms by which environmental exposure to the model chemical Bisphenol A (BPA) can cause heritable effects lasting for several generations after direct exposure. Specifically, we found that BPA causes reproductive defects and a heritable decrease in repressive histone marks in the germlines of worms that are ancestrally exposed. The inherited decrease in repressive histone marks and reproductive defects can be rescued by modulating the activity of histone modifying enzymes. Lastly, our work investigates the specific mechanisms through which BPA can induce reproductive defects that are inherited through the germline. We find that BPA affects the maintenance of meiotic processes, partly through disruption of double strand break repair pathways in a transgenerational manner. This in turn indicates the need for a larger transgenerational assessment focusing on the entire meiotic process that includes researching pairing, synapsis, recombination, and checkpoint pathways. These findings shine a light on how artificial environmental exposures can be biologically integrated and transgenerationally inherited. It highlights the importance of comprehensively examining our chemical environmental for its potential effects on our germline epigenome, which can in turn allow us to find interventional means to prevent transmission of effects to future generations.

The dissertation of Jessica Aimee Camacho is approved.

Amander Therese Clark

Curtis D Eckhert

Robert H Schiestl

Patrick Allard, Committee Chair

University of California, Los Angeles

2019

Dedicated to the two most important people in my world, Mom and Dad.

TABLE OF CONTENTS

Chapter 1: Introduction and Background……1

References……..…13

Chapter 2: Development and validation of a chemical epigenetic reporter system……..……16

References…….26

Chapter 3: The memory of environmental chemical exposure in *C. elegans* is dependent on the Jumonji demethylases *jmjd-2* and *jmjd-3/utx-1*……35

References……..…48

Chapter 4: Transgenerational germline dysfunction due to BPA exposure in *C. elegans*…...….70

References……..…81

Chapter 5: Summary and Discussion…….89

References……..…96

Appendix: Fast Functional Germline and Epigenetic Assays in the Nematode *Caenorhabdits elegans*……...100

Histone Modifications: Epigenetic Mediators of Environmental Exposure Memory……109

List of Tables and Figures

Chapter 1

Introduction and Background: Germline and Transgenerational impacts of Toxicant Exposures (Previously published in '*ToxicoEpigenetics: Core Principles and Applications'* textbook):

Figure 1.1: Changes in global methylation levels during early embryonic development 6

Figure 1.2: Multi- versus transgenerational exposures in rodents and in *C. elegans.* 9

Chapter 2

Development and validation of a chemical epigenetic reporter system:

Figure 2.1: Characterization of chemical epigenetic reporter system 31

Figure 2.2: Transgenerational effects of HDAC inhibitors *in C. elegans* 33

Figure 2.3: Following transgenerational heritability effects 34

Figure 2.4: Validation of chemical epigenetic reporter system with environmental toxicants 35

Chapter 3

The memory of environmental chemical exposure in *C. elegans* is dependent on the jumonji demethylases *jmjd-2* and *jmjd-3/utx-1* (Previously published in *Cell Reports*):

Figure 3.1: BPA exposure elicits a transgenerational desilencing of a repetitive array 40

Figure 3.2: BPA-induced transgenerational reduction in H3K9me3 and H3K27me3 identified by ChIP-seq 42

Figure 3.3: BPA treatment causes transgenerational intra-chromosomal redistribution of histone modifications 43

Figure 3.4: Ancestral BPA exposure decreases H3K9me3 and H3K27me3 levels in F3 germlines 44

Figure 3.5: Ancestral BPA exposure leads to a sharp decrease in H3K9me3 and H3K27me3

on autosomes, x chromosomes, and an extrachromosomal array and an upregulation of x-linked genes 45

Figure 3.6: Transgenerational impact of BPA on fertility 46

Figure 3.7: *jmjd-2* and *jmjd-3/utx-1* demethylases are required for BPA-induced transgenerational response 47

Figure 3.S1: Epigenetic drug inhibitor assessment in P0 nematodes. Related to Figure 1 53

Figure 3.S2: Dose, window and sex dependent germline pkIs1582 array desilencing. Related to Figure 1 54

Figure 3.S3: Transgenerational impact of BPA on the germline transcriptome. Related to Figure 2 and 5 55

Figure 3.S4: Ancestral BPA exposure decreases H3K9me3 and H3K27me3 levels in F3 germlines carrying an extrachromosomal array. Related to Figure 4 56

Figure 3.S5: Ancestral BPA exposure does not decrease H3K9me3 and H3K27me3 levels in F7 germlines. Related to Figure 4 57

Figure 3.S6: Variation in embryonic lethality phenotype based on genotype and variation in germline desilencing based on mode of inheritance. Related to Figure 6 58

Figure 3.S7: Changes in H3K9me3, H3K27me3, and array desilencing in the F3 generation following RNAi. Related to Figure 7 59

Figure 3.S8: Rescue of F3 germline pkIs1582 array desilencing and embryonic lethality phenotypes by inhibitor drug exposures. Related to Figure 7 60

Table 3.S1: RNA-Seq. Related to Figure 2 61

Table 3.S2: Differentially expressed reproduction genes. Related to Figure S3 67

Table 3.S3: Broad peak counts. Related to Figure 2 and S3 68

Table 3.S4: ChIP-seq GO analysis. Related to Figure 2 69

Table 3.S5: Histone PTM quantitation. Related to Figure 2 and Figure 4 70

Chapter 4

Transgenerational germline dysfunction due to BPA exposure in *C. elegans*

Figure 4.1: Transgenerational BPA exposure perturbs chromosome segregation and induces aneuploidy 86

Figure 4.2: BPA's transgenerational effects on double strand breaks 87

Figure 4.3: BPA exposure has influence on RAD-51 kinetics during early phases of pachytene 88

Figure 4.4: Transgenerational BPA exposure affects meiotic crossover dynamics 89

Chapter 5

Summary and Discussion: Histone Modifications: Epigenetic Mediators of Environmental Exposure Memory (previously published as a commentary article in *Epigenetic Insights*):

Figure 5.1: BPA exposures in C. elegans reduces the levels of the repressive histone marks H3K9me3 and H3K27me3, regulated by the demethylasesjmjd-2 and jmjd-3/utx-1 99

Acknowledgements

Thank you to my wonderful PI, Dr. Patrick Allard, for allowing me to be part of his lab and take part of a project I've truly enjoyed from the beginning. His patience and guidance have shaped me into the scientist I am today. No matter how I felt about any experiment or result, he always helped me to see the bigger picture, kept things interesting, and always found something to keep exploring. I can safely say that I always look forward to going to lab.

I would also like to thank the past and present members of the Allard lab. You all have made our lab such an awesome place to work at, and even outside of the lab, you are all wonderful people. I would like to give a special thanks to Dr. Yichang Chen, a true genius, and my best friend for the past six years. And of course, Lisa Truong, the next Dr. to come out of the lab. Your excitement for science, our work, and friendship is truly admirable.

I would also like to thank all of my committee members, Dr. Schiestl, Dr. Clark, and Dr. Eckhert. Your guidance and mentorship are truly invaluable, and I am so grateful.

Thank you to my family and friends. You have all been the greatest support system, I couldn't have gotten this far without you.

Thank you to all of my funding sources from UCLA, NSF, ACT, SCCSOT and SOT, for allowing me to advance my scientific knowledge, and to share my work with a broader audience through multiple conferences and meetings.

Chapter 3 is a version of a previous publication: Camacho J, Truong L, Kurt Z, Chen Y-W, Morselli M, Gutierrez G, Pellegrini M, Yang X, and Allard P. The Memory of Environmental Chemical Exposure in *C. elegans* Is Dependent on the Jumonji Demethylases *jmjd-2* and *jmjd-3/utx-1*. Cell Reports. 2018 May;23(8):2392–404. I would like to acknowledge the contributions of the co-authors in the paper: Lisa Truong for her contribution to designing experiments, experimental work and writing, Kurt Zeyneb, Yen-Wei Chen, and Dr. Xia Yang for their help with interpretation of RNA-seq and ChIP-seq data, Gerardo Gutierrez for his contribution to

experimental work, Marco Morselli and Dr. Matteo Pellegrini for their assistance with RNA-seq experimental work, and Dr. Patrick Allard for designing experiments, interpretation of data, and assistance writing and editing the publication.

Dr. Patrick Allard is the principal investigator who directed and supervised the research in this dissertation. He contributed by providing insight regarding the writing and editing of each chapter.

Biographical sketch

Jessica Aimee Camacho

EDUCATION

University of California, Los Angeles — Los Angeles, CA
PhD Candidate, Molecular Toxicology – GPA: 3.97 — August 2012- March 2019

University of California, Berkeley — Berkeley, CA
B.S. Molecular Toxicology **–** GPA 3.25 — August 2006 - May 2010

EXPERIENCE & SKILLS

University of California, Los Angeles — Los Angeles, CA
Graduate Student Researcher- Dr. Allard — April 2013-Present

University of California, Los Angeles — Los Angeles, CA
Graduate Student Researcher/ Rotation Student- Dr. Schiestl — August 2012-April 2013

Children's Hospital Oakland Research Institute
Oakland, CA
Undergraduate Student Researcher- Dr. Reason — June 2009-August 2010

-Proficiency in Microsoft PowerPoint, Graph Pad Prism, and Excel
-Fluent in oral/written Spanish

INTERNSHIPS

US Food and Drug Administration, CFSAN/OFAS
College Park, MD
ORISE Fellow — August 2010 – July 2012

Children's Hospital Oakland Research Institute (CHORI)
Oakland, CA
Research Intern — June 2009 - August 2010

Energy Biosciences Institute, UC Berkeley
Berkeley, CA
Part- Time Lab Assistant — January 2009 - August 2009

AWARDS & HONORS

- Dissertation Year Fellowship, UCLA — 2018
- Graduate Student Travel Support Award, SOT — 2017
- Leadership Committee Award, SOT — 2015-2016
- North American Graduate Fellowship, ACT — 2015-2016
- Cellular & Molecular Mechanisms of Toxicity GRC-Outstanding Poster — 2015
- Judith Blake Award, UCLA — 2015
- NSF Graduate Research Fellowship — 2014
- Eugene-Cota Robles Fellowship, UCLA — 2012

- NSF AGEP Competitive Edge Grant, UCLA 2012
- Biology Fellows Program Grant, UC Berkeley 2009
- Children's Hospital Oakland Research Institute Grant 2009-2010

LEADERSHIP & MENTORING

- SOT Leadership committee, 2014-2016
- Southern California Chapter of SOT student representative, 2014-2016
- SCCSOT K-12 outreach representative, 2015-2016
- Student to Scientist Mentor (Cal-State Northridge & UCLA), 2015-2018

PUBLICATIONS, PRESENTATIONS, POSTERS

-Camacho J, Truong L, Kurt Z, Chen Y, Yen-Wei Chen, Morselli M, Gutierrez G, Pellegrini M, Yang X, Allard P. The memory of environmental chemical exposure in *C. elegans* is dependent on the Jumonji demethylases *jmjd-2* and *jmjd-3/utx-1*. Cell Reports (2018) (Publication)
-Camacho J. Allard P. "Germline and Transgenerational Impacts of Toxicant Exposures". *Special Considerations in ToxicoEpigenetics Research*. Print. ToxicoEpigenetics: Core Principles and Applications. (2019) (Book Chapter)
-**Camacho J**, Allard P. "Histone Modifications: Epigenetic Mediators of Environmental Exposure Memory." Epigenetics Insights (2018) (Publication)
-Lundby, Z., **Camacho J**., Allard P. "Fast Functional Germline and Epigenetic Assays in the Nematode Caenorhabditis elegans." *High-Throughput Screening Assays in Toxicology*. 1st ed. Vol. 1473. N.p.: Humana Press, 2016. 99-107. Print. Methods in Molecular Biology. (Book Chapter)
-Chapman A.*, Malkin D.*, **Camacho J**., Schiestl R. IL-13 Overexpression in Mouse Lungs Triggers Systemic Genotoxicity in Peripheral Blood. Mutation Research 769 (2014) 100–107 (Publication)
-Reason D., Liberato J., Sun J., **Camacho J**., Zhou J. Mechanism of Lethal Toxin Neutralization by a Human Monoclonal Antibody Specific for the PA20 Region of Bacillus anthracis Protective Antigen. Toxins. 2011; 3(8):979-990. (Publication)
-**Camacho J**., Lundby Z., Hosohama L., Clark A., Allard. P. Heritable environmental effects mediated by germline chromatin alterations. Gordon Research Conferences- Cellular & Molecular Mechanisms of Toxicity, August 2015, Andover, NH (Platform Talk, and Poster))
-**Camacho J**. Examining Environmental Effects on the Germline Epigenome. EHS 411 Seminar Series. January 2015. UCLA. (Oral Presentation)
-**Camacho J**., Truong L, Gutierrez G., Kurt Z, Morselli M, Gutierrez G, Pellegrini M, Yang X Allard P. Mechanism of transgenerational inheritance of reproductive dysfunction stemming from environmental Bisphenol A exposure in *C. elegans.*. Toxicologist (2018, Poster Abstract)
-**Camacho J**., Truong L, Gutierrez G., Allard P. Transgenerational Inheritance Mechanisms of Environmental Exposure Effects. Toxicologist 1338:80 (2017, Poster Abstract)
-**Camacho J**., Gentry N, Gutierrez G., Hosohama L., Clark A., Allard. P. Heritable environmental effects mediated by germline chromatin alterations. Toxicologist 1839:196 (2016, Poster Abstract)
-**Camacho J**., Lundby Z., Hosohama L., Clark A., Allard. P. Examining Environmental Effects on the Germline Epigenome. Genetics Society of America- *C. elegans* meeting, June 2015. Los Angeles Ca (Poster)
-**Camacho J**., Lundby Z., Hosohama L., Clark A., Allard. P. Examining Environmental Effects on the Germline Epigenome. Toxicologist 2241:481 (2015, Poster Abstract)
-**Camacho J**., Allard P. Developing a screen for Analysis of Environmental Epigenetic Effects. Toxicologist 1704:443 (2014, Poster Abstract)

CHAPTER 1

Introduction & Background
"Germline and Transgenerational impacts of Toxicant Exposures"

Introduction

Many factors are important when considering the effects environmental toxicants can have on our society on a daily basis. One must consider everything we come in contact with in our homes, at our respective work-places and out in the environment. For decades we have focused on direct exposures and their outcomes, but we must also consider how these can affect future generations. Emerging studies continue to highlight the impact in-utero exposures can have on offspring, grand offspring, and beyond (inter-, multi-, transgenerational effects) (1). Unfortunately, there is a lack of unifying methods to study heritable effects from the thousands of environmental toxicants that remain to be tested. This chapter will focus on the impact of environmental exposures on future generations, with a focus on germline mediated effects.

References

1. Heard, E. & Martienssen, R. A. Transgenerational epigenetic inheritance: myths and mechanisms. *Cell* 157, 95-109, (2014).

CHAPTER

4-1

Germline and Transgenerational Impacts of Toxicant Exposures

Jessica A. Camacho[*], *Patrick Allard*[†]

[*]Molecular Toxicology Interdepartmental Program, University of California, Los Angeles, Los Angeles, CA, United States [†]Institute for Society and Genetics, University of California, Los Angeles, Los Angeles, CA, United States

OUTLINE

Introduction 251
The Germline 252
Germline Specification and the Importance of the Epigenetic Repression of Somatic Fates 252
PGC's Epigenetic Reprogramming: A Critical Period 253
Transgenerational Effects Stemming From Environmental Exposures 255
From Multi- to Trans-Generational 255
Toward a Mechanism of Inheritance: It's Not Just About DNA Methylation 257
Nonmammalian Models and the Central Role of Histone Modifications 258
Final Considerations 259
References 260
Further Reading 262

INTRODUCTION

When a pregnant woman is exposed to an epigenotoxicant, it may directly impact not only her epigenome but also the epigenome of her offspring and grand offspring, commonly referred to as inter- or multigenerational effects. Much attention has been given to G0 exposure and F1 effects. Much less attention, however, has been given to direct effects of exposures

https://doi.org/10.1016/B978-0-12-812433-8.00011-3

on the germ line, the eventual F2 (grand offspring) generation. This may be due to the intense focus over the last decade on the potential for exposures to influence transgenerational effects (F3 and beyond). In this chapter, we will explore the impact of environmental exposures on future generations, mainly focusing on germ-cell-mediated effects. Thus, to explain the mechanisms of inheritance stemming from various environmental cues and some of the discussions in the field, we first need to understand the developmental odyssey that germ cells are subjected to.

THE GERMLINE

Germ cells are the bridge between generations. They are responsible for passing down information from one generation to the next and consequently are often referred to as "immortal cells." The specification of germ cells occurs early during embryogenesis, yet their growth and development can span multiple years in mammals. A comprehensive description of germ-line development and across species has been reviewed elsewhere (e.g., Robert et al., 2015) and is beyond the scope of this chapter. Below, we will examine several critical periods of germ-cell development, how they may offer windows of susceptibility, and how they relate to the question of transgenerational inheritance.

GERMLINE SPECIFICATION AND THE IMPORTANCE OF THE EPIGENETIC REPRESSION OF SOMATIC FATES

In most animals, primordial germ cells (PGCs), the precursors to gametes, are formed during embryogenesis. There are two well-understood modes of PGC specification. One is the "preformation" mode, in which PGCs are specified by a specialized maternal cytoplasm or germ plasm that is asymmetrically divided during oogenesis or after fertilization to specify the cells to enter the germ-line lineage. Preformation is common among model organisms like *Drosophila*, *Caenorhabditis elegans* (*C. elegans*), *Xenopus*, and zebra fish. The second mechanism is termed epigenesis, where PGCs are induced during early embryogenesis by extracellular signals promoting pluripotent progenitor differentiation into germ cells (Seydoux and Braun, 2006). This mode was first observed in mice (Tam and Zhou, 1996) and appears to be the most widespread mechanism of germ-cell specification in metazoans (Extavour and Akam, 2003). These two modes of germ-cell specification have obvious distinct implications for transgenerational inheritance as the cytoplasmic continuity offered by preformation and the germplasm could act as a vector of information across generations. However, despite these differences, both mechanisms rely on the inhibition of the expression of somatic genes (Seydoux and Braun, 2006). Indeed, germ-line formation is guided by the inhibition of transcription and the use of repressive chromatin modifications in both modes of specification (Seydoux and Braun, 2006). For example, in mice, *Blimp1* (also known as PR domain zinc finger protein 1 (*Prdm1*)) is expressed during PGC specification and has been hypothesized to promote the repression of the somatic program, consistent with its known activity as a transcriptional repressor (Keller and Maniatis, 1991). *Tcfap2c*, a putative Blimp1 target, is expressed in PGCs from E7.25 and functions downstream to suppress mesodermal

differentiation (Ohinata et al., 2005). In *Drosophila* and *C. elegans*, PGCs (preformation models), inhibition of RNA polymerase II is observed, alongside a decrease in zygotic mRNAs until hours post fertilization at the onset of gastrulation. This transcriptional silencing is mediated by germplasm components, PIE-1 in *C. elegans* (Batchelder et al., 1999), and *germ cell-less* (*gcl*) and *polar granule component* (*pgc*) in *Drosophila* (Leatherman et al., 2002; Martinho et al., 2004; Schaner and Kelly 2006). In addition to germplasm components, chromatin-based mechanisms play a large part in specification of germ cells. In *Drosophila*, there is a decrease in the activating histone mark H3K4me2 (Rudolph et al., 2007), whereas in *C. elegans*, there is also a decrease in H3K4me2 alongside an increase in the repressive mark H3K27me3 (Katz et al., 2009; Schaner and Kelly, 2006). As detailed in a later section, the deregulation of histone marks in the germ line following environmental exposure has recently been shown to serve as a potent transgenerational signal in species such as *C. elegans*.

PGC'S EPIGENETIC REPROGRAMMING: A CRITICAL PERIOD

In mammals, soon after their specification, PGCs initiate a dramatic remodeling of their chromatin, a stage referred to as the period of epigenetic reprogramming. The complex kinetics of epigenetic modifications unfold over the course of several days to several weeks, depending on the species, and include a dramatic loss of global DNA methylation and changes to the levels of various histone marks (reviewed in Tang et al. (2016)). It is that period of epigenetic reprogramming that conceptually forms the biggest barrier to epigenetic inheritance, as epigenetic marks such as DNA methylation are broadly erased to reach the lowest level of DNA methylation of any mammalian cell type (Gkountela et al., 2015; Hackett et al., 2013; Seisenberger et al., 2012) (Fig. 1). However, the identification of DNA demethylation-resistant loci and other epigenetic marks that are not erased may provide a mechanistic link bridging generations.

The process of DNA demethylation in PGCs is remarkably extensive, leading to the levels measured to near or below 10 % average CpG methylation across the genome in E13.5 mouse PGCs (Hackett et al., 2013; Seisenberger et al., 2012) and is comparable with the levels reached

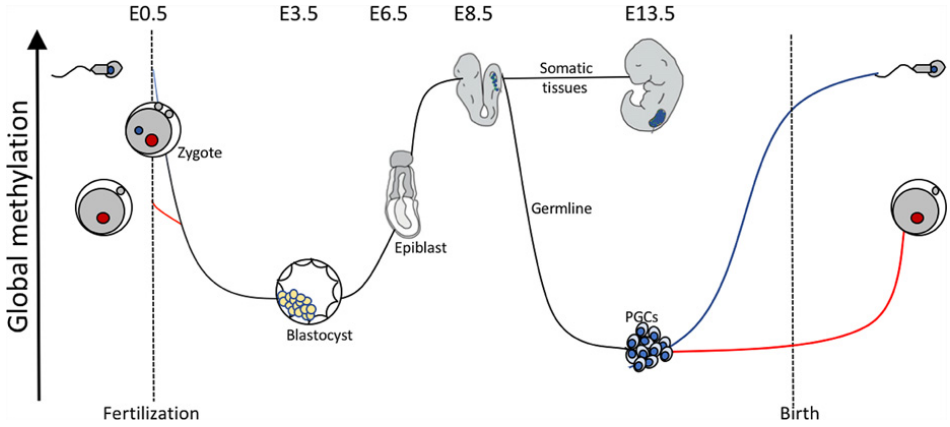

FIG. 1 Changes in global methylation levels during early embryonic development.

in human PGCs (Gkountela et al., 2015; Tang et al., 2015). The study of the dynamics and requirements for DNA demethylation in mouse primordial germ cells revealed that it is achieved in two phases. The first phase of DNA demethylation initiated in the mouse around E7.25 is both global and passive, that is, it is seen genome-wide and caused by the combination of active cellular replication and the simultaneous downregulation of expression of the *de novo* methyltransferases DNMT3A and DNMT3B, thus leading to the dilution of methylated CpGs over the course of several cell divisions (Grabole et al., 2013). In contrast, the second phase, which starts at E9.5, is dependent on the ten-eleven translocation (TET) enzymes, TET1 and TET2, and is more specific in its action (Hackett et al., 2013; Vincent et al., 2013). The methylation of imprinted control regions (ICRs), promoters of genes necessary for germ-cell formation and meiosis, and CpG islands of the inactive X chromosome in females survive the first wave of demethylation and appear to only reach full unmethylated state after the second wave of demethylation (Hackett et al., 2013; Hackett and Surani, 2013a,b; Tang et al., 2015). The supporting evidence includes the fact that *Tet1* and *Tet2* double knockout mice retain methylation at some ICRs and that *Tet1* is required for the demethylation of germ-cell- and meiosis-specific genes (Vincent et al., 2013; Yamaguchi et al., 2012). As mentioned above, while DNA methylation in PGCs is remarkably extensive, it is not complete. Notably, whole-genome bisulfite sequencing (WGBS) has revealed a total of 4730 loci that escape DNA demethylation in mouse PGCs, the vast majority of them being repeat associated (Hackett et al., 2013). These escapees are mainly evolutionarily young retrotransposons such as IAP elements in mice, which are known in other contexts to be sensitive to environmental exposures (see below) and LINE-1 L1HS elements in humans (Gkountela et al., 2015). Other regions also include pericentromeric satellite repeats (Tang et al., 2015) and subtelomeric regions (Guibert et al., 2012). There is clear interest in elucidating the consequence of perturbing the methylation at these loci, especially through the means of environmental exposures, and understanding how other epigenetic mechanisms, such as histone modifications, may be involved in the transcriptional repression of evolutionary older demethylated transposons.

However, in addition to DNA methylation erasure, histone modifications are also extensively reprogrammed during PGC differentiation. Notably, in mouse germ cells at around E8, there is a marked reduction in H3K9me2 that dovetails with an elevation of H3K27me3 (Kurimoto et al., 2015; Mansour et al., 2012; Seki et al., 2005, 2007; Shirane et al., 2016). The repressive mark H3K9me3 appears maintained throughout the reprogramming phase in the mouse and shows a "spotted" pattern in PGC nuclei corresponding to pericentromeric heterochromatin (Kim et al., 2014; Seki et al., 2007). One crucial factor for the regulation of these marks in PGCs is the N-methyltransferase SETDB1 that regulates H3K9me3 levels. Interestingly, the loss of SETDB1 leads to a reduction in H3K9me3 and H3K27me3 at IAPs and a reduction in DNA methylation at these loci (Leung et al., 2014; Liu et al., 2014) highlighting the importance of a concerted action between the different marks for transcriptional repression and the cross talk between these marks in PGCs. In other model organisms, such as *C. elegans*, where 5mC is not found, histone modifications are also remodeled during the germ-line cycle (Schaner and Kelly, 2006). However, as seen further below, the alteration of various histone marks, namely, H3K4me3, H3K9me3, and H3K27me3, has been associated with transgenerational inheritance of environmentally induced effects.

In summary, the transfer of epigenetic information across the period of PGC differentiation is a tightly regulated process that sees a global erasure of methylated CG dinucleotides and a remodeling of histone modifications. While it has been argued that this heavy remodeling

may prevent the inheritance of environmentally induced epimutations (heritable changes in gene activity not directly associated with the presence DNA mutations), the identification of demethylation-resistant young transposable elements among other loci and the stable expression of some histone marks, such as H3K9me3, open the possibility for a transfer of epimutations across that period.

TRANSGENERATIONAL EFFECTS STEMMING FROM ENVIRONMENTAL EXPOSURES

The possibility that organisms may pass down traits elicited by toxicant exposures has been controversial for a variety of reasons (Heard and Martienssen, 2014; Hughes, 2014), chief among them being an absence of clear mechanisms of transgenerational inheritance. However, recent developments from multiple laboratories, working with various model organisms, have reversed this situation such that there are now multiple lines of evidence that environmental exposures can lead to transgenerational effects and several proposed mechanisms for their inheritance. We will now highlight some of the critical findings in the field that were foundational to some recent exciting mechanistic discoveries.

FROM MULTI- TO TRANS-GENERATIONAL

An increasingly accepted nomenclature is used to distinguish between direct and indirect environmental effects on given generations: multigenerational versus transgenerational effects, respectively (Skinner, 2008). This nomenclature addresses the need to separate these effects as they would be born from different exposure windows and distinct mechanisms. In the multigenerational model of exposure, the F0 (sometimes more logically called "P0" for parental generation 0) is exposed to the environmental cue, thereby also exposing its germ cells. However, if the P0 parent is a pregnant mother, the exposure may also affect the fetus and the fetal germ cells, which represent the precursors to the filial generations F1 and F2, respectively. Thus, any health effects displayed by the P0, F1, and/or F2 may have been caused by the direct exposure to the environmental cue and may not be inherited. However, any effect shown by the F3 generation and beyond cannot be caused by direct exposure and therefore requires the transmission of a memory of the environmental exposure. This phenomenon is referred to as transgenerational exposure. The scenario is different if P0 male mice are used for exposure as only the P0 and the F1 germ cells are represented during the exposure; thus, any effects shown at the F2 and beyond represent a heritable transgenerational effect (Fig. 2).

The prior lack of agreement on a nomenclature may be leading to some confusion with regard to the ability of various environmental exposures to elicit transgenerational effects as defined above. The famous case of the Dutch famine is one such example (Ravelli et al., 1976). As described by Susser and others, pregnant women (P0) exposed to low calorie intake during pregnancy at the end of World War II gave birth to boys (F1) who showed a significant increase in their BMI at 19 years of age (Ravelli et al., 1976). A subsequent publication examined the F2 generation for various health end points and concluded that there was increased

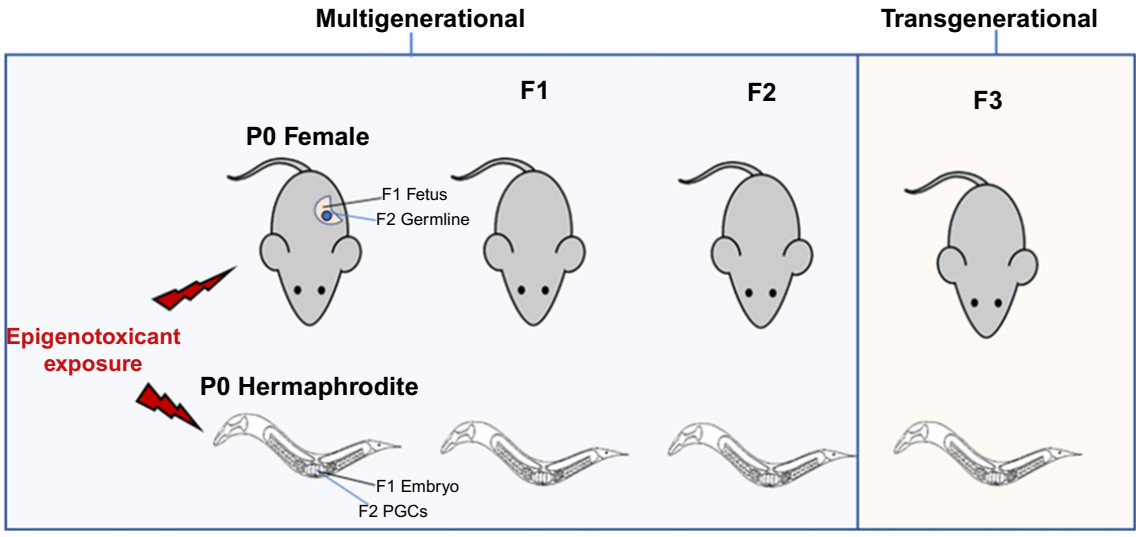

FIG. 2 Multi- versus transgenerational exposures in rodents and in *C. elegans*.

adiposity in that generation and thus transgenerational effect (Painter et al., 2008). In this exposure scenario, the F2 was represented as germ cells within the exposed fetus (F1). Therefore, one cannot exclude the possibility that the effects observed in the F2 are caused by direct exposure to low nutrient conditions as opposed to a heritable effect. Such studies however can be considered as foundational to transgenerational studies as they establish that the exposure in question has a direct effect on the fetus and that its germ cells and their epigenome may therefore also be impacted. The ability of *in utero* environmental exposures to alter health end points later in life led to the concept of the developmental origin of health and disease or DOHaD (Wadhwa et al., 2009). Importantly, it has now been clearly established that the type of environmental exposures able to act on the fetus is limited to not only "natural" environmental cues, such as diet, but also man-made ones, such as exposure to lead or plastics. In an important study carried by Dolinoy and colleagues, perinatal exposure to environmentally and physiologically relevant doses of the plastic manufacturing chemical bisphenol A led to an alteration of the DNA methylation levels of the *A*(*vy*) metastable epiallele involving an IAP element and leading to a change in its expression (Dolinoy et al., 2007). Together, these findings demonstrate a clear environmental impact on the fetus and extend the narrative related to early-life exposures to artificial environmental cues.

The ability of man-made environmental exposures to cause "true" transgenerational effects was established in 2005 by Skinner and colleagues (Anway et al., 2005). In their seminal study, gestational exposure (E8–E15) of rats by IP injection of high doses of the fungicide vinclozolin led to a strong effect on the reproductive function of males down to the F4 generation. These defects, which were transmitted through the male lineage, included a dramatic alteration of the testis morphology and a decrease in sperm count and quality (Anway et al., 2005). In line with the male lineage mode of inheritance, further analysis revealed that the F3 sperm carried a DNA methylation signature of ancestral vinclozolin exposure that consisted of 52 differentially methylated regions (DMRs) identified by MeDIP-chip (Guerrero-Bosagna

et al., 2010). This work was later extended to other compounds such as a mixtures of plastic compounds (BPA and phthalates) with similar conclusions (Manikkam et al., 2013). Some of these studies have since come under scrutiny for the chemical doses used (reviewed in (Hughes, 2014)), and it remains to be determined whether transgenerational effects of these compounds could be detected at environmentally relevant levels and routes of exposure. In those carefully defined and relevant conditions, it will also be important to test whether the identified epimutations caused by environmental exposure resist the period of DNA demethylation observed in PGCs and in early embryos, thus contributing to potential transgenerational inheritance. Nonetheless, it is undeniable that the studies by Skinner and colleagues ignited a vivid interest to examine toxicological end points over several generations and to investigate the role of the epigenome as a mechanism of transgenerational effects stemming from environmental chemicals.

TOWARD A MECHANISM OF INHERITANCE: IT'S NOT JUST ABOUT DNA METHYLATION

While not focused on environmental exposures, a recent study nonetheless demonstrated that overexpression of a histone lysine demethylase is sufficient to elicit a transmissible epigenetic impact on development (Siklenka et al., 2015). In this study, overexpression of the H3K4 demethylase KDM1A in transgenic male mice from only one generation was sufficient to result in transgenerational (F2 and beyond in this case) effects including a variety of severe developmental defects and a decrease in offspring survival. Interestingly, while there was a multigenerational decrease in H3K4me2 levels at 2300 loci corresponding to developmental genes in transgenic animals, this was not observed in nontransgenic animals and therefore, by inference, transgenerationally. Furthermore, DNA methylation was not altered in the sperm of transgenic or nontransgenic animals at loci where H3K4me2 levels were changed or genome-wide. However, gene expression in both sperm and embryos generated from sperm with ancestral KDM1A overexpression altered transgenerationally indicating that while the ancestral initiating event may be the change in H3K4me2, it is transmitted and exerts its developmental effects through another mechanism. This work is important because it suggests that an exposure-mediated change in expression levels of the epigenetic machinery might be sufficient to elicit transgenerational effects. It also emphasizes the fact that changes in DNA methylation are not necessary for the manifestation of transgenerational effects of environmental exposures.

A series of elegant and paradigm-shifting studies from several laboratories have also highlighted the importance of small tRNA-like RNAs in the transfer of information related to paternal diet to the next generation where they regulate metabolism. Rando and colleagues demonstrated that a low-protein paternal diet is sufficient to induce a metabolic reprogramming in the next generation, including an alteration in hepatic cholesterol production (Carone et al., 2010). However, sperm methylome profiling under various dietary condition revealed that diet alone had little influence on sperm methylation patterns (Shea et al., 2015). Instead, the low-protein diet led to the accumulation of small ~28–34 nt tRNA fragments that appear to be derived from the 5′ ends of tRNAs (Sharma et al.,

2016). A significant amount of those tRNA fragments is provided to the sperm during its passage through the epididymis through vesicles called epididymosomes that originate from the epididymal epithelium (Caballero et al., 2013). Importantly, injection of the sperm-derived small RNAs from low- versus high-protein males in zygotes was sufficient to differentially alter gene expression in preimplantation embryos, suggesting that later metabolic defects may be caused by the initial transcriptional landscape established by the presence of the small RNAs (Sharma et al., 2016). The effects of paternal high-fat diet (HFD) were also transmissible to the offspring, causing impaired glucose tolerance and insulin resistance (Chen et al., 2016). Injection of the sperm head from HFD males directly into the oocyte of female fed with a normal diet was sufficient to induce these changes (Chen et al., 2016). Furthermore, the injection of small 30–40 nucleotide RNAs, but not smaller or larger RNAs, isolated from these sperm into a zygote generated from normal diet mice was also sufficient to induce these metabolic phenotypes in the offspring (Chen et al., 2016). Finally, the authors were able to monitor the expression changes of genes in early embryos and in islets from mice obtained from injected embryos and showed that metabolic genes are perturbed in both cases, suggesting an alteration of these genes throughout the differentiation history of the islet cells.

Together, these studies highlight the role of small RNAs in the inheritance of paternal diet exposures; however, it is not clear whether any of these effects are transmissible to the subsequent generation (i.e., beyond the F1) or whether other paternal environmental conditions may also lead to the transfer of phenotypes to the next generation *via* small RNAs. Interestingly, a study on trauma and stress in mice has also shown that injection of sperm RNA was sufficient to induce behavioral and metabolic changes in the offspring (Gapp et al., 2014), suggesting it is possible that the sperm RNA content may transmit a wide range of paternal life experience.

NONMAMMALIAN MODELS AND THE CENTRAL ROLE OF HISTONE MODIFICATIONS

Transgenerational effects have also been identified in a variety of nonmammalian models (Baker et al., 2014; Brookheart and Duncan, 2016; Rankin, 2015). Crucially, some of these "alternative" models have been particularly conducive to the dissection of the mechanisms underlying environmental inheritance. This is particularly true of the nematode *C. elegans*, which offers the significant advantages of a short generation time (3–4 days) and a high level of genetic tractability.

The short generation time of the nematode and its utility for transgenerational studies are highlighted by a recent study on the effect of high temperature on the epigenome of the worm (Klosin et al., 2017). The authors examined the alteration of chromatin repression *via* desilencing of a heterochromatin-like repetitive transgene reporter following a five-generation high-temperature exposure. The study showed that such high-temperature exposure caused a derepression of the transgene expression lasting for 14 generations before returning to basal levels. The authors then examined the genetic requirement underlying this inheritance and showed that the transgene desilencing correlated with a decrease of the repressive mark H3K9me3 in the germ line. SET-25, the methyltransferase responsible for

H3K9 trimethylation, is required for the silencing of the reporter, and its deletion suppresses the difference between ancestrally exposed worms and nonexposed controls.

A variety of histone marks have been implicated in the inheritance of environmental effects that might be a reflection of the different environmental cues used in the studies. For example, exposure to arsenite leads to reproductive health defects, including reduction in brood size in *C. elegans*, in P0 generation and in subsequent generations (F1–F5) (Yu and Liao, 2016). In this case, the effects of arsenite are dependent on the levels of H3K4me2, a transcriptionally activating histone modification, as there is a decrease in the expression of the H3K4me2 demethylase, spr-5, together with an increase in H3K4me2 levels in the arsenite-exposed P0 generation and subsequent F1–F3 generations (Yu and Liao, 2016). H3K4 methylation has also been implicated as a mediator of the effects of various environmental exposures and stressors such as arsenite exposure, hyperosmosis, and starvation (Kishimoto et al., 2017). Exposure to these stressors during development resulted in an increased resistance to proteotoxicity and to the normally lethal oxidative stressor hydrogen peroxide that lasted until the F3 generation; however, worms with inactivating mutations in H3K4 methyltransferase complex components (*wdr-5.1* and *set-2*) failed to inherit resistance, reinforcing the role of H3K4 methylation in the transmission of the effect (Kishimoto et al., 2017). By comparing different exposures, this study suggests that the transgenerational effects that result from independent exposures may be transmitted through similar mechanisms. By contrast, a recent study identified the regulation of both H3K9me3 and H3K27me3 as mediators of memory of BPA exposure (Camacho et al., 2018) raising several hypotheses discussed below.

It is important to note that beside histone modifications, small RNAs have also been implicated as a mechanism of transgenerational inheritance in *C. elegans*. Starvation of worms, larvae, for example, induces the expression of several small RNAs, termed STGs for "small RNAs targeting a given gene." These STGs regulate nutrient reserves and have been detected in the both starved generation (P0) and their descendants through the F3 generation. Inheritance of the STGs is dependent on the presence of the argonaute proteins RDE-4 and HRDE-1 (Rechavi et al., 2014). Such small RNA mechanisms may work in concert with histone marks to regulate transgenerational inheritance as recently demonstrated in another study (Lev et al., 2017). That study examined the progressive mortal germ-line phenotype of the *met-2* mutants defective in H3K9 mono and dimethylation. In these worms, there was a progressive reduction in fertility that unfolds over 10–30 generations. Interestingly, the argonaute factor *hdre-1*, associated with small RNAs, is required for the progressive sterility phenotype of *met-2* mutant. From these results and others, the authors propose a model of inheritance where MET-2 functions to suppress the transgenerational transfer of small RNAs via the regulation of H3K9me. These findings directly link repressive histone marks and small RNAs; however, whether a similar connection can be established for environmentally induced phenotype remains to be explored.

FINAL CONSIDERATIONS

As illustrated above, there is currently not a single mechanism responsible for the transfer of environmental exposure effects from one generation to the next. The potential cross talk between epigenetic mechanisms, as observed in *C. elegans*, may explain why various

epigenetic marks have independently been shown to be important for the inheritance of exposure effects. Distinct environmental exposures may also act through different individual, or combinations of, epigenetic modifications. Efforts to distinguish between these possibilities would benefit greatly from a concerted and comprehensive effort between investigators in which standardized approaches are used to examine DNA methylation, histone modifications, and small RNAs simultaneously. As discussed earlier, it is also important for the community to establish a common nomenclature (e.g., definition of multi-, inter-, or transgenerational) and corresponding guidelines to examine these new models of inheritance. A movement in that direction has already been proposed by several key actors in the field (Bohacek and Mansuy, 2017; Skinner, 2008). Future studies must also determine whether a connection exists between specific environmental exposures and alterations in specific epigenetic factors. Similarly, there is also a need to examine how environmentally altered levels or distribution of epigenetic marks in germ cells may modify the function of adult organs. In conclusion, it is now well established that organisms have the ability to transmit various environmental cues across generations. This provides a fascinating reshaping of Darwinist evolutionary views to leave room to a certain degree of environmental responsiveness of animals over several generations. Despite these advances, we have yet to fully understand how environmental exposures alter the epigenome, how epimutations persist through developmental epigenetic reprogramming, and how epigenetic alterations in germ cells influence organ structure and function.

References

Anway, M.D., Cupp, A.S., Uzumcu, M., Skinner, M.K., 2005. Epigenetic transgenerational actions of endocrine disruptors and male fertility. Science 308, 1466–1469.

Baker, T.R., King-Heiden, T.C., Peterson, R.E., Heideman, W., 2014. Dioxin induction of transgenerational inheritance of disease in zebrafish. Mol. Cell. Endocrinol. 398, 36–41.

Batchelder, C., Dunn, M.A., Choy, B., Suh, Y., Cassie, C., Shim, E.Y., et al., 1999. Transcriptional repression by the caenorhabditis elegans germ-line protein pie-1. Genes Dev. 13, 202–212.

Bohacek, J., Mansuy, I.M., 2017. A guide to designing germline-dependent epigenetic inheritance experiments in mammals. Nat. Methods 14, 243–249.

Brookheart, R.T., Duncan, J.G., 2016. Drosophila melanogaster: an emerging model of transgenerational effects of maternal obesity. Mol. Cell. Endocrinol. 435, 20–28.

Caballero, J.N., Frenette, G., Belleannee, C., Sullivan, R., 2013. Cd9-positive microvesicles mediate the transfer of molecules to bovine spermatozoa during epididymal maturation. PLoS One 8, e65364.

Camacho, J., Truong, L., Kurt, Z., Chen, Y.W., Morselli, M., Gutierrez, G., Pellegrini, M., Yang, X., Allard, P., 2018. The memory of environmental chemical exposure in *C. elegans* is dependent on the Jumonji demethylases *jmjd-2* and *jmjd-3/utx-1*. Cell Rep. 23 (8), 2392–2404.

Carone, B.R., Fauquier, L., Habib, N., Shea, J.M., Hart, C.E., Li, R., et al., 2010. Paternally induced transgenerational environmental reprogramming of metabolic gene expression in mammals. Cell 143, 1084–1096.

Chen, Q., Yan, M., Cao, Z., Li, X., Zhang, Y., Shi, J., et al., 2016. Sperm tsrnas contribute to intergenerational inheritance of an acquired metabolic disorder. Science 351, 397–400.

Dolinoy, D.C., Huang, D., Jirtle, R.L., 2007. Maternal nutrient supplementation counteracts bisphenol a-induced DNA hypomethylation in early development. Proc. Natl. Acad. Sci. U. S. A. 104, 13056–13061.

Extavour, C.G., Akam, M., 2003. Mechanisms of germ cell specification across the metazoans: Epigenesis and preformation. Development 130, 5869–5884.

Gapp, K., Jawaid, A., Sarkies, P., Bohacek, J., Pelczar, P., Prados, J., et al., 2014. Implication of sperm rnas in transgenerational inheritance of the effects of early trauma in mice. Nat. Neurosci. 17, 667–669.

Gkountela, S., Zhang, K.X., Shafiq, T., Liao, W.-W., Hargan-Calvopina, J., Chen, P.-Y., Clark, A.T., 2015. DNA demethylation dynamics in the human prenatal germline. Cell 161, 1425–1436.

Grabole, N., Tischler, J., Hackett, J.A., Kim, S., Tang, F., Leitch, H.G., et al., 2013. Prdm14 promotes germline fate and naive pluripotency by repressing fgf signalling and DNA methylation. EMBO Rep. 14, 629–637.
Guerrero-Bosagna, C., Settles, M., Lucker, B., Skinner, M.K., 2010. Epigenetic transgenerational actions of vinclozolin on promoter regions of the sperm epigenome. PLoS One. 5.
Guibert, S., Forne, T., Weber, M., 2012. Global profiling of DNA methylation erasure in mouse primordial germ cells. Genome Res. 22, 633–641.
Hackett, J.A., Sengupta, R., Zylicz, J.J., Murakami, K., Lee, C., Down, T.A., Surani, M.A., 2013. Germline DNA demethylation dynamics and imprint erasure through 5-hydroxymethylcytosine. Science 339 (6118), 448–452.
Hackett, J.A., Surani, M.A., 2013b. DNA methylation dynamics during the mammalian life cycle. Philos. Trans. R. Soc. Lond. Ser. B: Biol. Sci. 368 (1609), 20110328.
Hackett, J.A., Surani, M.A., 2013a. Beyond DNA: programming and inheritance of parental methylomes. Cell 153, 737–739.
Heard, E., Martienssen, R.A., 2014. Transgenerational epigenetic inheritance: myths and mechanisms. Cell 157, 95–109.
Hughes, V., 2014. Epigenetics: the sins of the father. Nature 507, 22–24.
Katz, D.J., Edwards, T.M., Reinke, V., Kelly, W.G., 2009. A *C. elegans* lsd1 demethylase contributes to germline immortality by reprogramming epigenetic memory. Cell 137, 308–320.
Keller, A.D., Maniatis, T., 1991. Identification and characterization of a novel repressor of beta- interferon gene expression. Genes Dev. 5, 868–879.
Kim, S., Gunesdogan, U., Zylicz, J.J., Hackett, J.A., Cougot, D., Bao, S., et al., 2014. Prmt5 protects genomic integrity during global DNA demethylation in primordial germ cells and preimplantation embryos. Mol. Cell 56, 564–579.
Kishimoto, S., Uno, M., Okabe, E., Nono, M., Nishida, E., 2017. Environmental stresses induce transgenerationally inheritable survival advantages via germline-to-soma communication in *Caenorhabditis elegans*. Nat. Commun. 8:14031, https://dx.doi.org/10.1038/ncomms14031.
Klosin, A., Casas, E., Hidalgo-Carcedo, C., Vavouri, T., Lehner, B., 2017. Transgenerational transmission of environmental information in *C. elegans*. Science 356, 320–323.
Kurimoto, K., Yabuta, Y., Hayashi, K., Ohta, H., Kiyonari, H., Mitani, T., et al., 2015. Quantitative dynamics of chromatin remodeling during germ cell specification from mouse embryonic stem cells. Cell Stem Cell 16, 517–532.
Leatherman, J.L., Levin, L., Boero, J., Jongens, T.A., 2002. Germ cell-less acts to repress transcription during the establishment of the drosophila germ cell lineage. Curr. Biol. 12, 1681–1685.
Leung, D., Du, T., Wagner, U., Xie, W., Lee, A.Y., Goyal, P., et al., 2014. Regulation of DNA methylation turnover at ltr retrotransposons and imprinted loci by the histone methyltransferase setdb1. Proc. Natl. Acad. Sci. U. S. A. 111, 6690–6695.
Lev, I., Seroussi, U., Gingold, H., Bril, R., Anava, S., Rechavi, O., 2017. Met-2-dependent h3k9 methylation suppresses transgenerational small rna inheritance. Curr. Biol. 27, 1138–1147.
Liu, S., Brind'Amour, J., Karimi, M.M., Shirane, K., Bogutz, A., Lefebvre, L., et al., 2014. Setdb1 is required for germline development and silencing of h3k9me3-marked endogenous retroviruses in primordial germ cells. Genes Dev. 28, 2041–2055.
Manikkam, M., Tracey, R., Guerrero-Bosagna, C., Skinner, M.K., 2013. Plastics derived endocrine disruptors (BPA, DEHP and DBP) induce epigenetic transgenerational inheritance of obesity, reproductive disease and sperm epimutations. PLoS One 8, e55387.
Mansour, A.A., Gafni, O., Weinberger, L., Zviran, A., Ayyash, M., Rais, Y., et al., 2012. The h3k27 demethylase utx regulates somatic and germ cell epigenetic reprogramming. Nature 488, 409–413.
Martinho, R.G., Kunwar, P.S., Casanova, J., Lehmann, R., 2004. A noncoding rna is required for the repression of rnapolii-dependent transcription in primordial germ cells. Curr. Biol. 14, 159–165.
Ohinata, Y., Payer, B., O'carroll, D., Ancelin, K., Ono, Y., Sano, M., et al., 2005. Blimp1 is a critical determinant of the germ cell lineage in mice. Nature 436, 207–213.
Painter, R.C., Osmond, C., Gluckman, P., Hanson, M., Phillips, D.I., Roseboom, T.J., 2008. Transgenerational effects of prenatal exposure to the dutch famine on neonatal adiposity and health in later life. BJOG: Int. J. Obstet. Gynaecol. 115, 1243–1249.
Rankin, C.H., 2015. A review of transgenerational epigenetics for rnai, longevity, germline maintenance and olfactory imprinting in *Caenorhabditis elegans*. J. Exp. Biol. 218, 41–49.
Ravelli, G.P., Stein, Z.A., Susser, M.W., 1976. Obesity in young men after famine exposure in utero and early infancy. N. Engl. J. Med. 295, 349–353.

Rechavi, O., Houri-Ze'evi, L., Anava, S., Goh, W.S., Kerk, S.Y., Hannon, G.J., et al., 2014. Starvation-induced transgenerational inheritance of small rnas in *C. elegans*. Cell 158, 277–287.
Robert, V.J., Garvis, S., Palladino, F., 2015. Repression of somatic cell fate in the germline. Cell. Mol. Life Sci. 72, 3599–3620.
Rudolph, T., Yonezawa, M., Lein, S., Heidrich, K., Kubicek, S., Schafer, C., et al., 2007. Heterochromatin formation in drosophila is initiated through active removal of h3k4 methylation by the lsd1 homolog su(var)3-3. Mol. Cell 26, 103–115.
Schaner, C.E., Kelly, W.G., 2006. Germline chromatin. In: WormBook: The Online Review of *C. elegans* Biology. WormBook, Pasadena, CA, pp. 1–14.
Seisenberger, S., Andrews, S., Krueger, F., Arand, J., Walter, J., Santos, F., et al., 2012. The dynamics of genome-wide DNA methylation reprogramming in mouse primordial germ cells. Mol. Cell 48, 849–862.
Seki, Y., Hayashi, K., Itoh, K., Mizugaki, M., Saitou, M., Matsui, Y., 2005. Extensive and orderly reprogramming of genome-wide chromatin modifications associated with specification and early development of germ cells in mice. Dev. Biol. 278, 440–458.
Seki, Y., Yamaji, M., Yabuta, Y., Sano, M., Shigeta, M., Matsui, Y., et al., 2007. Cellular dynamics associated with the genome-wide epigenetic reprogramming in migrating primordial germ cells in mice. Development 134, 2627–2638.
Seydoux, G., Braun, R.E., 2006. Pathway to totipotency: lessons from germ cells. Cell 127, 891–904.
Sharma, U., Conine, C.C., Shea, J.M., Boskovic, A., Derr, A.G., Bing, X.Y., et al., 2016. Biogenesis and function of trna fragments during sperm maturation and fertilization in mammals. Science 351, 391–396.
Shea, J.M., Serra, R.W., Carone, B.R., Shulha, H.P., Kucukural, A., Ziller, M.J., et al., 2015. Genetic and epigenetic variation, but not diet, shape the sperm methylome. Dev. Cell 35, 750–758.
Shirane, K., Kurimoto, K., Yabuta, Y., Yamaji, M., Satoh, J., Ito, S., et al., 2016. Global landscape and regulatory principles of DNA methylation reprogramming for germ cell specification by mouse pluripotent stem cells. Dev. Cell 39, 87–103.
Siklenka, K., Erkek, S., Godmann, M., Lambrot, R., McGraw, S., Lafleur, C., et al., 2015. Disruption of histone methylation in developing sperm impairs offspring health transgenerationally. Science 350, aab2006.
Skinner, M.K., 2008. What is an epigenetic transgenerational phenotype? F3 or f2. Reprod. Toxicol. 25, 2–6.
Tam, P.P., Zhou, S.X., 1996. The allocation of epiblast cells to ectodermal and germ-line lineages is influenced by the position of the cells in the gastrulating mouse embryo. Dev. Biol. 178, 124–132.
Tang, W.W., Dietmann, S., Irie, N., Leitch, H.G., Floros, V.I., Bradshaw, C.R., et al., 2015. A unique gene regulatory network resets the human germline epigenome for development. Cell 161, 1453–1467.
Tang, W.W., Kobayashi, T., Irie, N., Dietmann, S., Surani, M.A., 2016. Specification and epigenetic programming of the human germ line. Nat. Rev. Genet. 17, 585–600.
Vincent, J.J., Huang, Y., Chen, P.Y., Feng, S., Calvopina, J.H., Nee, K., et al., 2013. Stage-specific roles for tet1 and tet2 in DNA demethylation in primordial germ cells. Cell Stem Cell 12, 470–478.
Wadhwa, P.D., Buss, C., Entringer, S., Swanson, J.M., 2009. Developmental origins of health and disease: brief history of the approach and current focus on epigenetic mechanisms. Semin. Reprod. Med. 27, 358–368.
Yamaguchi, S., Hong, K., Liu, R., Shen, L., Inoue, A., Diep, D., et al., 2012. Tet1 controls meiosis by regulating meiotic gene expression. Nature 492, 443–447.
Yu, C.W., Liao, V.H., 2016. Transgenerational reproductive effects of arsenite are associated with h3k4 dimethylation and spr-5 downregulation in *Caenorhabditis elegans*. Environ. Sci. Technol. 50, 10673–10681.

Further Reading

Allergrucci, C., 2005. Reproduction.
Blackwell, T.K., 2004. Germ cells: finding programs of mass repression. Curr. Biol. 14, R229–R230.
Chiquoine, A.D., 1954. The identification, origin, and migration of the primordial germ cells in the mouse embryo. Anat. Rec. 118 (2), 135–146. https://dx.doi.org/10.1002/ar.1091180202. PMID 13138919.
Chuva De Sousa Lopes, S.M., Hayashi, K., Shovlin, T.C., Mifsud, W., Surani, M.A., Mclaren, A., 2008. X chromosome activity in mouse XX primordial germ cells. PLoS Genetics 4, e30.
Copeland, N.G., Gilbert, D.J., Cho, B.C., Donovan, P.J., Jenkins, N.A., Cosman, D., et al., 1990. Mast cell growth factor maps near the steel locus on mouse chromosome 10 and is deleted in a number of steel alleles. Cell 63, 175–183.

Fullston, T., et al., 2013. FASEB J. 27, 4226–4243.
Ginsburg, M., Snow, M.H., McLaren, A., 1990. Primordial germ cells in the mouse embryo during gastrulation. Development 110 (2), 521–528.
Greer, E.L., et al., 2011. Nature 479, 365–371.
Hajkova, P., Ancelin, K., Waldmann, T., Lacoste, N., Lange, U.C., Cesari, F., Lee, C., Almouzni, G., Schneider, R., Surani, M.A., 2008. Chromatin dynamics during epigenetic reprogramming in the mouse germ line. Nature 452 (7189), 877–881.
Hajkova, P., Jeffries, S.J., Lee, C., Miller, N., Jackson, S.P., Surani, M.A., 2010. Genome-wide reprogramming in the mouse germ line entails the base excision repair pathway. Science 329 (5987), 78–82.
Huang, E., Nocka, K., Beier, D.R., Chu, T.Y., Buck, J., Lahm, H.W., et al., 1990. The hematopoietic growth factor KL is encoded by the Sl locus and is the ligand of the c-kit receptor, the gene product of the W locus. Cell 63, 225–233.
Kohli, R.M., Zhang, Y., 2013. TET enzymes, TDG and the dynamics of DNA demethylation. Nature 502 (7472), 472–479.
Lambrot, R., et al., 2013. Nat. Commun. 4, 2889.
Lawson, K.A., Hage, W.J., 1994. In: Clonal analysis of the origin of primordial germ cells in the mouse. Ciba Foundation Symposium. Novartis Foundation Symposia, 182, pp. 68–84. discussion 84–91.
Maatouk, D.M., Resnick, J.L., 2006. DNA methylation is a primary mechanism for silencing postmigratory primordial germ cell genes in both germ cell and somatic cell lineages. Development 133, 3411–3418.
Marczylo, E.L., Amoako, A.A., Konje, J.C., Gant, T.W., Marczylo, T.H., 2012. Epigenetics 7, 432–439.
Messerschmidt, D.M., Knowles, B.B., Solter, D., 2014. DNA methylation dynamics during epigenetic reprogramming in the germline and preimplantation embryos. Genes Dev. 28, 812–828.
Ng, S.-F., et al., 2010. Nature 467, 963–966.
Ohinata, Y., Ohta, H., Shigeta, M., Yamanaka, K., Wakayama, T., Saitou, M., 2009. A signaling principle for the specification of the germ cell lineage in mice. Cell 137, 571–584.
Pembrey, M.E., et al., 2006. Eur. J. Hum. Genet. 14, 159–166.
Saitou, M., Barton, S.C., Surani, M.A., 2002. A molecular programme for the specification of germ cell fate in mice. Nature 418, 293–300.
Saitou, M., Kagiwada, S., Kurimoto, K., 2012. Epigenetic reprogramming in mouse pre-implantation development and primordial germ cells. Development 139, 15–31.
Wei, Y., et al., 2014. Proc. Natl. Acad. Sci. U. S. A. 111, 1873–1878.
Yamaji, M., Seki, Y., Kurimoto, K., Yabuta, Y., Yuasa, M., Shigeta, M., et al., 2008. Crit- ical function of Prdm14 for the establishment of the germ cell lineage in mice. Nature Genetics 40, 1016–1022.
Yoshimizu, T., Obinata, M., Matsui, Y., 2001. Stage-specific tissue and cell interactions play key roles in mouse germ cell specification. Development 128, 481–490.
Zwaka, T.P., Thomson, J.A., 2005. A germ cell origin of embryonic stem cells? Development 132, 227–233.

CHAPTER 2
Development and validation of a chemical epigenetic reporter system

Summary

We are continually exposed to tens of thousands of environmental chemicals that have not been tested for epigenetically-mediated inherited effects. We must address the epigenetic toxicity of these chemicals, but this poses a challenge because we must consider their combinatory effects (mixtures) and the vast number of toxicity endpoints that can be affected. Importantly, we must identify model organisms that will enable us to quickly, economically, and ethically assess chemical safety. Epigenetic toxicity studies will need to focus on germ cells to analyze perturbations passed down from generation to generation. Germ cell development occurs over many months to many years in mammalian species, presenting challenges for comprehensive germ cell toxicity assays because the germ cells are difficult to access at all stages of development. This chapter centers on development and validation of an epigenetic reporter system and serves as a prelude to the work that was ultimately published in Chapter 3. Our work developed a protocol (1), the first of its kind, for the assessment of environmental toxicant effects on the epigenome in a quick and efficient manner.

Introduction

Many factors challenge our ability to assess the safety of thousands of chemicals found in the environment. These factors include the number of toxicity endpoints, concentrations, and combinations of chemicals to be tested. The potential effect of chemicals on the germline and its epigenome is of particular importance because exposures to chemicals can alter biological processes over several generations, as have been observed in the cases of the reproductive toxicants DES, vinclozolin, and BPA (2–5). Epigenetics, as a field, examines changes in gene expression or cellular phenotype that are caused by genome modifications that do not alter the underlying DNA sequence. This is achieved through various chromatin modifications including DNA methylation, histone modifications and small RNAs. While DNA methylation has been the focus of most early studies, recent work has focused on the other mechanisms. Unfortunately,

there is clear paucity of methods that allow us to quickly and efficiently examine the mechanisms underlying heredity of germline epigenome effects resulting from toxicant exposures.

Our goal is to explore the influence of environmental chemicals on the germline epigenome. Though tightly regulated, germ cells are vulnerable to outside influence as these cells undergo periods of profound DNA demethylation and histone marks modification (6). In mammals, these events take place early during embryogenesis, which creates issues of accessibility to the cells and ease of study. The powerful genetic system *Caenorhabditis elegans (C. elegans)* allows us quickly and efficiently address these accessibility issues. Additionally, *C. elegans* offer many advantages that will allow us to study impacts of chemical exposure over time including their genetic tractability, accessible germ line, short generation time and well-characterized distribution and regulation of chromatin marks (7–9). These features can enable us to dissect the intricate mechanisms of inherited effects from toxicant exposures.

Characterization of a chemical epigenetic reporter system

We proposed that *C. elegans* strains containing a highly repetitive GFP transgene array (**NL2507, PD7271)** could be utilized to follow environmental toxicant effects on the germline epigenome. The strains carry a repetitive transgene that is regulated similarly to repetitive elements silencing in mammalian germ cells (10,11). Constructed by William Kelly and colleagues, this strain was initially utilized to study repetitive transgenes and how these arrays mimic a subset of the repressive mechanisms regulating X chromatin assembly (12). In adult worms, it was found that gene silencing correlates with enrichment of repressive histone marks (H3K9me) in the array chromatin, as well as an absence of activating histone marks (H3K4me). These studies strongly implicated a predominant role for chromatin structure in the silencing process. While this approach has been previously used with success to identify genetic factors required for epigenetic homeostasis in the germline (13,14), it has not been adapted and validated for chemical screening. Therefore, epigenetic maintenance of the repetitive transgene can be

manipulated by chemical exposure and allow for easy visualization of GFP expression after disruption of silencing mechanisms.

Results

Epigenetic reporter validation with histone modifying chemicals

The strain used by Kelly & Fire (14) contains a repetitive let-858::gfp reporter array, and like other low complexity arrays, it is silenced in the adult germline (Figure 1A) (14). Here, we will demonstrate the powerful use of this reporter to examine epigenetic regulation in the *C. elegans* germline after chemical exposure. Our novel approach was developed by characterizing the *C. elegans* reporter, testing several screening conditions, and finally exposing worms to various histone modifying chemicals to validate our method.

We first assessed baseline germline GFP expression in two different worm strains containing the same repetitive let-858::GFP reporter array: NL2507 and PD7271. At the standard maintenance temperature of 20°C, baseline GFP expression for PD727 and NL2507 ranged from 7-10%, respectively (worms with germline GFP expression /total worms = %Germline GFP expression). In contrast, expression at 25°C ranged from 10% for PD7271 and 21% for NL2507 (Figure 1B). The larger range of induction for the NL2507 strain at both of the temperatures tested could prove beneficial to our chemical assessments, given the dynamic range it could offer when studying chemicals that could either increase or decrease germline GFP expression.

To further investigate which strain was more suitable for our work, we tested several chemicals with known effects on histone modifications. For these experiments, a short exposure window of 24 hours from L4 to adult day 1 stage was used for the following chemicals: histone deacetylase inhibitors (valproic acid, vorinostat, trichostatin), histone methyltransferase inhibitors (bix-01338, chaetocin), a histone acetyltransferase inhibitor (anacardic acid), and a histone demethylase inhibitor (methylstat). All chemicals were tested at a concentration of 100μM, with

exception of chaetocin (10μM) due to its induction of lethality after a 24-hour exposure to worms at a 100μM concentration. Following a 24-hour exposure to histone modifying chemicals at 20°C (standard maintenance temperature), replicated twice, several chemicals increased germline GFP expression levels compared to our DMSO control (Figure 1C). The histone deacetylase inhibitor Valproic acid (VA) showed a 1.2-fold GFP de-silencing increase from the control in the NL2507 strain, compared to 0.5-fold in the PD7272 strain. The range of induction between control and VA treatment demonstrated that it was a viable candidate for follow-up studies.

We next sought a suitable exposure paradigm to assess the effects of chemical exposure on the germline. We tested additional windows of exposure, determined based on the developmental timeline of the worm germline and the temperature/conditions of transgene would be disrupted. Using VA as our candidate chemical for its GFP de-silencing capabilities, we tested 48- or 65-hour exposures in liquid culture. We found that a 48-hour exposure, encompassing the L4 stage to day 2 of adulthood, resulted in a tighter and more significant range of worms displaying germline GFP de-silencing (48hr: DMSO 9.0±1.1%, VA=17.7±2.3% $P<0.01$, 65hr: DMSO 7.5±1.7% VA 17.3±3.2%, $P<0.05$, Figure 1D). In contrast, the 65-hour exposure had several disadvantages including food shortage, worm aging, and bagging. In general, the worms exposed for 48 hours were phenotypically healthier. We also examined the effect of incubation temperature on VA exposure. We expected an increase in de-silencing (i.e., higher GFP expression) following VA exposure, therefore it was ideal to start from the lower baseline expression levels observed at 20°C. Additionally at 25°C, worms age more quickly, disrupting the window of exposure we previously identified as ideal (48h from L4 to day 2 adulthood). For these reasons, the standard protocol determined: 1.5ml tubes, 500μL total volume: M9 (saline buffer), 1:10 Harvard OP50 bacteria as food, 0.5μL chemical concentration, 200-300 L4 stage worms, for 48 hours (Figure 1E).

Using these conditions, we tested chemicals with known histone modifying capabilities, including a few previously tested in the 24-hr strain assessment. We observed differences in germline GFP expression and the effect direction correlated with the expected activity of each chemical as either an activators or. repressors (Figure 1F).

Analysis of transgenerational effects of histone modifying compounds

We advanced these studies by testing the trans-generational effects following the initial direct exposure. VA is a histone deacetylase (HDAC) inhibitor that showed de-silencing of GFP transgene activity in the initial short-term 24-hour and 48-hour exposures. Similarly, the histone deacetylase inhibitor sodium butyrate significantly increased germline GFP expression following a 48-hr exposure. When a higher concentration of 1mM (Figure 1F) was used there was a significant increase in germline GFP expression without causing evident changes to phenotype or mortality (DMSO 14.3±1.6%, sodium butyrate 32.5±3.1%, $P<0.001$). Next, we exposed L4 worms to histone deacetylase inhibitors sodium butyrate and valproic acid for 48 hours, then assessed the F1, F2, and F3 generations (Figure 2A). Importantly, F3 is the first transgenerational group and was not directly exposed during the initial P0 parental exposure. The parent (in our case hermaphrodite worm), carries her embryos (F1 generation) and the germline of her embryos (F2 generation) all within the 48-hour window of exposure. Therefore, if any effects are evident at F3, three generations after the initial parental exposure, this means the effects were mediated through the germline as these are the only cells that are passed down to the next generation. Interestingly, VA did not show a strong de-silencing effect when compared to our DMSO control, other than in the parental generation directly exposed (P0: DMSO 13.2±0.9% VA 21.6±1.7%, $P<0.01$, Figure 2B right). In contrast, sodium butyrate had a significant increase in percentage of worms with germline GFP expression that lasted until the F3 transgenerational generation, displaying heritability of effects (P0: DMSO 13.2±0.9% SB 34.8±2.8%, $P<0.001$, F2: DMSO

29.2±3.5% SB 47.2±3.4%, P<0.01, F3: DMSO 13.2±0.9% SB 49.4±3.3%, P<0.001, Figure 2B left).

Our analysis of worms from P0 to F3 was done in a mixed population of worms, with some expressing low or high GFP levels. We were therefore interested in following expressers and non-expressers to further examine heredity. We altered our selection of worm offspring by separating them based on the GFP expression of the P0 parental generation after exposure (showing a de-silencing effect or lack-of, Figure 3A). By separating the worms, heritability of effects seen at the P0 generation can be followed. Groups were labelled (+) or (-) and followed up to the F3 generation. Results show that even in cases where worms do not show a de-silencing effect (GFP expression) after being directly exposed to either VA or sodium butyrate, effects can be seen in later generations (Figure 3B). Most strikingly, the majority of offspring of GFP expressers, remain GFP positive for the F1 generation, and in the case of VA and sodium butyrate, these effects last up to the F3 generation. Results reached a significant 2 to 3-fold induction in both F2 and F3 generations after the separation of GFP expressers, displaying an evident picture of heritable epigenetic effects (Figure 3B). To summarize, worms display germline de-silencing of a normally epigenetically silenced repetitive GFP transgene when directly exposed to histone modifying chemicals.

One interesting finding throughout the worm analysis of GFP de-silencing in different generations, was the appearance of what we called “super bright” worms. During our initial analysis in the worms we called ‘positive,’ we saw GFP expression that was slightly less bright than the somatic GFP expression throughout the worm (Figure 3C). In F1 and later generations (F1-F3), we saw a third category we called ‘super bright’, given its germline GFP expression was just as bright as that of the rest of the worm (Figure 3D). We brought in this categorization to our analysis as a more clear-cut way to identify true positives from those worms that seemed questionable, but the results did not differ between examples, even controls (Figure 3E).

Reporter application to environmental toxicants

With a system in place to visualize de-silencing effects after exposure to histone modifying chemicals, the next approach is to analyze environmental chemicals and their transgenerational effects. Using the same exposure conditions described previously, our next experiments focused was on two environmental chemicals, Vinclozolin and BPA. Vinclozolin and BPA have been proven to cause a variety of epigenetically-mediated effects in rodent models, including transgenerational reproductive effects (2,3). Worms were exposed to the environmental toxicants at 100μM. The P0 generation showed a significant increase of germline GFP expression for both BPA and vinclozolin when compared to the DMSO control (P0: DMSO 15.3±1.7%, BPA 27.5±1.7%, Vinclozolin 31.0±2.1%, $P<0.001$ Figure 4A), indicating effects on germline chromatin. We followed the offspring of the P0 parental generation until the transgenerational group (F3). At F3, we continued to see a significant difference of germline GFP expression (DMSO 21.2±1.7% BPA 45.4±4.8%, $P<0.01$, Vinclozolin 40.6±5.7% $P<0.05$), even 3 generations after direct exposure, indicating a transgenerational effect (Figure 4B).

To summarize, BPA and vinclozolin exposed worms display germline transgene de-silencing when directly exposed to these environmental toxicants. Furthermore, this effect is heritable and even increases for at least three generations after initial parental exposure. Vinclozolin and BPA have similar effects in early generations, but the effect of BPA becomes stronger than vinclozolin in later generations. These results indicate that BPA and vinclozolin exposures cause de-silencing of a normally epigenetically silenced repetitive GFP transgene in the *C. elegans* germline. Follow-up studies will look closely at the generations between P0-F3 and after, to examine the enduring nature of this heritability. Additionally, we will examine how these epigenetic effects are mediated how the disruption of chromatin in the germline can affect reproduction and development.

Conclusions

C. elegans are an emerging animal model for toxicological assays and are used in various screening efforts from the National Institute of Environmental Health Sciences (NIEHS) and the National Toxicology Program (NTP) (15,16). In several recent publications, the *C. elegans* model was established as a viable alternative to rodent models for both mechanistic and comprehensive analyses. *C. elegans* offer enormous advantages for the study of germ cells and epigenetic regulation. We can take advantage of genetic and epigenetic tools available in a 'lower' model organism, but do not remain confined to it. We can use our findings in *C. elegans* as foundation and validate in rodent models. The mobilization of evolutionary conserved features that we can study across several species brings a unique angle to the research. It also ensures that the work proposed remains relevant and gives confidence in using model system data for risk assessment purposes. Additionally, our studies focus on endpoints that are particularly difficult to observe in mammalian settings. By studying *C. elegans* and their conserved reproductive processes, we can take full advantage of its biology and genetic tools to carry experiments on all stages of germ cell development and over multiple generations, in a large-scale setting. Thus, these studies will address existing gaps in our efforts to examine environmental effects that are of tremendous health importance for ours, and future generations.

Experimental procedures

Culture conditions and strains: Standard methods of culturing and handling of *C. elegans* were followed (17). Worms were maintained on nematode growth medium (NGM) plates streaked with OP50 E. coli. Strains used in this chapter were obtained from the *C. elegans* Genetics Center (CGC) and include the following: NL2507 (pkIs1582[let-858::GFP;rol-6(su1006)]), and PD7271 (pha-1(e2123) III; ccEx7271).

Chemical exposure protocol and GFP scoring: The exposure and GFP germline de-silencing assessment were performed as described in Lundby et al., 2016 (see Appendix). Chemicals tested were obtained from Sigma Aldrich and were dissolved in DMSO to a stock concentration of 100mM. Worms were synchronized by bleaching an adult population of either strain, plating the eggs and allowing the population to reach L4 larval stage (50-52 hours). Worms were then exposed for 48 hours, and After 48 hours, then allowed to recover on NGM plates for 1-2 hours (mixed population) or immediately plated as individual worms to separately labeled 35 mm seeded NGM plates (GFP+/- population sorting) and recovered there.

Statistical analyses

Unless indicated otherwise, an unpaired t-test assuming unequal variance with Welch's correction was applied. For multi-group comparisons, a one-way ANOVA with Sidak correction or two-way ANOVA was used.

References

1. Lundby Z, Camacho J, Allard P. Fast Functional Germline and Epigenetic Assays in the Nematode Caenorhabditis elegans. In: Zhu H, Xia M, editors. High-Throughput Screening Assays in Toxicology [Internet]. New York, NY: Springer New York; 2016 [cited 2018 Aug 24]. p. 99–107. Available from: http://link.springer.com/10.1007/978-1-4939-6346-1_11

2. Manikkam M, Tracey R, Guerrero-Bosagna C, Skinner MK. Plastics Derived Endocrine Disruptors (BPA, DEHP and DBP) Induce Epigenetic Transgenerational Inheritance of Obesity, Reproductive Disease and Sperm Epimutations. Shioda T, editor. PLoS ONE. 2013 Jan 24;8(1):e55387.

3. Anway MD. Epigenetic Transgenerational Actions of Endocrine Disruptors and Male Fertility. Science. 2005 Jun 3;308(5727):1466–9.

4. Nelson KG, Sakai Y, Eitzman B, Steed T, McLachlan J. Exposure to diethylstilbestrol during a critical developmental period of the mouse reproductive tract leads to persistent induction of two estrogen-regulated genes. Cell Growth & Differentiation. 1994 Jun 1;5(6):595.

5. Doherty LF, Bromer JG, Zhou Y, Aldad TS, Taylor HS. In Utero Exposure to Diethylstilbestrol (DES) or Bisphenol-A (BPA) Increases EZH2 Expression in the Mammary Gland: An Epigenetic Mechanism Linking Endocrine Disruptors to Breast Cancer. Horm Cancer. 2010 Jun;1(3):146–55.

6. Tang WWC, Kobayashi T, Irie N, Dietmann S, Surani MA. Specification and epigenetic programming of the human germ line. Nat Rev Genet. 2016;17(10):585–600.

7. Bessler JB, Andersen EC, Villeneuve AM. Differential Localization and Independent Acquisition of the H3K9me2 and H3K9me3 Chromatin Modifications in the Caenorhabditis elegans Adult Germ Line. Copenhaver GP, editor. PLoS Genetics. 2010 Jan 22;6(1):e1000830.

8. Ho JWK, Jung YL, Liu T, Alver BH, Lee S, Ikegami K, et al. Comparative analysis of metazoan chromatin organization. Nature. 2014 Aug 27;512:449.

9. Liu T, Rechtsteiner A, Egelhofer TA, Vielle A, Latorre I, Cheung M-S, et al. Broad chromosomal domains of histone modification patterns in C. elegans. Genome Research. 2011 Feb 1;21(2):227–36.

10. Schaner CE, Kelly WG. Germline chromatin [Internet]. WormBook; 2006 [cited 2019 Jan 24]. Available from: https://www.ncbi.nlm.nih.gov/books/NBK19753/

11. Leitch HG, Tang WWC, Surani MA. Chapter Five - Primordial Germ-Cell Development and Epigenetic Reprogramming in Mammals. In: Heard E, editor. Current Topics in Developmental Biology [Internet]. Academic Press; 2013 [cited 2019 Jan 24]. p. 149–87. (Epigenetics and Development; vol. 104). Available from: http://www.sciencedirect.com/science/article/pii/B978012416027900005X

12. Kelly WG, Xu S, Montgomery MK, Fire A. Distinct Requirements for Somatic and Germline Expression of a Generally Expressed Caernorhabditis elegans Gene. Genetics. 1997 May 1;146(1):227–38.

13. Leung MCK, Williams PL, Benedetto A, Au C, Helmcke KJ, Aschner M, et al. Caenorhabditis elegans: An Emerging Model in Biomedical and Environmental Toxicology. Toxicol Sci. 2008 Nov;106(1):5–28.

14. Kelly WG, Fire A. Chromatin silencing and the maintenance of a functional germline in Caenorhabditis elegans. Development. 1998 Jul;125(13):2451–6.

15. Boyd WA, McBride SJ, Freedman JH. Effects of Genetic Mutations and Chemical Exposures on Caenorhabditis elegans Feeding: Evaluation of a Novel, High-Throughput Screening Assay. PLOS ONE. 2007 Dec 5;2(12):e1259.

16. Boyd WA, Smith MV, Kissling GE, Freedman JH. Medium- and high-throughput screening of neurotoxicants using C. elegans. Neurotoxicology and Teratology. 2010 Jan 1;32(1):68–73.

17. Stiernagle T. Maintenance of C. elegans. WormBook [Internet]. 2006 [cited 2019 Jan 30]; Available from: http://www.wormbook.org/chapters/www_strainmaintain/strainmaintain.html

Figure Legends

Figure 1: Characterization of chemical epigenetic reporter system on P0 generation

A: brightfield images of *c. elegans* germline (left panels), GFP (FITC) images showing a negative germline (top right) and positive germline (bottom right). Red arrows indicate somatic cells. Scale bar = 50μm. B: table showing percentage of germline GFP positive worms for NL2507 and PD7271 strains at 20ºC and 25°C. N=3, 30 worms each. C: Percentage germline GFP expression assessment of 24-hour exposures of two strains to histone modifying chemicals. N=2, 30 worms each. D: Percentage germline GFP expression assessment of valproic acid in NL2507 strain for 48 hours (left) and 65 hours (right). N=4-5, 30 worms each. E: Conditions tested with PD7271 and NL2507 including maintenance temperature, exposure temperature, and exposure time. Red indicates strain and conditions chosen as standard for all of the experiments that followed. F: Validation of histone modifying chemicals using standard parameters seen in E in a P0 population. Chemicals grouped based on expected chromatin effect. Chemicals are grouped based on their suspected chromatin effect: active (green), repressive (red) or carrying pleiotropic activity (grey). Unless indicated otherwise, all chemicals were tested at 100μM. N=5-9, 25 worms each, *P≤0.05, ****P≤0.0001. One way ANOVA,Sidak correction. All data are represented as mean +/- SEM.

Figure 2: Transgenerational effects of HDAC inhibitor in *C. elegans*

A: P0 exposure paradigm, showing multigenerational and transgenerational categorization. B: percentage GFP expression of HDAC inhibotors Sodium butyrate and Valproic acid, following generations from P0 to F3. N=5, 30 worms each, *P≤0.05, **P≤0.01 ***P≤0.001. One-way ANOVA, Sidak correction. All data are represented as mean +/- SEM.

Figure 3: Following transgenerational heritability effects

A: Diagram showing how to follow heritability of effects after direct chemical exposure. Selection and separation of GFP positive and GFP negative worms done at P0, then their offspring is followed until the F3. B: Transgenerational germline GFP expression analysis of HDAC inhibitors, following separated populations based on P0 expression. N=5, 30 worms each. C: GFP positive NL2507 strain worm at 40X (germline circled in white). D: GFP 'super bright' positive NL2507 strain worm at 40X (germline circled in white). Scale bar = 50μm. E: Percentage germline GFP expression in F1 generation after HDAC inhibitor exposure. Red line indicates percentage of super bright worms within the positive population N=3, 30 worms each.

Figure 4: Validation of chemical epigenetic reporter system with environmental toxicants

Transgenerational validation of epigenetic toxicants with NL2507 strain, P0 (left) and F3 (right). . N=5-10, 30 worms each, *P≤0.05, **P≤0.01 ***P≤0.001. One way ANOVA,Sidak correction. All data are represented as mean +/- SEM.

Figure 1.

A

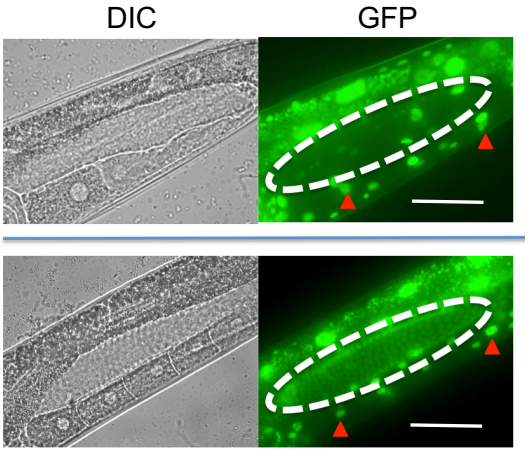

B

Strain/Temp	25°C	20°C
NL2507	21	10
PD7271	10	7

C

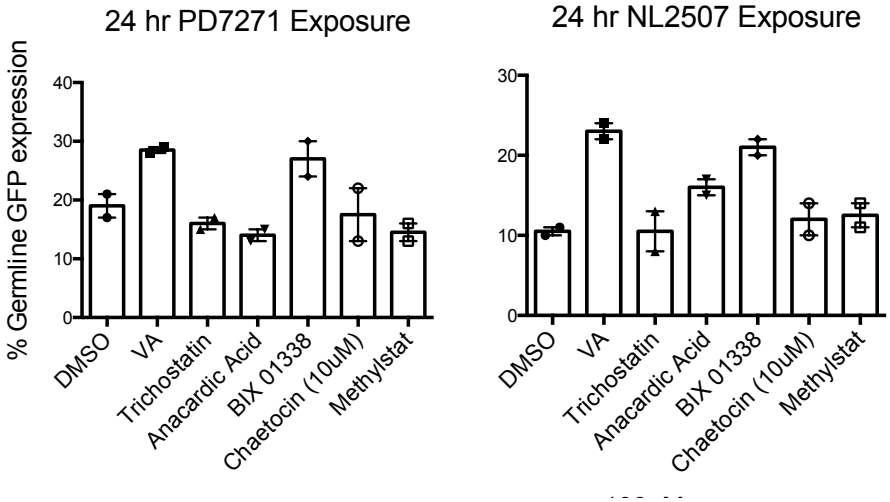

D

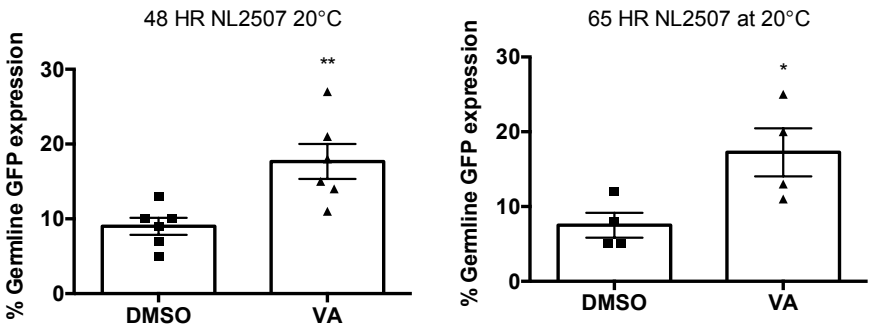

Figure 1 (continued)

E

Strain	Maintenance Temperature (°C)	Exposure Temperature (°C)	Exposure Time (hrs)
PD7271	**20**	**20**	24
NL2507	22.5	22.5	**48**
	25	25	65
	27	27	72

F

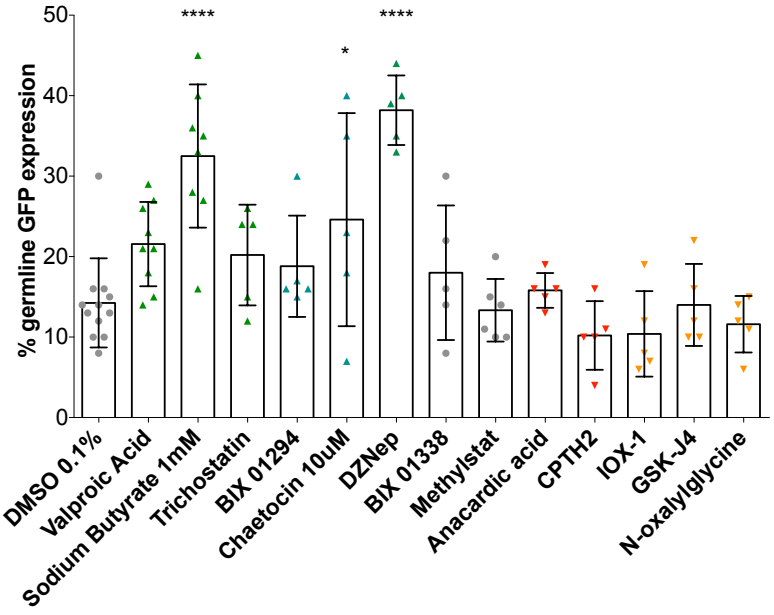

Figure 2.

A

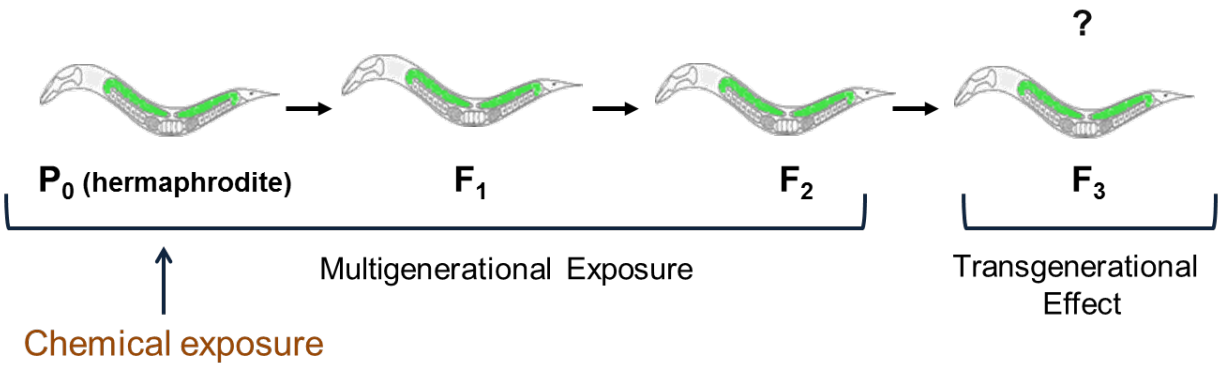
?
P0 (hermaphrodite)
F1
F2
F3
Multigenerational Exposure
Transgenerational Effect
Chemical exposure

B

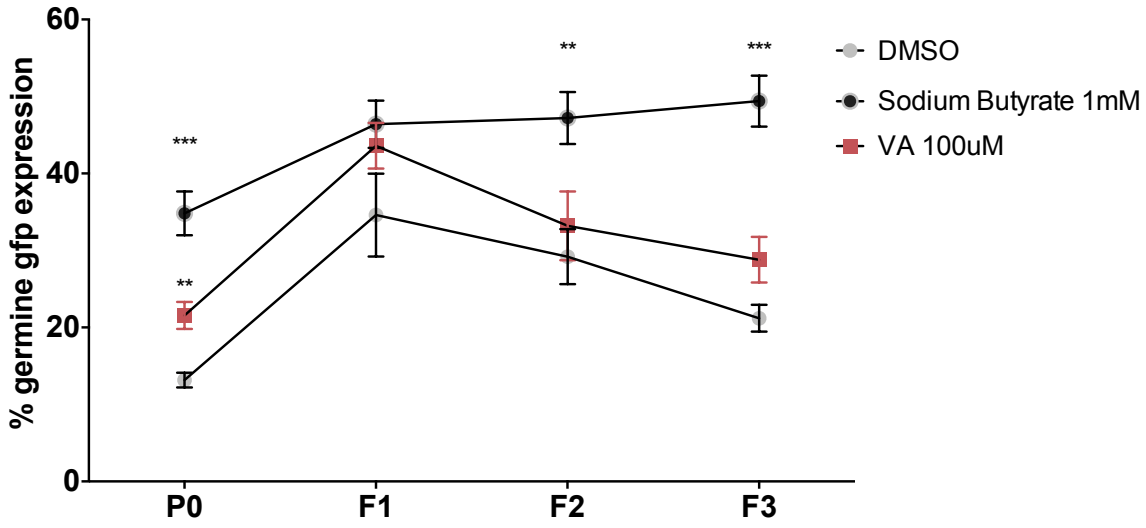
% germine gfp expression
60
40
20
0
P0
F1
F2
F3
***
**
**
***
DMSO
Sodium Butyrate 1mM
VA 100uM

Figure 3.

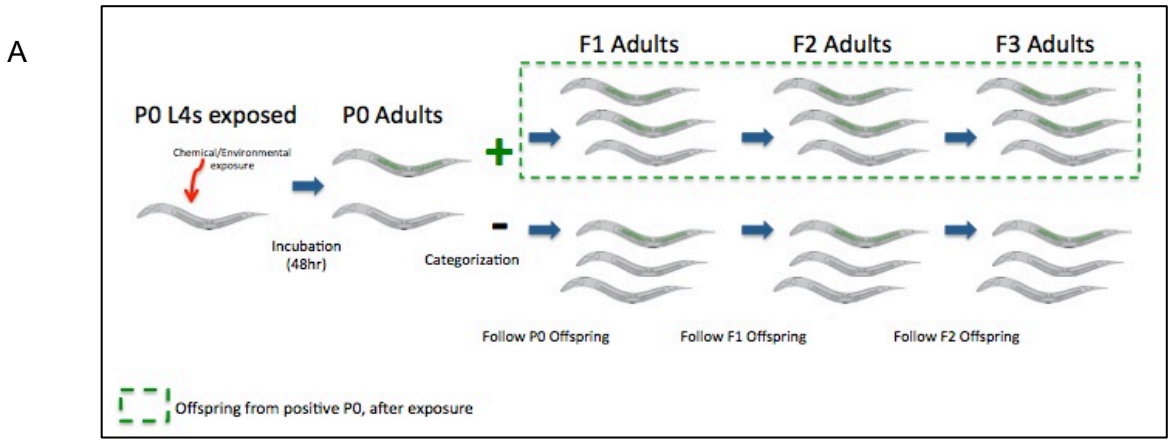
A
F1 Adults
F2 Adults
F3 Adults
P0 L4s exposed
P0 Adults
Chemical/Environmental exposure
Incubation (48hr)
Categorization
Follow P0 Offspring
Follow F1 Offspring
Follow F2 Offspring
Offspring from positive P0, after exposure

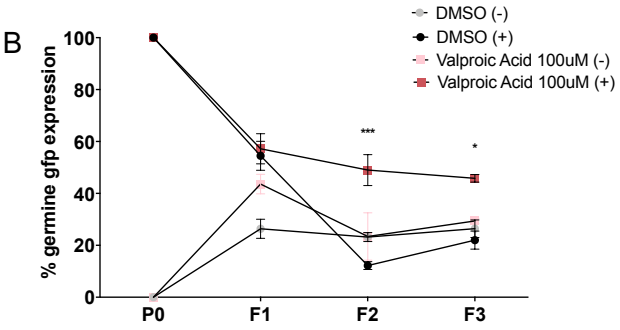
B
DMSO (-)
DMSO (+)
Valproic Acid 100uM (-)
Valproic Acid 100uM (+)
% germine gfp expression
P0
F1
F2
F3

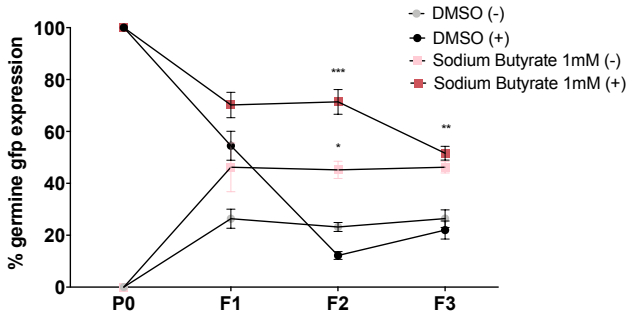
DMSO (-)
DMSO (+)
Sodium Butyrate 1mM (-)
Sodium Butyrate 1mM (+)
% germine gfp expression
P0
F1
F2
F3

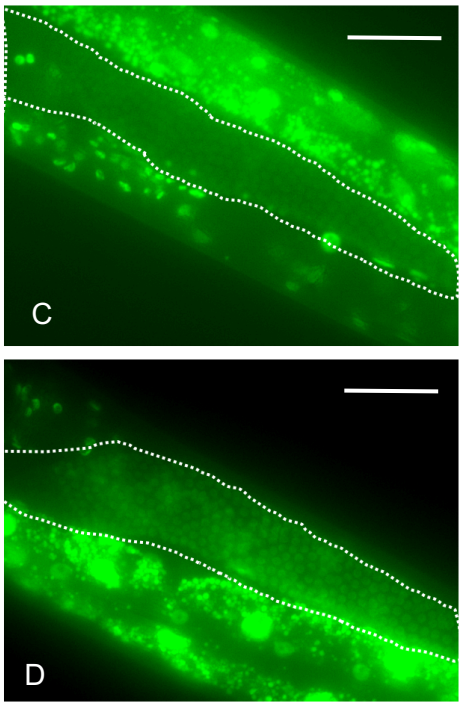
C
D

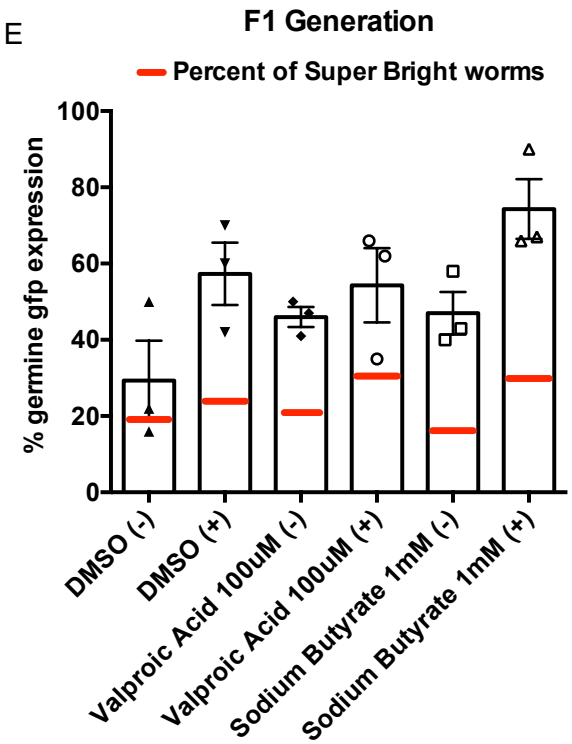
E
F1 Generation
Percent of Super Bright worms
% germine gfp expression
DMSO (-)
DMSO (+)
Valproic Acid 100uM (-)
Valproic Acid 100uM (+)
Sodium Butyrate 1mM (-)
Sodium Butyrate 1mM (+)

Figure 4.

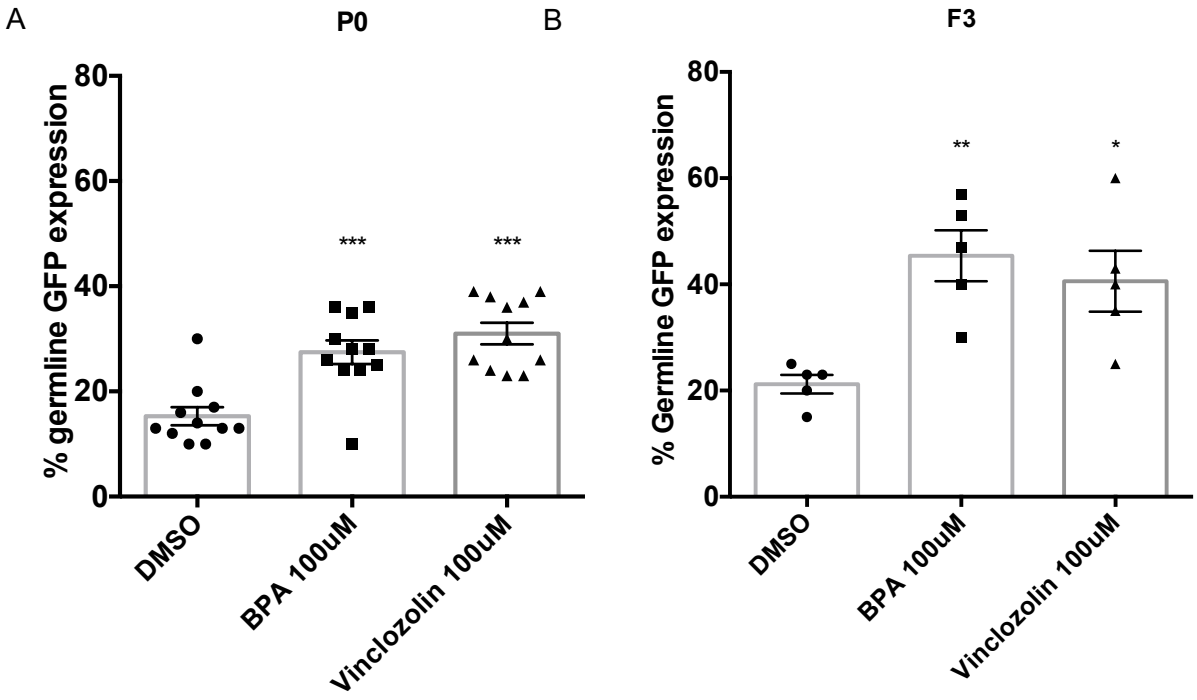
A
P0
B
F3
% germline GFP expression
% Germline GFP expression
0
20
40
60
80
***
***
**
*
DMSO
BPA 100uM
Vinclozolin 100uM
DMSO
BPA 100uM
Vinclozolin 100uM

CHAPTER 3

The memory of environmental chemical exposure in *c. Elegans*

Is dependent on the jumonji demethylases *jmjd-2* and *jmjd-3/utx-1*

Introduction

The identification of a proper epigenetic reporter allowed us to conduct further experiments on BPA for both its effects on the epigenome and transgenerational phenotypes. Previous studies on BPA have revealed that developmental exposure to BPA can change offspring phenotype by altering the epigenome, specifically, decreased DNA methylation (1). DNA methylation (CpG methylation) was also altered in pre-adolescent girls, where higher BPA concentrations were associated with decreased methylation. The decreased DNA methylation was observed various genes involving immune function and metabolism, showing the possibility of affecting both health and development (2). BPA not only affects DNA methylation, but also histone modifications, as seen in the study by Trapphoff et al (3). Their studies showed how BPA exposure caused a reduction in concentration of H3K9me3 in germinal vesicle oocytes. The literature clearly indicated the effects BPA exposures can have on the epigenome in various models, but the question remained on its effects on later generations. With our epigenetic reporter, we sought to answer the question of BPA's transgenerational effects and the mechanisms behind them.

References

1. Dolinoy DC, Huang D, Jirtle RL. Maternal nutrient supplementation counteracts bisphenol A-induced DNA hypomethylation in early development. Proc Natl Acad Sci USA. 2007;104:13056–13061.

2. Kim JH, Rozek LS, Soliman AS, et al. Bisphenol A-associated epigenomic changes in prepubescent girls: a cross-sectional study in Gharbiah, Egypt. Environ Health. 2013;12:33.

3. Trapphoff T, Heiligentag M, Hajj NE, Haaf T, Eichenlaub-Ritter U. Chronic exposure to a low concentration of bisphenol A during follicle culture affects the epigenetic status of germinal vesicles and metaphase II oocytes. Fertil Steril. 2013;100:1758. e1–1767.e1.

Cell Reports

Article

The Memory of Environmental Chemical Exposure in *C. elegans* Is Dependent on the Jumonji Demethylases *jmjd-2* and *jmjd-3/utx-1*

Graphical Abstract

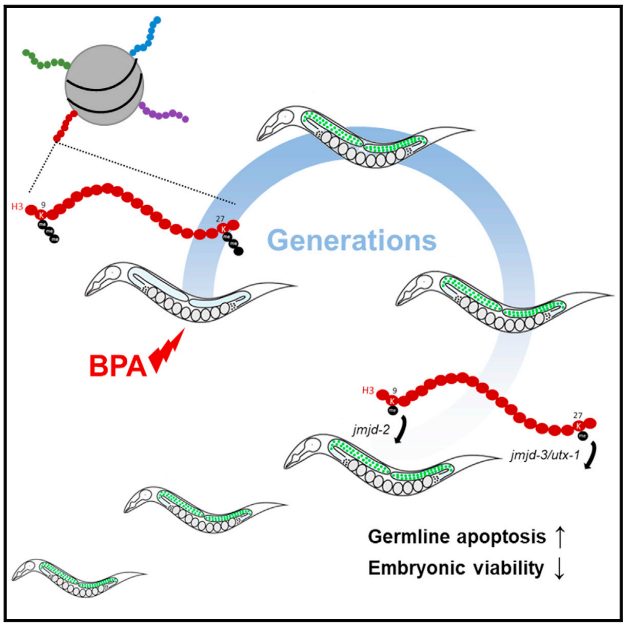

Authors

Jessica Camacho, Lisa Truong, Zeyneb Kurt, ..., Matteo Pellegrini, Xia Yang, Patrick Allard

Correspondence

pallard@ucla.edu

In Brief

Little is known about the mechanisms of inheritance of artificial environmental exposures. Camacho et al. describe the transgenerational reproductive dysfunctions caused by ancestral exposure to the model environmental compound Bisphenol A, and they provide a role for the regulation of repressive histone marks by histone demethylases in this process.

Highlights

- Bisphenol A elicits a 5-generation germline array desilencing effect in *C. elegans*
- The desilencing response tracks with germline apoptosis and embryonic lethality
- Ancestrally exposed F3 germlines show a dramatic reduction in H3K9me3 and H3K27me3
- JMJD-2 and JMD-3/UTX-1 demethylases are required for BPA's transgenerational effects

Data and Software Availability

GSE113187
GSE113266

Camacho et al., 2018, Cell Reports *23*, 2392–2404
May 22, 2018
https://doi.org/10.1016/j.celrep.2018.04.078

OPEN ACCESS
CellPress

Cell Reports
Article

The Memory of Environmental Chemical Exposure in *C. elegans* Is Dependent on the Jumonji Demethylases *jmjd-2* and *jmjd-3/utx-1*

Jessica Camacho,[1] Lisa Truong,[2] Zeyneb Kurt,[3] Yen-Wei Chen,[1] Marco Morselli,[4] Gerardo Gutierrez,[1,5] Matteo Pellegrini,[4] Xia Yang,[1,3,6,7,8] and Patrick Allard[1,8,9,10,*]

[1]Molecular Toxicology Interdepartmental Program, University of California, Los Angeles, Los Angeles, CA 90095, USA
[2]Human Genetics and Genomic Analysis Training Program, University of California, Los Angeles, Los Angeles, CA 90095, USA
[3]Department of Integrative Biology and Physiology, University of California, Los Angeles, Los Angeles, CA 90095, USA
[4]Molecular, Cell and Developmental Biology Department, University of California, Los Angeles, Los Angeles, CA 90095, USA
[5]Department of Environmental and Occupational Health, California State University, Northridge, CA 91330, USA
[6]Bioinformatics Interdepartmental Program, University of California, Los Angeles, Los Angeles, CA 90095, USA
[7]Institute for Quantitative and Computational Biosciences, University of California, Los Angeles, Los Angeles, CA 90095, USA
[8]Molecular Biology Institute, University of California, Los Angeles, Los Angeles, CA 90095, USA
[9]Institute for Society and Genetics, University of California, Los Angeles, Los Angeles, CA 90095, USA
[10]Lead Contact
*Correspondence: pallard@ucla.edu
https://doi.org/10.1016/j.celrep.2018.04.078

SUMMARY

How artificial environmental cues are biologically integrated and transgenerationally inherited is still poorly understood. Here, we investigate the mechanisms of inheritance of reproductive outcomes elicited by the model environmental chemical Bisphenol A in *C. elegans*. We show that Bisphenol A (BPA) exposure causes the derepression of an epigenomically silenced transgene in the germline for 5 generations, regardless of ancestral response. Chromatin immunoprecipitation sequencing (ChIP-seq), histone modification quantitation, and immunofluorescence assays revealed that this effect is associated with a reduction of the repressive marks H3K9me3 and H3K27me3 in whole worms and in germline nuclei in the F3, as well as with reproductive dysfunctions, including germline apoptosis and embryonic lethality. Furthermore, targeting of the Jumonji demethylases JMJD-2 and JMJD-3/UTX-1 restores H3K9me3 and H3K27me3 levels, respectively, and it fully alleviates the BPA-induced transgenerational effects. Together, our results demonstrate the central role of repressive histone modifications in the inheritance of reproductive defects elicited by a common environmental chemical exposure.

INTRODUCTION

The elicitation and inheritance of phenotypes from environmental cues have been the subject of intense research and debate. Best understood is the transfer of biological information triggered by natural exposures, such as temperature, hyperosmotic stress, diet, or starvation, thanks to research advances in a variety of model systems from plants to rodents (reviewed in Heard and Martienssen, 2014). Recent reports have shown that the heritability of effects elicited by such natural cues across generations is conditioned by changes in the epigenome, or the molecular tags that alter gene expression and that are mitotically and/or meiotically heritable but do not entail a change in DNA sequence (Wu and Morris, 2001). These mechanisms include small RNA-based pathways (Gapp et al., 2014; Rechavi et al., 2014; Zhong et al., 2013) as well as through the regulation of the complex collection of covalent modifications of histone proteins (Gaydos et al., 2014; Greer et al., 2014; Kishimoto et al., 2017; Klosin et al., 2017; Siklenka et al., 2015). By contrast, the transgenerational inheritance of man-made environmental chemicals has remained controversial, particularly in mammalian settings. Several rodent studies have indicated that a one-generation parental (P)0 exposure to compounds, such as the fungicide Vinclozolin (Anway et al., 2005), or to mixtures of plastic compounds, such as Bisphenol A (BPA) and phthalates (Manikkam et al., 2013), is sufficient to cause a transgenerational decrease in the number and quality of germ cells in F3 and F4 adults, and it correlates with an alteration of DNA methylation patterns (Anway et al., 2005, 2006). However, some of these studies have been challenged (Heard and Martienssen, 2014; Hughes, 2014), have not provided a clear mechanism of inheritance, and have not explored the involvement of other epigenetic marks besides DNA methylation, such as histone modifications.

The nematode *Caenorhabditis elegans* has proven to be a valuable model system to study the effects of environmental exposures on the epigenome due to its ability to respond to a variety of stressors (Kishimoto et al., 2017; Klosin et al., 2017; Rechavi et al., 2014; Rudgalvyte et al., 2017). Here, we exploited the tractability of *C. elegans* to study the transgenerational impact of chemical exposure on reproductive function and dissect its underlying mechanisms of inheritance. These experiments were

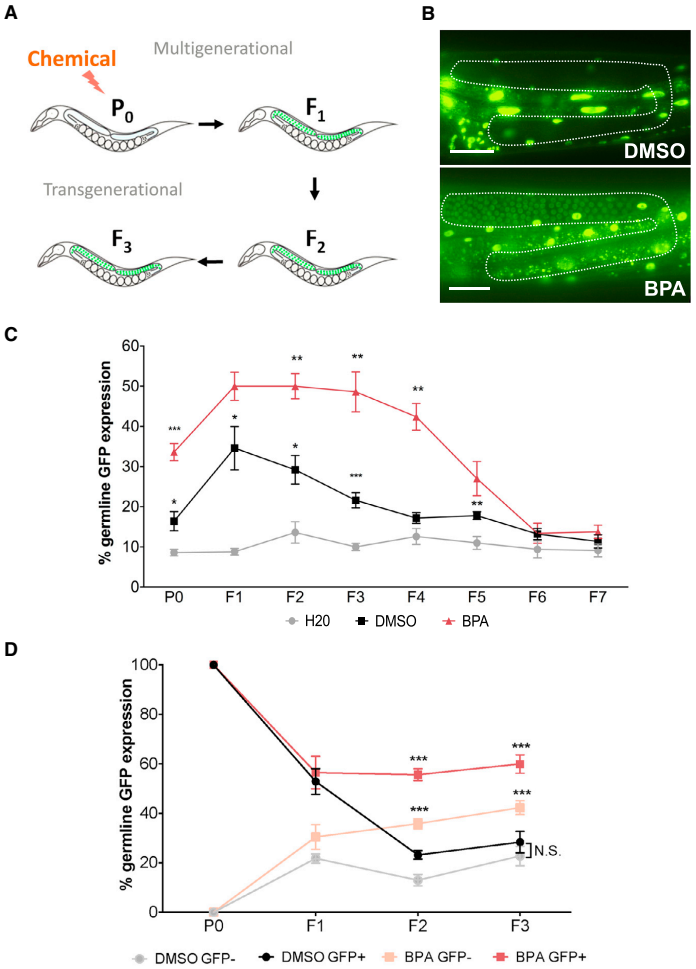

Figure 1. BPA Exposure Elicits a Transgenerational Desilencing of a Repetitive Array

(A) Exposure scheme. Nematodes are exposed to the chemicals of interest for 48 hr at the parental (P0) generation. Worms carrying the integrated array *pkIs1582* [*let-858*::GFP; *rol-6*(*su1006*)] express GFP in all somatic nuclei but silence the array in the germline. This strain is used to monitor the array desilencing over multiple generations.

(B) Representative example of silenced (top) and desilenced (bottom) *pkIs1582* array expression in F3 germlines (dashed lines). Scale bar, 50 μm.

(C) Percentage of worms displaying germline desilencing (y axis) at each generation (x axis). n = 5–10, 30 worms each; *p ≤ 0.05, **p ≤ 0.01, and ***p ≤ 0.001. Significance is indicated for BPA versus DMSO above the BPA line and DMSO versus water above the DMSO line.

(D) Lineage analysis of the germline desilencing response. Worms were sorted following exposure at the P0 generation based on their germline GFP expression. Their progeny was then followed and examined for 3 additional generations. n = 5–10, 30 worms each; ***p ≤ 0.001. BPA is compared to DMSO within each GFP status category (e.g., BPA/GFP+ versus DMSO/GFP+). All data are represented as mean ± SEM.

greatly facilitated by the nematode's short generation time, approximately 4 days at 20°C; its well-characterized distribution and regulation of chromatin marks (Bessler et al., 2010; Ho et al., 2014; Liu et al., 2011); and its ability to silence repetitive transgenes in the germline via repressive histone modifications in a fashion similar to the silencing of repetitive elements in mammalian germ cells (Kelly and Fire, 1998; Liu et al., 2014). Using these features, we investigated the mechanism of transgenerational inheritance following exposure to the model environmental chemical BPA. BPA is a widely used, high-production volume plastic manufacturing chemical highly prevalent in human samples (Vandenberg et al., 2010). We show that ancestral BPA exposure causes a histone 3, lysine 9 (H3K9) and a histone 3, lysine 27 (H3K27) trimethylation-dependent transgenerational chromatin-desilencing response in the germline that spans five generations and is associated with germline dysfunction and elevated progeny lethality.

RESULTS

Germline Transgene Desilencing following Chemical Exposure

To capture single, multi-, and transgenerational environmental effects stemming from chemical exposure, we used a germline desilencing reporter (Kelly et al., 1997). The assay that we developed (Figure 1A) is based on the strain NL2507 carrying an integrated low-complexity, highly repetitive array composed of a transgene coding for a fusion product between nuclear-localized LET-858 and GFP (*pkIs1582[let-858::GFP; rol-6(su1006)]*). This transgene is expressed in somatic cells, but it is transcriptionally silenced in the germline (Figure 1B) via accumulation of the repressive marks H3K9me3 and H3K27me3 (Kelly and Fire, 1998; Schaner and Kelly, 2006).

We first tested the reporter NL2507 strain in a chemical assay by using a variety of well-characterized inhibitors of chromatin-modifying enzymes (Figure S1). All drug exposures were performed at the P0 generation for 48 hr, encompassing the window of L4 stage to day 1 of adulthood. Drug responses were compared to the vehicle DMSO in the context of which a low rate of desilencing is observed (14.3% ± 1.6%). Following treatment with all tested inhibitors of H3K9 or H3K27 demethylases,

of non-selective methyltransferases or demethylases, as well as of histone acetyltransferases, the transgene expression remained silenced at levels comparable to the DMSO control. Conversely, HDAC inhibitors or methyltransferase inhibitors against either H3K9 or H3K27 all led to an increase in *pkIs1582* germline expression, with exposure to the class I HDAC inhibitor sodium butyrate and the SAM and EZH2 inhibitor 3-Deazaneplanocin A (DZnep) showing the highest levels of desilencing at P0, 32.5% ± 3.1% and 38.2% ± 1.9%, respectively ($p \leq 0.0001$ for both). Together, these results indicate that the desilencing of the *pkIs1582* array may serve as a sensitive and relevant indicator of chromatin mark-regulated transcriptional modulation.

BPA Exposure Causes a Heritable, Transgenerational Chromosomal Array-Desilencing Response

BPA was chosen as a test compound in the array-desilencing assay based on several lines of evidence that include changes in H3K27 histone methyltransferase Enhancer of Zeste homolog 2 (EZH2) expression (Bhan et al., 2014) and decreases in H3K9me3 levels in post-natal mouse oocytes (Trapphoff et al., 2013) and in H3K9 and H3K27 methylation levels in a variety of somatic cell types (Doherty et al., 2010; Singh and Li, 2012; Yeo et al., 2013).

First, we tested a range of BPA concentrations (10, 50, 100, and 500 μM), chosen based on previous dose-response analyses (Chen et al., 2016), to identify the lowest dose that led to a maximal desilencing effect. We initially performed the exposures at a single generation (P0) at L4 stage for 48 hr. We observed a dose-response relationship of the germline array desilencing across generations, reaching saturation at 100 μM (45.0% ± 3.3% desilencing at the F3, $p \leq 0.001$) (Figure S2A). We also tested additional 48-hr exposure windows, including from L1 to L4 (Figure S2B) and from day 0 of adulthood (24 hr post-L4) to day 2 (Figure S2C). In all cases, we observed a significant desilencing of the germline array in the F3, although the generational kinetics varied between exposure windows and none reached the maximum F3 desilencing levels achieved by the L4-to-day 1 exposure window (Figure S2A). Thus, for all subsequent experiments, we exposed the worms to a single 100-μM BPA dose from L4 to day 1. This external dose is below previously characterized *C. elegans* doses measured by gas chromatography-mass spectrometry (GC-MS) to lead to an internal BPA concentration within human physiological range (Chen et al., 2016).

We then examined the rate of array desilencing over six generations following the single P0 generation BPA exposure at 100 μM (Figure 1C). The solvent control DMSO led to a pronounced elevation in desilencing in F1 animals (34.6% ± 5.4% of worms display GFP expression in their germline) compared to water alone (8.6% ± 0.8%). However, GFP levels in the DMSO group sharply declined after the F1 generation and were statistically indistinguishable from the water control at the F4 generation. This effect of DMSO is likely due to its described positive activity in DNA relaxation, transcription enhancement, and promotion of an active chromatin state (Iwatani et al., 2006; Juang and Liu, 1987; Kim and Dean, 2004). By contrast, BPA exposure led to a dramatic increase in desilencing in the F1 generation (50.0% ± 3.5%). This BPA-induced desilencing rate was consistently higher than DMSO's and remained that way until the F5 generation. These results therefore indicate a potent transgenerational desilencing response stemming from BPA exposure and spanning 5 generations (P0–F4).

To determine whether most of the desilencing effect observed in the first transgenerational (F3) generation is primarily caused by descendants of strong P0 responders, we performed a series of lineage studies where individual P0 worms were segregated based on their germline GFP expression following BPA or DMSO exposure. Worms that showed germline desilencing at P0 following BPA exposure gave rise to F1, F2, and F3 progenies with a high rate of desilencing, nearing 60% (Figure 1D). By contrast, DMSO-exposed animals, whether silenced or desilenced at P0, showed a reduced rate of desilencing in the F2 and F3 generations, nearing 20%. Surprisingly, BPA-treated but GFP-negative P0 worms gave rise to progeny showing a higher rate of desilencing at each subsequent generation, such that there was a statistically significant difference when compared to DMSO in the F2 and F3 generations. In the latter, the proportion of descendants of BPA-exposed but GFP-negative P0s showing germline desilencing reached 42.3% ± 2.8% ($p \leq 0.01$ versus DMSO/GFP−). Interestingly, the mating of ancestrally exposed F1 hermaphrodites with unexposed males did not rescue the germline desilencing response, indicating that the primary mode of inheritance of BPA's effect is through the female germline (Figure S2D).

Collectively, these findings identify a matrilineal transgenerational inheritance of a repetitive array-desilencing response that is only partially conditioned by the ancestral (P0) response to BPA exposure.

BPA Exposure Causes a Transgenerational Alteration of the Germline Transcriptome

To investigate the impact of ancestral BPA exposure on the germline and distinguish it from that of DMSO, which also led to a mild transgenerational germline desilencing in the F3 compared to water, we performed RNA sequencing (RNA-seq) analysis on isolated F3 germlines. We identified a total of 264 transcripts that were differentially up- or downregulated at $p \leq 0.05$ in F3 germlines ancestrally exposed to BPA compared to DMSO, with 152 transcripts having a fold induction ≤ 0.5 or ≥ 1.5 (Table S1; Figure S3A). There was little overlap between the transcripts that were differentially expressed in all 3 groups, BPA versus DMSO, BPA versus water, and DMSO versus water (Figure S3B), suggesting that DMSO's transgenerational impact on the germline transcriptome is mostly distinct from that of BPA. A gene ontology analysis of the functional categories represented by the differentially expressed transcripts also highlighted the lack of overlap between the different treatment group comparisons. Interestingly, however, the second most represented functional category in the BPA versus DMSO group was reproduction, which was not represented in the DMSO versus water group (Figure S3C). This category includes 61 genes, many of them normally expressed in the germline tissue and essential for germline function (Table S2). These results therefore suggest that ancestral BPA exposure may deregulate reproductive processes by altering the germline transcriptome.

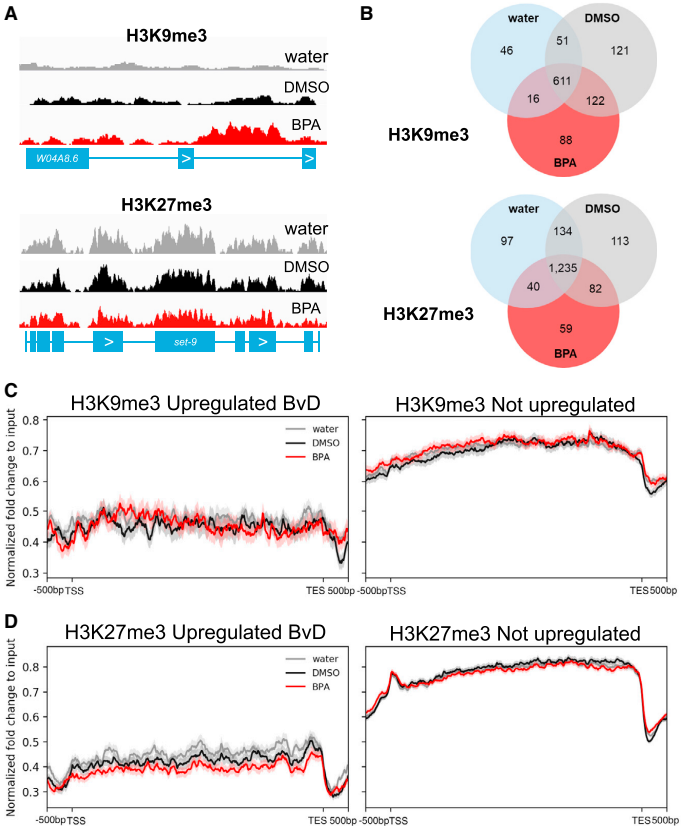

Figure 2. BPA-Induced Transgenerational Reduction in H3K9me3 and H3K27me3 Identified by ChIP-Seq

(A) Examples of ChIP-seq gene plots for H3K9me3 and H3K27me3 from F3 nematodes.

(B) Venn diagram from genes with peak calling in each of the treatment groups.

(C) Average H3K9me3 histone modification fold enrichment signals from gene bodies of either silenced upregulated genes (left panel) or silenced non-upregulated genes (right panel) after BPA treatment. Lightly shaded regions indicate the SE.

(D) Average H3K27me3 histone modification fold enrichment signals from gene bodies of either silenced upregulated genes (left panel) or silenced non-upregulated genes (right panel) after BPA treatment. Lightly shaded regions indicate the SE.

Ancestral BPA Exposure Leads to a Deregulation of Repressive Histone Marks in F3 Nematodes

Several recent reports in *C. elegans* have implicated various histone modifications as important mediators of a variety of environmental effects across generations (Kishimoto et al., 2017; Klosin et al., 2017). We therefore assessed whether BPA exposure in P0 worms could lead to observable changes in the chromatin of F3 worms. To this aim, we performed chromatin immunoprecipitation sequencing (ChIP-seq) in whole adult worms at the F3 generation ancestrally exposed to BPA, DMSO, and water. Just as for the RNA-seq analysis, these experiments were performed on a large population of worms that were not selected based on their GFP expression. We focused our analysis on two repressive marks, H3K9me3 and H3K27me3, which have both been previously implicated in chromatin silencing in the germline of a wide range of species as well as in the repression of low-complexity transgenes in the *C. elegans* germline (Bessler et al., 2010; Greer et al., 2014; Leung et al., 2014; Liu et al., 2014; Schaner and Kelly, 2006; Towbin et al., 2012).

We first mined the ChIP-seq data to identify genes with significantly altered H3K9me3 and H3K27me3 levels (see the Experimental Procedures; Figures 2A and 2B). Among the three conditions, water, DMSO, and BPA, we identified between 3,740 and 4,951 broad peaks for H3K9me3 and between 19,019 and 21,741 for H3K27me3 (Table S3). A total of 1,055 and 1,780 genes were associated with broad peak calls, i.e., showed enrichment in their gene bodies, for H3K9me3 and H3K27me3, respectively. The majority of these peak calls were shared among all three treatment groups, although the BPA treatment group generated 88 and 59 unique peaks for H3K9me3 and H3K27me3, respectively (Figure 2B). The gene ontology (GO) analysis of biological processes at false discovery rate (FDR) < 0.05 and $p < 0.001$ for the genes associated with a loss of H3K27me3 broad peaks in BPA samples compared to DMSO confirmed the relevance of the epigenomic effect detected, as the second most prominent GO category was related to the response to steroid hormone stimulus, in line with BPA's well-described estrogenic activity (Table S4).

Next we compared the ChIP-seq and RNA-seq datasets by examining the levels of H3K9me3 and H3K27me3 under all 3 treatment conditions in genes that either had a low expression level in DMSO (first quartile, i.e., silenced genes) and were not upregulated or were upregulated >2-fold based on the RNA-seq data. As expected, we found that upregulated genes had on average 40%–50% lower H3K9me3 and H3K27me3 compared to their not-upregulated counterparts (Figures 2C and 2D). The levels and distributions of the marks were consistent with their described patterns in the *C. elegans* larval chromatin, where both H3K9me3 and H3K27me3 predominantly occupy the gene body of silenced genes (Ho et al., 2014). Comparing the three treatment groups, we did not observe a difference in H3K9me3 based on expression levels, perhaps due to

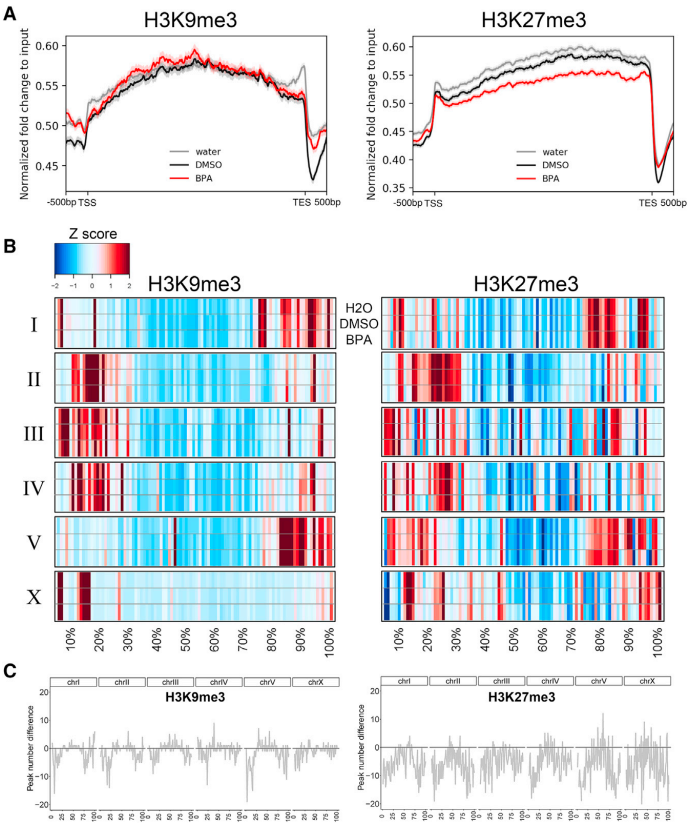

Figure 3. BPA Treatment Causes Transgenerational Intra-chromosomal Redistribution of Histone Modifications

(A) Average H3K9me3 (left) and H3K27me3 (right) histone modification fold enrichment signals from gene bodies of all genes. Shaded regions indicate SE.

(B) Heatmap of averaged H3K9me3 (left) and H3K27me3 (right) histone modification fold enrichment signals in 100 sub-regions across all chromosomes. *Z* scores were calculated on averaged values in each chromosome and sample.

(C) Difference in unique peak-calling numbers between BPA and DMSO from H3K9me3 (left) and H3K27me3 (right) along all chromosome sub-regions. The y axis indicates unique peak numbers calculated by BPA minus DMSO by region.

the tissue sources used for the two datasets (whole worms for ChIP-seq and isolated germlines for RNA-seq). However, we observed a decrease in H3K27me3 in the BPA treatment group compared to DMSO and water for genes that were upregulated (Figure 2D, lightly shaded area indicates SE). These results were similar for all genes, irrespective of expression level, where H3K27me3 was significantly reduced in the gene body compared to DMSO and water groups (Figure 3A).

Finally, we asked whether ancestral BPA exposure might not only affect H3K9me3 and H3K27me3 gene body levels but also their distribution along the chromosome axes. To this aim, we calculated the average fold enrichment of each mark over input by 1% increments along all 6 chromosomes. The data were normalized using a *Z* score for each individual chromosome and treatment group to allow the visualization of the marks' redistribution (Figure 3B). For each 1% increment, we also identified the number of peaks that were present in BPA but absent in DMSO (Figure 3C). These two complementary chromosome-wide analyses revealed a reduction of both marks from the distal chromosomal regions, largely heterochromatic (Garrigues et al., 2015), and a slight enrichment in the chromosome centers when comparing BPA to DMSO (Figures 3B and 3C). It also suggested a decrease of the marks' levels on the X chromosome. We validated the decrease in the levels of the marks by performing a multiplex histone post-translation modification (PTM) quantitation assay on pooled F3 whole-worm extracts (Table S5). The assay revealed a 25%–33% decrease in H3K9 mono-, di-, and trimethylation and a more pronounced 29%–56% decrease in H3K27 di- and trimethylation at the F3 generation in BPA-exposed P0 nematodes compared to DMSO. Conversely, another histone modification, H3K36me3, remained largely unchanged. Together, these results indicate a potent transgenerational impact of BPA on the chromatin, altering both the levels of the two repressive marks H3K9me3 and H3K27me3 as well as their distribution along chromosomal axes.

Ancestral BPA Exposure Leads to a Deregulation of Repressive Histone in the Germline

A transgenerational effect implies that the epigenomic alterations described above must also occur in the germline in order to be inherited. We therefore performed immunofluorescence against H3K9me3 and H3K27me3 in dissected germlines of the NL2507 strain containing the integrated *pkIs1582* transgene at the F3, when desilencing is pronounced, and at the F7, when germline desilencing has returned to control levels. At the pachytene stage of the F3 germline, we observed significant 26% and 24% reductions in global H3K9me3 and H3K27me3 levels, respectively, between BPA and DMSO (Figures 4A and 4B). By contrast, no significant differences were observed between water and DMSO. A similar decrease of total nuclear levels of these marks was seen in the strain PD7271, where the transgene is episomally maintained (*ccEx7271*): 23.3% and 34.6% reductions for H3K9me3 and H3K27me3, respectively (Figure S4). At the F7 generation, the germline levels of H3K9me3 and

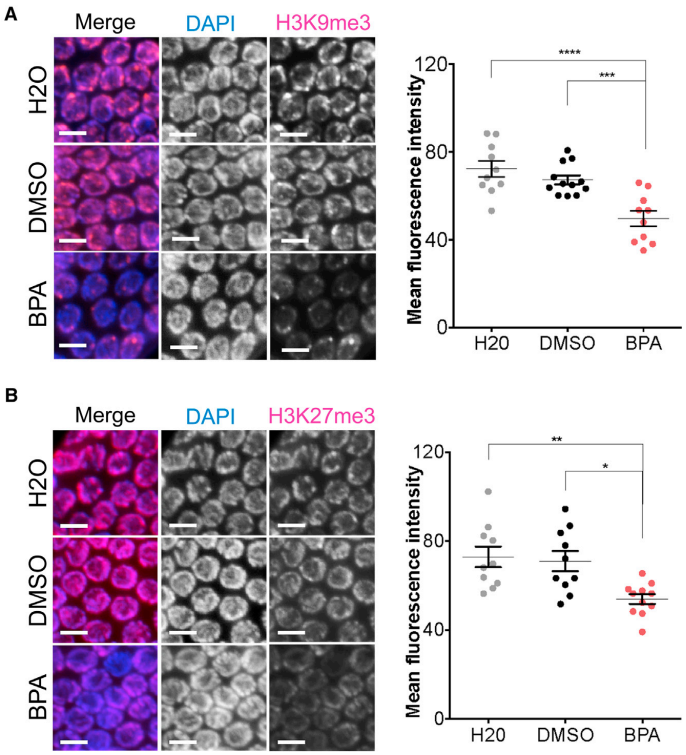

Figure 4. Ancestral BPA Exposure Decreases H3K9me3 and H3K27me3 Levels in F3 Germlines

(A and B) Immunofluorescence images of mid-to-late pachytene germline nuclei from F3 worms ancestrally exposed to DMSO or BPA and stained for H3K9me3 (A) or H3K27me3 (B). DAPI is represented in blue and the histone mark of interest in magenta in the merge. All images shown were selected representative images of the mean values obtained after quantification of all germline nuclei from that exposure group. The corresponding fluorescence intensity quantification is shown on the right panels. n = 11–12 worms, 10 nuclei per worm; *p ≤ 0.05, **p ≤ 0.01, ***p ≤ 0.001, and ****p ≤ 0.0001, one-way ANOVA with Sidak correction. Scale bar, 5 μm. All data are represented as mean ± SEM.

H3K27me3 in the BPA group were statistically indistinguishable from DMSO controls (Figure S5).

The use of the PD7271 *ccEx7271* array-bearing strain also allowed us to separately examine the levels of repressive modifications on the autosomes; the X chromosomes, which tend to lay apart from the rest of the chromosomes during the pachytene stage in hermaphrodites (Schaner and Kelly, 2006); and the extrachromosomal array (Figures 5A and 5B). We observed marked decreases in both H3K9me3 and H3K27me3 on autosomes (24.8% and 34.3%, respectively), X chromosomes (25.3% and 41.5%), and the extrachromosomal array (39.6% and 51.3%). We examined whether the trend toward a larger decrease of these marks on the X chromosomes compared to autosomes was significant by measuring the X:A ratio for each germline nucleus (Figure 5C). F3 germline nuclei showed a significant X:A ratio decrease in H3K27me3 levels when ancestrally exposed to BPA compared to DMSO (0.98 versus 1.09, respectively, a 10% decrease; p = 0.03), while H3K9me3 showed a trend toward a decreased X:A ratio between DMSO and BPA. Consistent with these results and with the described role of H3K27me3 in X silencing in the germline (Bender et al., 2006; Gaydos et al., 2012), we observed a modest but significant (p = 0.01) 2.36% increase in overall X-related genes with fragments per kilobase of transcript per million (FPKM) > 1 in our F3 germline RNA-seq data (Figure 5D).

Taken together, these experiments indicate a broad transgenerational impact on the germline chromatin of F3 nematodes not only confined to the repetitive arrays but also affecting the autosomes and the X chromosomes.

BPA Exposure Elicits a Transgenerational Increase in Embryonic Lethality and Germline Dysfunction

Next, we examined whether the transgenerational alteration of the germline chromatin was associated with reproductive defects. For these and all subsequent experiments, we chose to only compare BPA to DMSO, as BPA is dissolved in DMSO and the RNA-seq and ChIP-seq data indicated chromatin and expression BPA signatures distinct from those of DMSO. While the number of embryos produced was not dependent on ancestral exposure (Figure 6A), we observed a significant 85% (D = 3.83 and B = 7.07) increase in embryonic lethality in F3 worms ancestrally exposed to BPA when compared to DMSO (Figure 6B). We also examined the rate of embryonic lethality at the F7, a generation at which desilencing is not observed. Surprisingly, a trend between DMSO and BPA was still apparent even if it did not reach significance (86%, D = 3.58 and B = 6.67) (Figure 6B). The F3 embryonic lethality defect was not caused by the spurious expression of the *pkIs1582* transgene in the germline, as it was also observed in wild-type (N2) worms (Figure S6). Additionally, we assessed whether the increased embryonic lethality correlated with the transgene desilencing by separately assessing the embryonic survival of GFP-negative and GFP-positive F3 worms' progeny (Figure 6C). We observed a significantly higher level of embryonic lethality in the offspring of GFP-positive F3 worms ancestrally exposed to BPA when compared to both GFP-negative/BPA F3 offspring and GFP-positive/DMSO F3 offspring.

Finally, we monitored germline health by measuring the induction of germline apoptosis using acridine orange staining

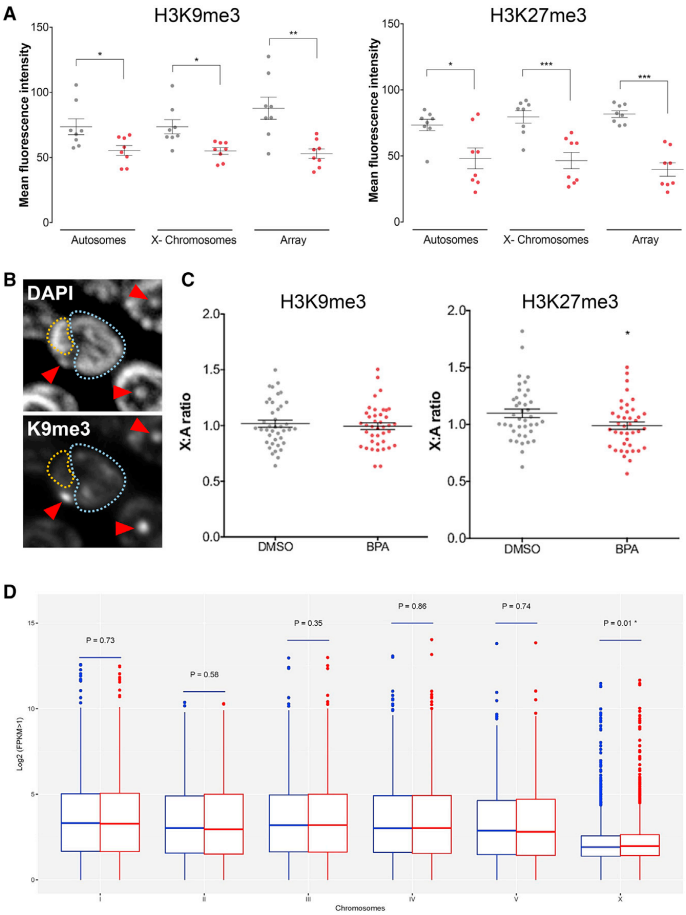

Figure 5. Ancestral BPA Exposure Leads to a Sharp Decrease in H3K9me3 and H3K27me3 on Autosomes, X Chromosomes, and an Extrachromosomal Array and an Up-regulation of X-Linked Genes

(A) Quantification of H3K9me3 and H3K27me3 levels on autosomes, X chromosomes, and an extrachromosomal array in the F3 generation following P0 exposure to either DMSO or BPA. Gray, DMSO; red, BPA. n = 8 worms, 5 nuclei per worm; *p $\leq$ 0.05, **p $\leq$ 0.01, and ***p $\leq$ 0.001.

(B) DAPI- (top) and H3K9me3- (bottom) stained nuclei. The colored dashed lines identify the autosomes (blue) and the X chromosomes (orange). The red arrowheads identify the extrachromosomal array that is enriched in H3K9me3.

(C) Fluorescence intensity quantification of H3K9me3 and H3K27me3 levels is shown on the right. Gray is the X:A ratio for DMSO and red for BPA. n = 8 worms, 5 nuclei per worm; *p $\leq$ 0.05.

(D) Gene expression data from dissected F3 germlines showing all transcripts with FKPM > 1 following ancestral DMSO (blue) or BPA (red) exposure. X-linked genes show a modest but significant overall 2.36% increase in expression (p = 0.01). All data are represented as mean ± SEM.

(Gartner et al., 2008) at the late prophase stage, when synapsis and recombination-dependent checkpoint activation results in programmed germline nuclear culling (Bhalla and Dernburg, 2005; Gartner et al., 2008). We observed a significant increase in germline apoptosis in F3 worms ancestrally exposed to BPA when compared to DMSO (Figures 6D and 6E), which was lost at the F7. Thus, together, these results show that ancestral BPA exposure elicits a clear transgenerational reproductive dysfunction effect. They also indicate that BPA-induced transgenerational effects mostly resolve by the F7.

Jumonji Histone Demethylase Activity Is Required for the Inheritance of BPA-Induced Transgenerational Effects

Since BPA exposure at the P0 generation was correlated with a decrease in repressive histone modifications in the germline of the F3 worms, we hypothesized that BPA's effects may be dependent on levels of these marks and on the activity of the enzymes that regulate them. This hypothesis was partially supported by the RNA-seq data from which 7 differentially expressed chromatin factors were identified: *sir-2.4*, ZK1127.3, *sop-2*, TO7E3.3, *met-2*, *jmjd-1.2*, and *set-26* (Table S1). MET-2, a SET domain histone H3 lysine 9 histone methyltransferase (HMTase) (Bessler et al., 2010), was significantly downregulated, while *set-26*, another H3K9 methyltransferase (Greer et al., 2014), was represented by two functionally equivalent transcript isoforms, one upregulated and one downregulated. Therefore, to functionally implicate the dysregulation of H3K9me3 and H3K27me3 in BPA's transgenerational outcomes, we attempted to rescue its effects by genetically or chemically modulating several histone demethylases after the initial P0 exposure but prior to the F3 (Figures 7A and S8A).

We first assessed whether the deregulation of repressive H3-lysine methylation marks by BPA is required for the transgenerational inheritance of BPA-induced effects. To this end, we used a feeding RNAi strategy to downregulate the expression of *jmjd-2* (H3K9me3/H3K36me3 histone lysine demethylase [KDM]) (Greer et al., 2014; Whetstine et al., 2006) or *jmjd-3/utx-1* (H3K27me3 KDM) (Agger et al., 2007), and we monitored two hallmarks of BPA's transgenerational effects, namely, the germline array desilencing as well as the increase in embryonic lethality. When compared to control RNAi, the downregulation of *jmjd-2* or *jmjd-3/utx-1* at the F1-to-F2 transition was sufficient to increase the levels of H3K9me3 and H3K27me3, respectively,

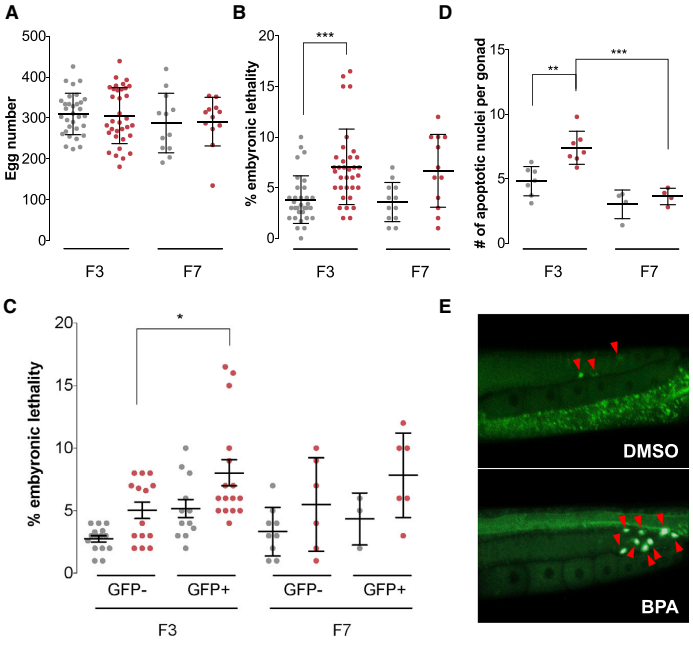

Figure 6. Transgenerational Impact of BPA on Fertility

(A) Number of eggs produced by F3 or F7 worms following P0 exposure to DMSO control (gray) or BPA (red).

(B) Percentage of lethality of embryos generated by F3 or F7 worms ancestrally exposed to either DMSO control or BPA. n = 23–33; ***p $\leq$ 0.001, two-way ANOVA.

(C) Embryonic lethality of F3 or F7 worms' progeny based on the GFP expression in the germline of F3 or F7 worms. n = 10; *p $\leq$ 0.05, two-way ANOVA.

(D) Number of apoptotic nuclei per gonadal arms of F3 or F7 worms. n = 7 repeats, 20 worms each; **p $\leq$ 0.01 and ***p $\leq$ 0.001, two-way ANOVA.

(E) Representative examples of acridine orange-stained F3 nematodes following P0 DMSO or BPA exposure. All data are represented as mean ± SEM.

in the F3 germlines (Figure 7B; quantification shown in Figure S7A). Also, while the control RNAi conditions slightly elevated the rates of desilencing and embryonic lethality compared to no-RNAi conditions, the downregulation of either *jmjd-2* or *jmjd-3/utx-1* led to a complete rescue of BPA-induced responses in the F3, except for the embryonic lethality effect under *jmjd-2* RNAi conditions, which was strongly reduced but did not reach significance (Figure 7C). Interestingly, single RNAi against *jmjd-3* or *utx-1* dramatically increased the proportion of desilenced germlines under both ancestral DMSO and BPA exposures, suggesting a partial compensation between *jmjd-3* and *utx-1* in the *C. elegans* germline (Figure S7B). This increase is similar to that of RNAi against the H3K27 HMT Polycomb Group complex member *mes-6* or against the SET domain H3K36 HMT *mes-4*, which functions to limit H3K27me3 spreading away from silenced chromatin (Figure S7B) (Gaydos et al., 2012).

We further implicated the deregulation of H3K9me3 and H3K27me3 as central to BPA's transgenerational effects by performing drug rescue experiments using the KDM4/JMJD-2 inhibitor IOX-1 (King et al., 2010), which has been shown to elevate H3K9me3 levels *in vitro* and in cell culture settings, (Hu et al., 2016; King et al., 2010; Schiller et al., 2014), and the potent selective Jumonji JMJD-3/UTX-1 H3K27 demethylase inhibitor GSK-J4 (Kruidenier et al., 2012). We first examined whether a combination of the two histone demethylase inhibitors would be sufficient to decrease the germline array desilencing and embryonic lethality effects. The co-treatment of the F1 generation with 100 μM IOX-1 and 100 μM GSK-J4 led to a significant reduction in BPA-induced array desilencing and embryonic lethality by 15.8% and 27.0%, respectively (Figure S8B). Finally, we tested the effect of the two inhibitors independently. Remarkably, F1 exposure to either IOX-1 or GSK-J4 was sufficient to suppress the elevation in array desilencing and embryonic lethality in P0 BPA-exposed worms compared to DMSO (Figure S8C). Thus, two distinct means of rescuing BPA's transgenerational effects, by RNAi or chemical inhibitors, indicate that the activity of either JMJD-2 or JMD-3/UTX-1 is required for the inheritance of BPA-induced reproductive effects.

DISCUSSION

In the present study, we aimed to characterize the molecular mechanisms of memory of environmental exposures using BPA as a model chemical. We showed that ancestral BPA exposure leads to a transgenerational decrease in the germline levels of H3K9me3 and H3K27me3 dependent on the activity of the JMJD-2 and JMJD-3/UTX-1 demethylases. Interestingly, our results indicate that, while the overt germline desilencing effect lasts only up to 5 generations, some modest impacts on reproduction extend at least until the F7 generation. These results therefore suggest that the transgenerational impact of BPA may differ depending on the type of genetic loci examined, with repetitive loci, such as the transgene, being less affected than other loci controlling *C. elegans* reproductive function.

We found that modulation of either JMJD-2 or JMJD-3/UTX-1 activity, chemically or genetically, is sufficient to dramatically reduce the inheritance of transgenerational effects. While JMJD-2 acts as both an H3K9me3 and H3K36me3 demethylase, the ability of *jmjd-2* RNAi to rescue desilencing's effects is likely caused by its action on H3K9me3, as H3K36me3 is considered an active mark in the *C. elegans* germline (Gaydos

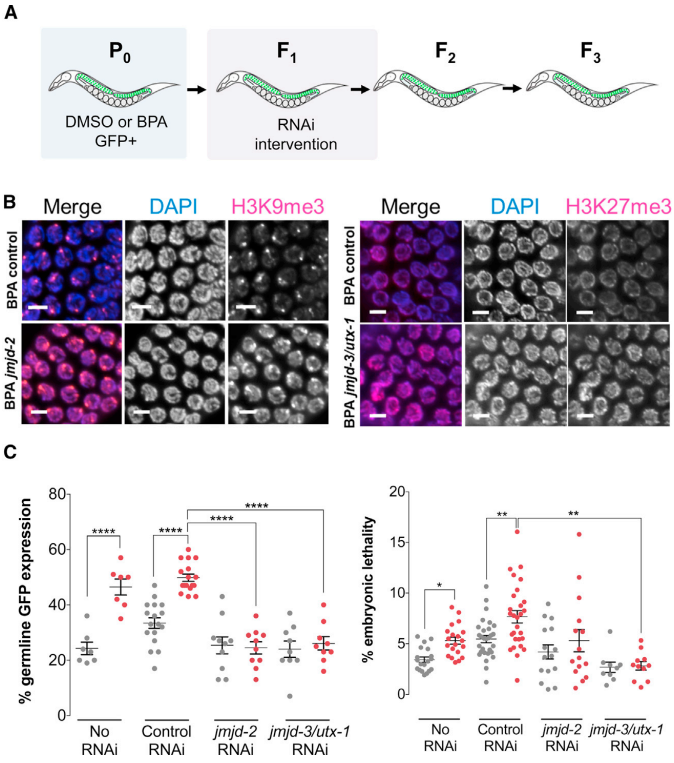

Figure 7. *jmjd-2* and *jmjd-3/utx-1* Demethylases Are Required for BPA-Induced Transgenerational Response

(A) Exposure and rescue experimental scheme. Following exposure to DMSO or BPA at the P0 generation, the progeny of GFP-positive P0 worms was collected and subjected to feeding RNAi until the F2. F3 worms were then collected and analyzed.

(B) Immunofluorescence images of mid-to-late pachytene germline nuclei from F3 worms ancestrally exposed to BPA and GFP-positive at the P0, stained for H3K9me3 or H3K27me3. DAPI is represented in blue and the histone mark of interest in magenta in the merge. All images shown were selected representative images of the mean values obtained after quantification of all germline nuclei from that exposure group (Figure S7A). Scale bar, 5 μm.

(C) RNAi rescue of ancestral DMSO- (gray) or BPA- (red) induced effects following either no F1 treatment, empty vector control, *jmjd-2*, or *jmjd-3/utx-1* feeding RNAi. n = 7–17 repeats, 30 worms each for desilencing assay and n = 4–8 repeats, 3–4 worms each for the embryonic lethality assay; $^{*}p \leq 0.05$, $^{**}p \leq 0.01$, and $^{****}p \leq 0.0001$, two-way ANOVA. All data are represented as mean ± SEM.

et al., 2012) and RNAi against *jmjd-2* increases its levels (Whetstine et al., 2006), which is inconsistent with the observed decrease in BPA-induced desilencing in *jmjd-2* RNAi F3 animals. Our results thus suggest a cooperation between H3K9me3 and H3K27me3 for proper chromatin silencing in the *C. elegans* germline. Such cooperation is understood in mammalian embryonic stem cells (ESCs) to emerge from the interaction between Jarid2/Jumonji and Polycomb Repressive Complex 2 (PRC2) (Pasini et al., 2010; Peng et al., 2009) and to be important for heterochromatin formation and/or maintenance through PRC2's effect on increasing the binding efficiency of HP1 to H3K9me3 (Boros et al., 2014). In *C. elegans*' embryonic or larval chromatin, there is a strong overlap between H3K27me3 and H3K9me3 at genome-wide levels (Garrigues et al., 2015; Ho et al., 2014). This overlap is particularly significant at chromosomal arms of heterochromatic nature as well as lamina-associated domains (Ho et al., 2014), something also observed in our data (Figure 3B). In the *C. elegans* meiotic germline, the overlap between H3K27me3 and H3K9me3 chromosomal distribution is likely to be high, as H3K27me3 distribution is greater than that of H3K9me3 (Bender et al., 2004; Bessler et al., 2010; Schaner and Kelly, 2006).

Our results are consistent with previous observations in mouse germ cells, where exposure of growing oocytes to low BPA concentrations decreased H3K9me3 levels (Trapphoff et al., 2013). However, the effect of BPA may also be context dependent, as an increase in EZH2 expression and, consequently, an elevation of H3K27me3 was detected in mammary tissues following BPA exposure (Doherty et al., 2010). Our work suggests that, at least in *C. elegans*, the tight regulation of H3K9 and H3K27 methylation is central to the epigenetic memory of ancestral exposures. It will be crucial to examine how histone-based epimutations may be inherited across generations in mammalian models, since the mammalian epigenome undergoes two distinct waves of reprogramming, once in the primordial germ cells (PGCs) and a second time after fertilization in the pre-implantation embryo (reviewed in Tang et al., 2016). During the first reprogramming in PGCs, there is a wide fluctuation in H3K9me2 level, which becomes depleted (Seki et al., 2005), and in H3K27me3 level, which is gradually enriched globally (Hajkova et al., 2008). However, H3K9me3 is maintained in a dotted pattern in the pericentric heterochromatic regions as well as on endogenous retroviruses (Liu et al., 2014; Seki et al., 2005). Thus, H3K9me3 could serve in mammals as a molecular mediator of exposure memory in the germline.

The centrality of H3K9me3 in the inheritance of natural environmental effects has recently been further highlighted in *C. elegans*, where temperature-mediated alteration of transgene expression was detected for up to 14 generations (Klosin et al., 2017). However, other environmental cues, such as starvation or hyperosmosis, have been shown, depending on the studies,

to require small RNA-based mechanisms and/or H3K4 trimethylase activity (Kishimoto et al., 2017; Rechavi et al., 2014). While these pathways may be mechanistically related, it will be necessary to examine whether a unifying mechanism of environmental inheritance can be identified, especially as we also identified a requirement for the regulation of H3K27 methylation for the transgenerational inheritance of BPA's exposure. Finally, our findings on the transgenerational memory of exposure to the model toxicant BPA and its impact on the germline's epigenome and reproduction also raise important questions for human risk from exposure, as our work identified transgenerational reproductive effects even in the absence of such a response in the earlier generations and at BPA concentrations lower than those previously characterized and that yielded internal concentrations close to those found in human reproductive tissues (Chen et al., 2016; Schönfelder et al., 2002; Vandenberg et al., 2010).

In conclusion, we have uncovered a transgenerational effect on reproduction stemming from exposure to the environmental chemical BPA and mediated in part by a deregulation of repressive histone modifications. These findings, therefore, highlight the need to comprehensively examine the effect of our chemical environment on the unique context of the germline epigenome, and they also offer interventional means to prevent the transmission of such effects across generations.

EXPERIMENTAL PROCEDURES

Culture Conditions and Strains

Standard methods of culturing and handling of *C. elegans* were followed (Stiernagle, 2006). Worms were maintained on nematode growth medium (NGM) plates streaked with OP50 *E. coli*, and all experiments were performed at 20°C (at 25°C, a pronounced desilencing of pkIs1582 is observed in the germline). Strains used in this study were obtained from the *C. elegans* Genetics Center (CGC) and include the following: NL2507 (*pkIs1582[let-858*::GFP; *rol-6*(*su1006*)]), PD7271 (*pha-1(e2123)* III*; ccEx7271*), and N2 (wild-type).

Chemical Exposure and GFP Scoring

The exposure and GFP germline desilencing assessments were performed as previously described (Lundby et al., 2016). Briefly, all chemicals tested were obtained from Sigma-Aldrich and were dissolved in DMSO to a stock concentration of 100 mM. Worms were synchronized by bleaching an adult population of the strain of interest, plating the eggs, and allowing the synchronized population to reach L4 larval stage (approximately 50 hr). These were then collected and incubated for 48 hr in 50 μL OP50 bacteria, 500 μL M9, and 0.5 μL of the chemical of interest for a final chemical concentration of 100 μM. After 48 hr, the worms were collected and allowed to recover on NGM plates for 1–2 hr (mixed population) or immediately plated as individual worms to separately labeled 35-mm seeded NGM plates (GFP+/− population sorting) and recovered there. Worms were scored for germline GFP expression using a Nikon H600L microscope at 40× magnification.

Apoptosis Assay and Embryonic Lethality Assessment

Apoptosis assay was performed by acridine orange staining on synchronized adult hermaphrodites collected at 20–24 hr post-L4, as previously described (Allard and Colaiácovo, 2011; Chen et al., 2016). Embryonic lethality was performed by monitoring the numbers of embryos produced by each worm of each day of its reproductive life and subsequent larvae hatched from these embryos. The ratio of the latter measure by the former and multiplied by 100 generates the rate of embryonic lethality.

Chemical Rescue

F1 L4 larvae were obtained from DMSO- or BPA-exposed GFP-positive P0 worm populations, and they were exposed for 48 hr to the chemical rescue drugs IOX-1 and GSK-J4 dissolved in DMSO to a stock concentration of 100 mM. In combination treatments, one drug was prepared at a higher concentration so that the final DMSO concentration never exceeded 0.11%. The exposed F1 adult worms were then allowed to recover on NGM plates, and their offspring were followed until the F3 generation for GFP scoring and embryonic lethality assessment.

RNAi Experiments

Worms were exposed to RNAi by feeding (Kamath and Ahringer, 2003) with *E. coli* strains containing either an empty control vector (L4440) or expressing double-stranded RNA. RNAi constructs against *jmjd-2*, *jmjd-3*, *utx-1*, *mes-4*, and *mes-6* were obtained from the Ahringer RNAi library and sequence verified. P0 worms were exposed to BPA or DMSO for 48 hr following the procedure described above. For *jmjd-2* and *jmjd-3*/*utx-1* RNAi, F1 adult worms from GFP-positive P0 worms were placed on plates of *E. coli* containing an empty control vector (L4440) or expressing double-stranded RNA to lay overnight. F2 worms were grown on RNAi bacteria from hatching until the first day of adulthood, at which point they were transferred to non-RNAi OP50 plates. The subsequent generation (F3) was collected at adulthood (24 hr post-L4) for further analysis. For *mes-4* and *mes-6* RNAi, the same procedure was followed but from the F2 to F3 generation to circumvent their associated maternal sterility phenotype.

Immunofluorescence

Immunofluorescence images were collected at 0.5-μm z intervals with an Eclipse Ni-E microscope (Nikon) and a cooled charge-coupled device (CCD) camera (model CoolSNAP HQ, Photometrics) controlled by the NIS Elements AR system (Nikon). The images presented and quantified are projections approximately halfway through 3D data stacks of *C. elegans* gonads, which encompass entire nuclei. Images were subjected to 3D landweber deconvolution analysis (5 iterations) with the NIS Elements AR analysis program (Nikon). H3K27me3 and H3K9me3 quantification in mid-late pachytene germ cell nuclei was performed with the ImageJ software. F3 worms were staged at L4, and gonad dissection and immunofluorescence were performed 20–24 hr post-L4, as previously described (Chen et al., 2016). Primary antibodies were used at the following dilutions: rabbit α-H3K9me3, 1:500 (Abcam); and mouse α-H3K27me2me3, 1:200 (Active Motif). Secondary antibodies were used at the following dilutions: Cy3 α-rabbit, 1:700; and TxRed α-mouse, 1:200, (Jackson ImmunoResearch).

Germline RNA Amplification and RNA-Seq Analysis

Total RNA was extracted from needle-dissected gonads of F3 adult worms obtained from a mixed population of H_2O-, DMSO-, and BPA-exposed P0 nematodes. The experiments were performed on 4 biological replicates of 30 gonads each that were processed through the NucleoSpin RNA XS, Macherey Nagel kit. cDNA was synthesized using the SMART-Seq v4 Ultra Low Input RNA Kit for sequencing, amplified 10×, and purified using agentcourt AMPure beads.

Nextera XT Library Prep Kit was used to prepare the sequencing libraries from 1 ng cDNA. Single-end sequencing at 50-bp length was performed on an Illumina Hiseq 4000 system (Illumina, CA, USA), and a total of ~350 million reads was obtained for 12 samples (3 treatment groups × 4 replicates/group). Data quality checks were performed using the FastQC tool (http://www.bioinformatics.babraham.ac.uk/projects/fastqc). RNA-seq reads passing quality control (QC) were analyzed using a pipeline comprised of HISAT (Kim et al., 2015), StringTie (Pertea et al., 2015), and Ballgown (Frazee et al., 2015) tools. HISAT was used to align reads against the *C. elegans* genome to discover the locations from which the reads originated and to determine the transcript splice sites. Then, StringTie was used to assemble the RNA-seq alignments into potential transcripts. Ballgown was used to identify the transcripts and genes that were differentially expressed between the BPA and DMSO groups, between the BPA and control (water) groups, and between the DMSO and control groups. FPKMs for each transcript were obtained by Ballgown and used as the expression measure. We filtered out the low-abundance transcripts and kept those having a mean FPKM > 1 across all samples. To test the transcriptional impact of BPA on individual chromosomes, we applied a Student's t test to determine whether the differences in the mean

log2(FPKM + 1) values between the BPA and DMSO groups were significant for all transcripts with FPKM > 1 on each chromosome. $p \leq 0.05$ was considered significant.

ChIP-Seq and Multiplex PTM Assay

Histone modification H3K9me3 and H3K27me3 ChIP-seq data were generated as a service by Active Motif using their in-house antibodies from 3 biological repeats of frozen F3 nematode populations, with 200 μL worms per sample repeat. The sequencing data were obtained through Illumina Nextseq and mapped to ce10 genome by Burrows-Wheeler Aligner (BWA) algorithm (Li and Durbin, 2009). Following pooling of the sequencing data per exposure category (Yang et al., 2014), the data were normalized to input and million reads to produce a signal track file by MACS2 (Zhang et al., 2008). For chromosome-wide mark distribution analysis, each chromosome was divided into 100 sub-regions and average fold enrichment score per base in sub-regions. We normalized signals with *Z* score for each chromosome and each sample.

For gene body histone modification analysis, deepTools (Ramírez et al., 2014) was utilized to obtain aggregated signal from −500 bp of the upstream transcription start site (TSS) to +500 bp of the downstream transcription end site (TES). We first summarized genes with multiple transcripts into a single gene by the one with the most significant difference from BPA and DMSO from RNA-seq results. Silenced genes were defined as genes expressed in the lowest 25% (Q1, 1,801 genes) of all genes in the DMSO group, and upregulated genes were defined as silenced genes upregulated more than 2-fold after BPA treatment (244 genes) based on RNA-seq results. We called peaks by MACS2 broad peak function with q value = 0.1 (cutoff). Broad peak is used as a peak-calling category when analyzing data for protein-DNA association with broader DNA coverage, such as for H3K9me3 and H3K27me3. It joins nearby narrower peak calling into one broader peak. To compare differential peak, unique peak method was used to compare BPA and DMSO samples (Steinhauser et al., 2016). Non-overlapping broad peaks called by MACS2 were defined as unique peaks. Unique peaks from BPA and DMSO in 100 sub-regions along each chromosome were compared. We further define peaked genes as genes with any peak calling in gene body region. Unless specified, analyses were conducted by R 3.4.0 (R Core Team, 2017) and Bioconductor (Huber et al., 2015).

The multiplex PTM quantitation assay was also generated as service by Active Motif on a Luminex platform, and it was performed on pooled samples (totaling 100 μL) generated from 3–4 individual repeats per exposure condition.

Statistical Analyses

Unless indicated otherwise, an unpaired t test assuming unequal variance with Welch's correction was applied. For multi-group comparisons, a one-way ANOVA with Sidak correction or two-way ANOVA was used.

DATA AND SOFTWARE AVAILABILITY

The accession numbers for the ChIP-seq and RNA-seq data reported in this paper are GEO: GSE113187 and GSE113266.

SUPPLEMENTAL INFORMATION

Supplemental Information includes eight figures and five tables and can be found with this article online at https://doi.org/10.1016/j.celrep.2018.04.078.

ACKNOWLEDGMENTS

P.A. is supported by NIH/NIEHS R01 ES02748701 and the Burroughs Wellcome Foundation. J.C. received support from NIH/NIEHS T32 ES015457 Training in Molecular Toxicology, the North American Graduate Fellowship, the NSF AGEP Competitive Edge, the NSF Graduate Research Fellowship, and the Eugene-Cota Robles Fellowship. L.T. is supported by the NIH Training Grant in Genomic Analysis and Interpretation T32 HG002536. G.G. is supported by NIH/NIEHS R25 ES02550703. Z.K. was supported by an American Heart Association post-doctoral fellowship (17POST33670739) and the Iris Cantor-UCLA Executive Advisory Board/CTSI Pilot Award. M.M. was supported by a Dissertation Year Fellowship (University of California, Los Angeles). X.Y. is supported by NIH/NIDDK R01 DK104363 and NIH/NINDS R21 NS103088.

AUTHOR CONTRIBUTIONS

J.C., L.T., M.M., and G.G. performed the experiments. J.C., L.T., Z.K., Y.-W.C., M.P., X.Y., and P.A. analyzed and interpreted the results. J.C., L.T., Z.K., Y.-W.C., X.Y., and P.A. wrote the manuscript.

DECLARATION OF INTERESTS

The authors declare no competing interests.

Received: September 7, 2017
Revised: March 15, 2018
Accepted: April 17, 2018
Published: May 22, 2018

REFERENCES

Agger, K., Cloos, P.A., Christensen, J., Pasini, D., Rose, S., Rappsilber, J., Issaeva, I., Canaani, E., Salcini, A.E., and Helin, K. (2007). UTX and JMJD3 are histone H3K27 demethylases involved in HOX gene regulation and development. Nature *449*, 731–734.

Allard, P., and Colaiácovo, M.P. (2011). Mechanistic insights into the action of Bisphenol A on the germline using C. elegans. Cell Cycle *10*, 183–184.

Anway, M.D., Cupp, A.S., Uzumcu, M., and Skinner, M.K. (2005). Epigenetic transgenerational actions of endocrine disruptors and male fertility. Science *308*, 1466–1469.

Anway, M.D., Leathers, C., and Skinner, M.K. (2006). Endocrine disruptor vinclozolin induced epigenetic transgenerational adult-onset disease. Endocrinology *147*, 5515–5523.

Bender, L.B., Cao, R., Zhang, Y., and Strome, S. (2004). The MES-2/MES-3/MES-6 complex and regulation of histone H3 methylation in C. elegans. Curr. Biol. *14*, 1639–1643.

Bender, L.B., Suh, J., Carroll, C.R., Fong, Y., Fingerman, I.M., Briggs, S.D., Cao, R., Zhang, Y., Reinke, V., and Strome, S. (2006). MES-4: an autosome-associated histone methyltransferase that participates in silencing the X chromosomes in the C. elegans germ line. Development *133*, 3907–3917.

Bessler, J.B., Andersen, E.C., and Villeneuve, A.M. (2010). Differential localization and independent acquisition of the H3K9me2 and H3K9me3 chromatin modifications in the Caenorhabditis elegans adult germ line. PLoS Genet. *6*, e1000830.

Bhalla, N., and Dernburg, A.F. (2005). A conserved checkpoint monitors meiotic chromosome synapsis in Caenorhabditis elegans. Science *310*, 1683–1686.

Bhan, A., Hussain, I., Ansari, K.I., Bobzean, S.A., Perrotti, L.I., and Mandal, S.S. (2014). Histone methyltransferase EZH2 is transcriptionally induced by estradiol as well as estrogenic endocrine disruptors bisphenol-A and diethylstilbestrol. J. Mol. Biol. *426*, 3426–3441.

Boros, J., Arnoult, N., Stroobant, V., Collet, J.F., and Decottignies, A. (2014). Polycomb repressive complex 2 and H3K27me3 cooperate with H3K9 methylation to maintain heterochromatin protein 1α at chromatin. Mol. Cell. Biol. *34*, 3662–3674.

Chen, Y., Shu, L., Qiu, Z., Lee, D.Y., Settle, S.J., Que Hee, S., Telesca, D., Yang, X., and Allard, P. (2016). Exposure to the BPA-Substitute Bisphenol S Causes Unique Alterations of Germline Function. PLoS Genet. *12*, e1006223.

Doherty, L.F., Bromer, J.G., Zhou, Y., Aldad, T.S., and Taylor, H.S. (2010). In utero exposure to diethylstilbestrol (DES) or bisphenol-A (BPA) increases EZH2 expression in the mammary gland: an epigenetic mechanism linking endocrine disruptors to breast cancer. Horm. Cancer *1*, 146–155.

Frazee, A.C., Pertea, G., Jaffe, A.E., Langmead, B., Salzberg, S.L., and Leek, J.T. (2015). Ballgown bridges the gap between transcriptome assembly and expression analysis. Nat. Biotechnol. *33*, 243–246.

Gapp, K., Jawaid, A., Sarkies, P., Bohacek, J., Pelczar, P., Prados, J., Farinelli, L., Miska, E., and Mansuy, I.M. (2014). Implication of sperm RNAs in transgenerational inheritance of the effects of early trauma in mice. Nat. Neurosci. *17*, 667–669.

Garrigues, J.M., Sidoli, S., Garcia, B.A., and Strome, S. (2015). Defining heterochromatin in C. elegans through genome-wide analysis of the heterochromatin protein 1 homolog HPL-2. Genome Res. *25*, 76–88.

Gartner, A., Boag, P.R., and Blackwell, T.K. (2008). Germline survival and apoptosis. WormBook1-20.

Gaydos, L.J., Rechtsteiner, A., Egelhofer, T.A., Carroll, C.R., and Strome, S. (2012). Antagonism between MES-4 and Polycomb repressive complex 2 promotes appropriate gene expression in C. elegans germ cells. Cell Rep. *2*, 1169–1177.

Gaydos, L.J., Wang, W., and Strome, S. (2014). Gene repression. H3K27me and PRC2 transmit a memory of repression across generations and during development. Science *345*, 1515–1518.

Greer, E.L., Beese-Sims, S.E., Brookes, E., Spadafora, R., Zhu, Y., Rothbart, S.B., Aristizábal-Corrales, D., Chen, S., Badeaux, A.I., Jin, Q., et al. (2014). A histone methylation network regulates transgenerational epigenetic memory in C. elegans. Cell Rep. *7*, 113–126.

Hajkova, P., Ancelin, K., Waldmann, T., Lacoste, N., Lange, U.C., Cesari, F., Lee, C., Almouzni, G., Schneider, R., and Surani, M.A. (2008). Chromatin dynamics during epigenetic reprogramming in the mouse germ line. Nature *452*, 877–881.

Heard, E., and Martienssen, R.A. (2014). Transgenerational epigenetic inheritance: myths and mechanisms. Cell *157*, 95–109.

Ho, J.W., Jung, Y.L., Liu, T., Alver, B.H., Lee, S., Ikegami, K., Sohn, K.A., Minoda, A., Tolstorukov, M.Y., Appert, A., et al. (2014). Comparative analysis of metazoan chromatin organization. Nature *512*, 449–452.

Hu, Q., Chen, J., Zhang, J., Xu, C., Yang, S., and Jiang, H. (2016). IOX1, a JMJD2A inhibitor, suppresses the proliferation and migration of vascular smooth muscle cells induced by angiotensin II by regulating the expression of cell cycle-related proteins. Int. J. Mol. Med. *37*, 189–196.

Huber, W., Carey, V.J., Gentleman, R., Anders, S., Carlson, M., Carvalho, B.S., Bravo, H.C., Davis, S., Gatto, L., Girke, T., et al. (2015). Orchestrating high-throughput genomic analysis with Bioconductor. Nat. Methods *12*, 115–121.

Hughes, V. (2014). Epigenetics: The sins of the father. Nature *507*, 22–24.

Iwatani, M., Ikegami, K., Kremenska, Y., Hattori, N., Tanaka, S., Yagi, S., and Shiota, K. (2006). Dimethyl sulfoxide has an impact on epigenetic profile in mouse embryoid body. Stem Cells *24*, 2549–2556.

Juang, J.K., and Liu, H.J. (1987). The effect of DMSO on natural DNA conformation in enhancing transcription. Biochem. Biophys. Res. Commun. *146*, 1458–1464.

Kamath, R.S., and Ahringer, J. (2003). Genome-wide RNAi screening in Caenorhabditis elegans. Methods *30*, 313–321.

Kelly, W.G., and Fire, A. (1998). Chromatin silencing and the maintenance of a functional germline in Caenorhabditis elegans. Development *125*, 2451–2456.

Kelly, W.G., Xu, S., Montgomery, M.K., and Fire, A. (1997). Distinct requirements for somatic and germline expression of a generally expressed Caenorhabditis elegans gene. Genetics *146*, 227–238.

Kim, A., and Dean, A. (2004). Developmental stage differences in chromatin subdomains of the beta-globin locus. Proc. Natl. Acad. Sci. USA *101*, 7028–7033.

Kim, D., Langmead, B., and Salzberg, S.L. (2015). HISAT: a fast spliced aligner with low memory requirements. Nat. Methods *12*, 357–360.

King, O.N., Li, X.S., Sakurai, M., Kawamura, A., Rose, N.R., Ng, S.S., Quinn, A.M., Rai, G., Mott, B.T., Beswick, P., et al. (2010). Quantitative high-throughput screening identifies 8-hydroxyquinolines as cell-active histone demethylase inhibitors. PLoS ONE *5*, e15535.

Kishimoto, S., Uno, M., Okabe, E., Nono, M., and Nishida, E. (2017). Environmental stresses induce transgenerationally inheritable survival advantages via germline-to-soma communication in Caenorhabditis elegans. Nat. Commun. *8*, 14031.

Klosin, A., Casas, E., Hidalgo-Carcedo, C., Vavouri, T., and Lehner, B. (2017). Transgenerational transmission of environmental information in *C. elegans*. Science *356*, 320–323.

Kruidenier, L., Chung, C.W., Cheng, Z., Liddle, J., Che, K., Joberty, G., Bantscheff, M., Bountra, C., Bridges, A., Diallo, H., et al. (2012). A selective jumonji H3K27 demethylase inhibitor modulates the proinflammatory macrophage response. Nature *488*, 404–408.

Leung, D., Du, T., Wagner, U., Xie, W., Lee, A.Y., Goyal, P., Li, Y., Szulwach, K.E., Jin, P., Lorincz, M.C., and Ren, B. (2014). Regulation of DNA methylation turnover at LTR retrotransposons and imprinted loci by the histone methyltransferase Setdb1. Proc. Natl. Acad. Sci. USA *111*, 6690–6695.

Li, H., and Durbin, R. (2009). Fast and accurate short read alignment with Burrows-Wheeler transform. Bioinformatics *25*, 1754–1760.

Liu, T., Rechtsteiner, A., Egelhofer, T.A., Vielle, A., Latorre, I., Cheung, M.S., Ercan, S., Ikegami, K., Jensen, M., Kolasinska-Zwierz, P., et al. (2011). Broad chromosomal domains of histone modification patterns in C. elegans. Genome Res. *21*, 227–236.

Liu, S., Brind'Amour, J., Karimi, M.M., Shirane, K., Bogutz, A., Lefebvre, L., Sasaki, H., Shinkai, Y., and Lorincz, M.C. (2014). Setdb1 is required for germline development and silencing of H3K9me3-marked endogenous retroviruses in primordial germ cells. Genes Dev. *28*, 2041–2055.

Lundby, Z., Camacho, J., and Allard, P. (2016). Fast Functional Germline and Epigenetic Assays in the Nematode Caenorhabditis elegans. Methods Mol. Biol. *1473*, 99–107.

Manikkam, M., Tracey, R., Guerrero-Bosagna, C., and Skinner, M.K. (2013). Plastics derived endocrine disruptors (BPA, DEHP and DBP) induce epigenetic transgenerational inheritance of obesity, reproductive disease and sperm epimutations. PLoS ONE *8*, e55387.

Pasini, D., Cloos, P.A., Walfridsson, J., Olsson, L., Bukowski, J.P., Johansen, J.V., Bak, M., Tommerup, N., Rappsilber, J., and Helin, K. (2010). JARID2 regulates binding of the Polycomb repressive complex 2 to target genes in ES cells. Nature *464*, 306–310.

Peng, J.C., Valouev, A., Swigut, T., Zhang, J., Zhao, Y., Sidow, A., and Wysocka, J. (2009). Jarid2/Jumonji coordinates control of PRC2 enzymatic activity and target gene occupancy in pluripotent cells. Cell *139*, 1290–1302.

Pertea, M., Pertea, G.M., Antonescu, C.M., Chang, T.C., Mendell, J.T., and Salzberg, S.L. (2015). StringTie enables improved reconstruction of a transcriptome from RNA-seq reads. Nat. Biotechnol. *33*, 290–295.

R Core Team (2017). R: A language and environment for statistical computing (R Foundation for Statistical Computing).

Ramírez, F., Dündar, F., Diehl, S., Grüning, B.A., and Manke, T. (2014). deepTools: a flexible platform for exploring deep-sequencing data. Nucleic Acids Res. *42*, W187–W191.

Rechavi, O., Houri-Ze'evi, L., Anava, S., Goh, W.S.S., Kerk, S.Y., Hannon, G.J., and Hobert, O. (2014). Starvation-induced transgenerational inheritance of small RNAs in C. elegans. Cell *158*, 277–287.

Rudgalvyte, M., Peltonen, J., Lakso, M., and Wong, G. (2017). Chronic MeHg exposure modifies the histone H3K4me3 epigenetic landscape in Caenorhabditis elegans. Comp. Biochem. Physiol. C Toxicol. Pharmacol. *191*, 109–116.

Schaner, C.E., and Kelly, W.G. (2006). Germline chromatin. WormBook, 1–14.

Schiller, R., Scozzafava, G., Tumber, A., Wickens, J.R., Bush, J.T., Rai, G., Lejeune, C., Choi, H., Yeh, T.L., Chan, M.C., et al. (2014). A cell-permeable ester derivative of the JmjC histone demethylase inhibitor IOX1. ChemMedChem *9*, 566–571.

Schönfelder, G., Wittfoht, W., Hopp, H., Talsness, C.E., Paul, M., and Chahoud, I. (2002). Parent bisphenol A accumulation in the human maternal-fetal-placental unit. Environ. Health Perspect. *110*, A703–A707.

Seki, Y., Hayashi, K., Itoh, K., Mizugaki, M., Saitou, M., and Matsui, Y. (2005). Extensive and orderly reprogramming of genome-wide chromatin

modifications associated with specification and early development of germ cells in mice. Dev. Biol. *278*, 440–458.

Siklenka, K., Erkek, S., Godmann, M., Lambrot, R., McGraw, S., Lafleur, C., Cohen, T., Xia, J., Suderman, M., Hallett, M., et al. (2015). Disruption of histone methylation in developing sperm impairs offspring health transgenerationally. Science *350*, aab2006.

Singh, S., and Li, S.S. (2012). Epigenetic effects of environmental chemicals bisphenol A and phthalates. Int. J. Mol. Sci. *13*, 10143–10153.

Steinhauser, S., Kurzawa, N., Eils, R., and Herrmann, C. (2016). A comprehensive comparison of tools for differential ChIP-seq analysis. Brief. Bioinform. *17*, 953–966.

Stiernagle, T. (2006). Maintenance of C. elegans. WormBook, 1–11.

Tang, W.W., Kobayashi, T., Irie, N., Dietmann, S., and Surani, M.A. (2016). Specification and epigenetic programming of the human germ line. Nat. Rev. Genet. *17*, 585–600.

Towbin, B.D., González-Aguilera, C., Sack, R., Gaidatzis, D., Kalck, V., Meister, P., Askjaer, P., and Gasser, S.M. (2012). Step-wise methylation of histone H3K9 positions heterochromatin at the nuclear periphery. Cell *150*, 934–947.

Trapphoff, T., Heiligentag, M., El Hajj, N., Haaf, T., and Eichenlaub-Ritter, U. (2013). Chronic exposure to a low concentration of bisphenol A during follicle culture affects the epigenetic status of germinal vesicles and metaphase II oocytes. Fertil. Steril. *100*, 1758–1767.e1.

Vandenberg, L.N., Chahoud, I., Heindel, J.J., Padmanabhan, V., Paumgartten, F.J.R., and Schoenfelder, G. (2010). Urinary, circulating, and tissue biomonitoring studies indicate widespread exposure to bisphenol A. Environ. Health Perspect. *118*, 1055–1070.

Whetstine, J.R., Nottke, A., Lan, F., Huarte, M., Smolikov, S., Chen, Z., Spooner, E., Li, E., Zhang, G., Colaiacovo, M., and Shi, Y. (2006). Reversal of histone lysine trimethylation by the JMJD2 family of histone demethylases. Cell *125*, 467–481.

Wu, C.T., and Morris, J.R. (2001). Genes, genetics, and epigenetics: a correspondence. Science *293*, 1103–1105.

Yang, Y., Fear, J., Hu, J., Haecker, I., Zhou, L., Renne, R., Bloom, D., and McIntyre, L.M. (2014). Leveraging biological replicates to improve analysis in ChIP-seq experiments. Comput. Struct. Biotechnol. J. *9*, e201401002.

Yeo, M., Berglund, K., Hanna, M., Guo, J.U., Kittur, J., Torres, M.D., Abramowitz, J., Busciglio, J., Gao, Y., Birnbaumer, L., and Liedtke, W.B. (2013). Bisphenol A delays the perinatal chloride shift in cortical neurons by epigenetic effects on the Kcc2 promoter. Proc. Natl. Acad. Sci. USA *110*, 4315–4320.

Zhang, Y., Liu, T., Meyer, C.A., Eeckhoute, J., Johnson, D.S., Bernstein, B.E., Nusbaum, C., Myers, R.M., Brown, M., Li, W., and Liu, X.S. (2008). Model-based analysis of ChIP-Seq (MACS). Genome Biol. *9*, R137.

Zhong, S.H., Liu, J.Z., Jin, H., Lin, L., Li, Q., Chen, Y., Yuan, Y.X., Wang, Z.Y., Huang, H., Qi, Y.J., et al. (2013). Warm temperatures induce transgenerational epigenetic release of RNA silencing by inhibiting siRNA biogenesis in Arabidopsis. Proc. Natl. Acad. Sci. USA *110*, 9171–9176.

Cell Reports, Volume *23*

Supplemental Information

The Memory of Environmental Chemical Exposure in *C. elegans* Is Dependent on the Jumonji Demethylases *jmjd-2* and *jmjd-3*/*utx-1*

Jessica Camacho, Lisa Truong, Zeyneb Kurt, Yen-Wei Chen, Marco Morselli, Gerardo Gutierrez, Matteo Pellegrini, Xia Yang, and Patrick Allard

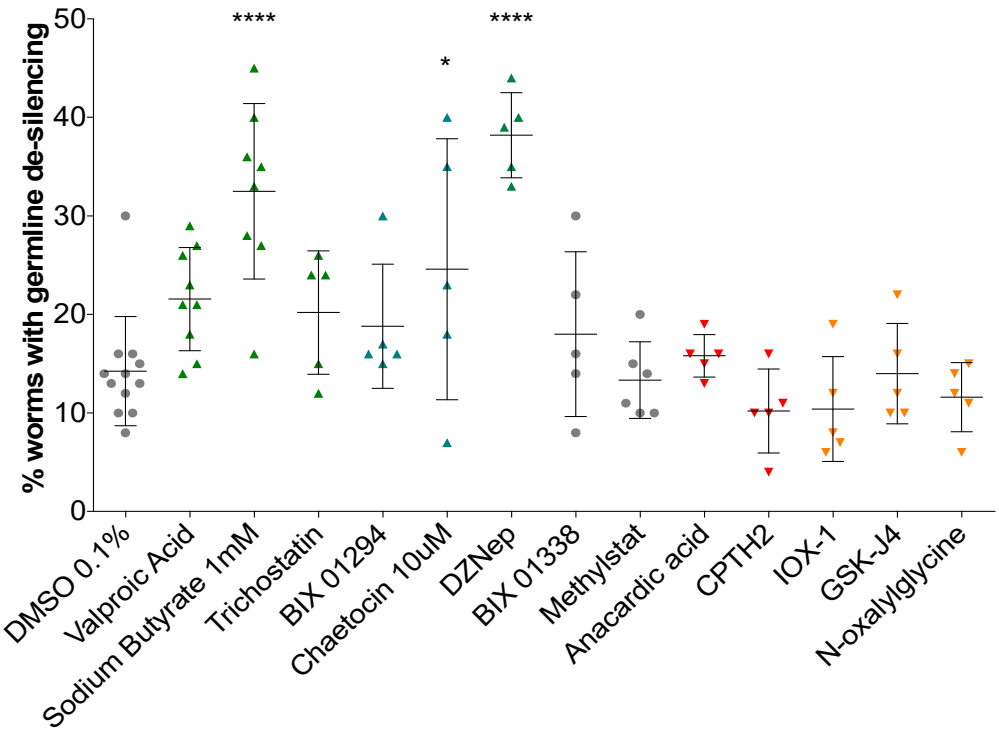

Figure S1: Epigenetic drug inhibitors assessment in P0 nematodes. Related to Figure 1. 13 drug inhibitors were tested for desilencing of the *pkIs1582* array in P0 worms. Chemicals are grouped based on their suspected chromatin effect: active (green), repressive (red) or carrying pleiotropic activity (grey). Unless indicated otherwise, all chemicals were tested at 100 µM. HDAC inhibitors are: Valproic acid, Sodium Butyrate and Trichostatin. Repressive H3K methyltransferase inhibitors are: BIX01294, Chaetocin and DZnep. Non-selective HMT and KDM inhibitors are: BIX 01338 and Methylstat. HAT inhibitors: Anacardic acid and CPTH2. Repressive H3K KDM inhibitors: IOX-1, GSK-J4 and N-oxalylglycine. N=5-9, 25 worms each, *P≤0.05, ****P≤0.0001. One way ANOVA, Sidak correction. All data are represented as mean +/- SEM.

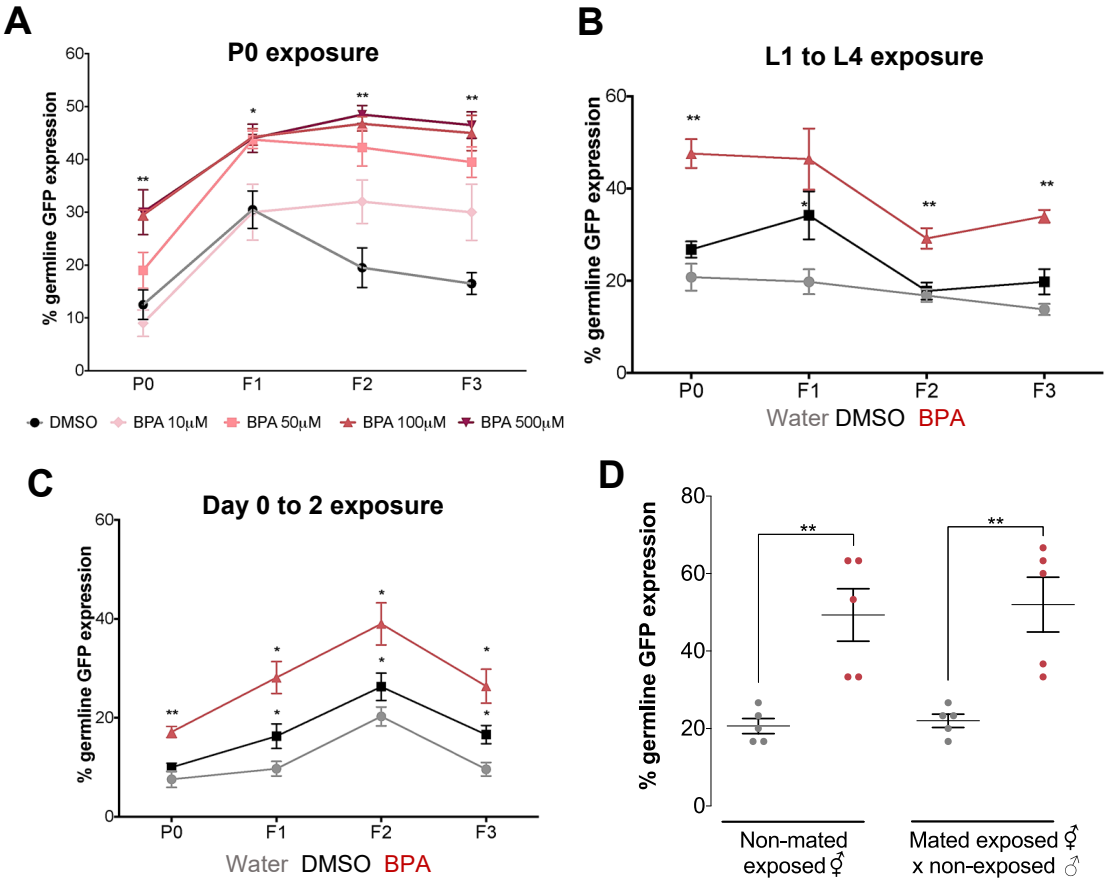

Figure S2: Dose, window and sex dependent germline *pkIs1582* array desilencing. Related to Figure 1. (A) Nematodes were exposed as L4 for 48 hours to BPA at the listed concentrations followed by monitoring of the proportion of worms with desilenced germlines. N=5-9, 25 worms each, *P≤0.05, **P≤0.01. A 100 μM dose was used to test two additional exposure windows, L1 to L4 (B) or Day 1 to Day 2 (C). N=5-9, 25 worms each, *P≤0.05, **P≤0.01. (D) Absence of rescue of ancestral BPA exposure-induced array desilencing in F3 germlines by mating. P0 nematodes were either exposed to DMSO (grey) or BPA (red) and the progeny of GFP-positive P0 worms was either not mated (left) or mated at the F1 generation with unexposed males (right). Expression of the *pkIs1582* integrated array was then monitored in F3 germlines. N=5, 30 worms each **P≤0.01. All data are represented as mean +/- SEM.

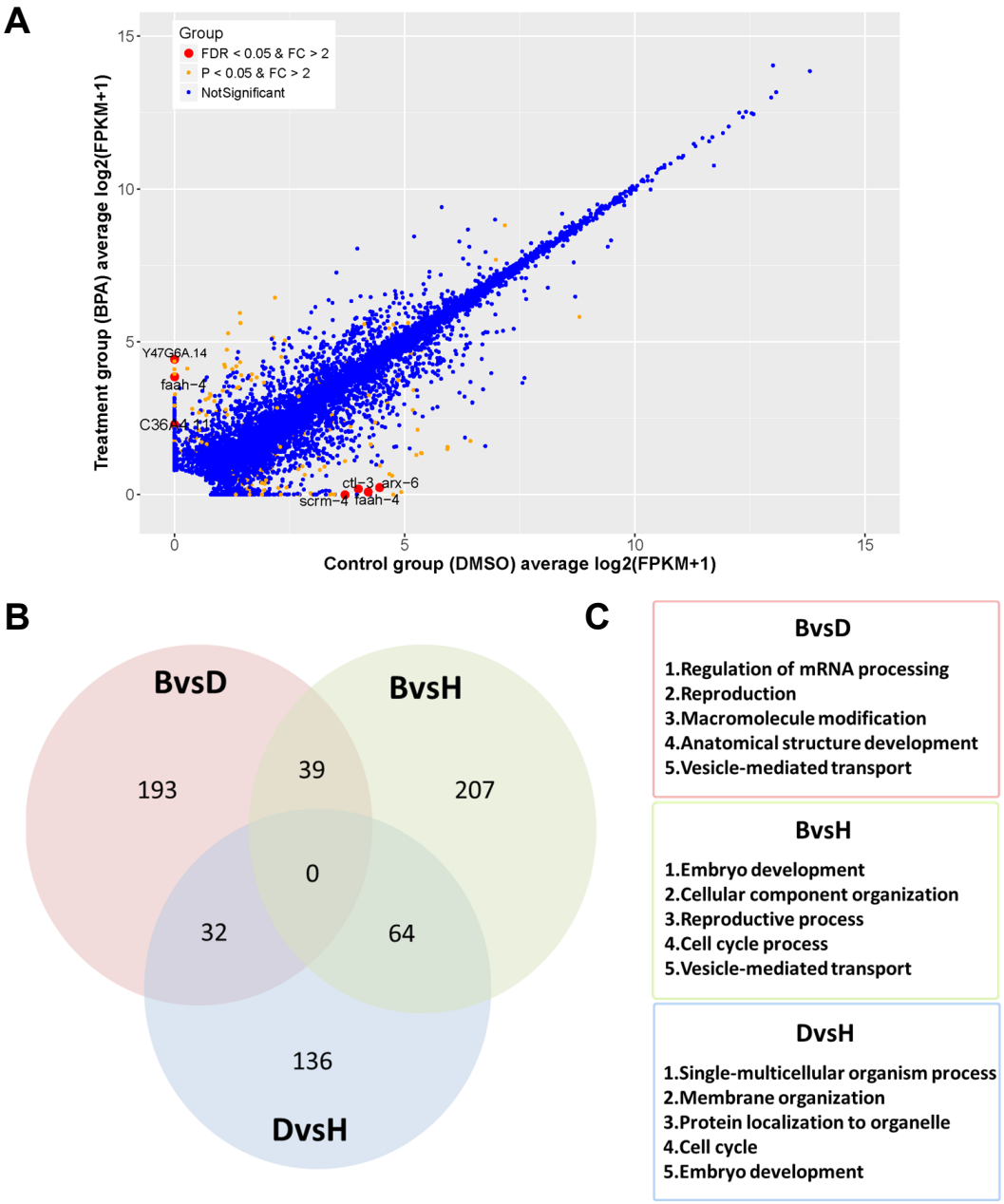

Figure S3: Transgenerational impact of BPA on the germline transcriptome. Related to Figure 2 and 5. A. The pair-wise comparison log2-transformed FKPM obtained by RNA-seq from BPA and DMSO samples. Red circles: FDR<0.05 and fold change >|2|, orange circles P<0.05 and fold change >|2|, blue no significant difference. (B) Venn diagram of transcripts identified in each treatment group. (C) Gene ontology analysis of unique transcripts ≤0.5 or ≥1.5 between all treatment pairs.

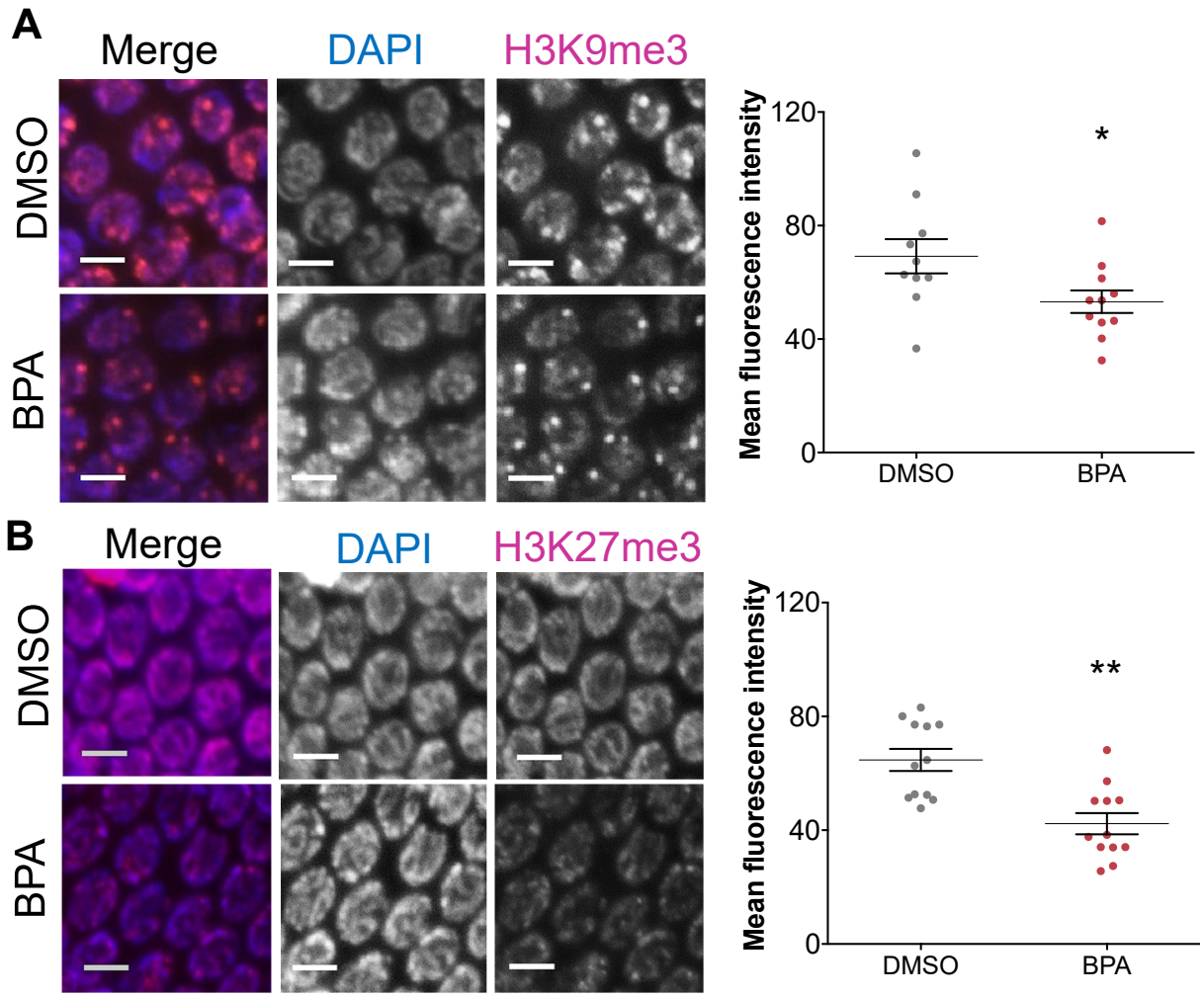

Figure S4: Ancestral BPA exposure decreases H3K9me3 and H3K27me3 levels in F3 germlines carrying an extrachromosomal array. Related to Figure 4. Immunofluorescence images of mid-to-late pachytene germline nuclei from F3 PD7271 (*pha-1(e2123)* III*; ccEx7271*) worms ancestrally exposed to DMSO or BPA and stained for H3K9me3 (A) or H3K27me3 (B). DAPI is represented in blue and the histone mark of interest in magenta in the merge. All images shown were selected representative images of the mean values obtained after quantification of all germline nuclei from that exposure group. The fluorescence intensity quantification is shown on the right panels. N=10-12 worms, 10 nuclei per worm, *P≤0.05, **P≤0.01. All data are represented as mean +/- SEM.

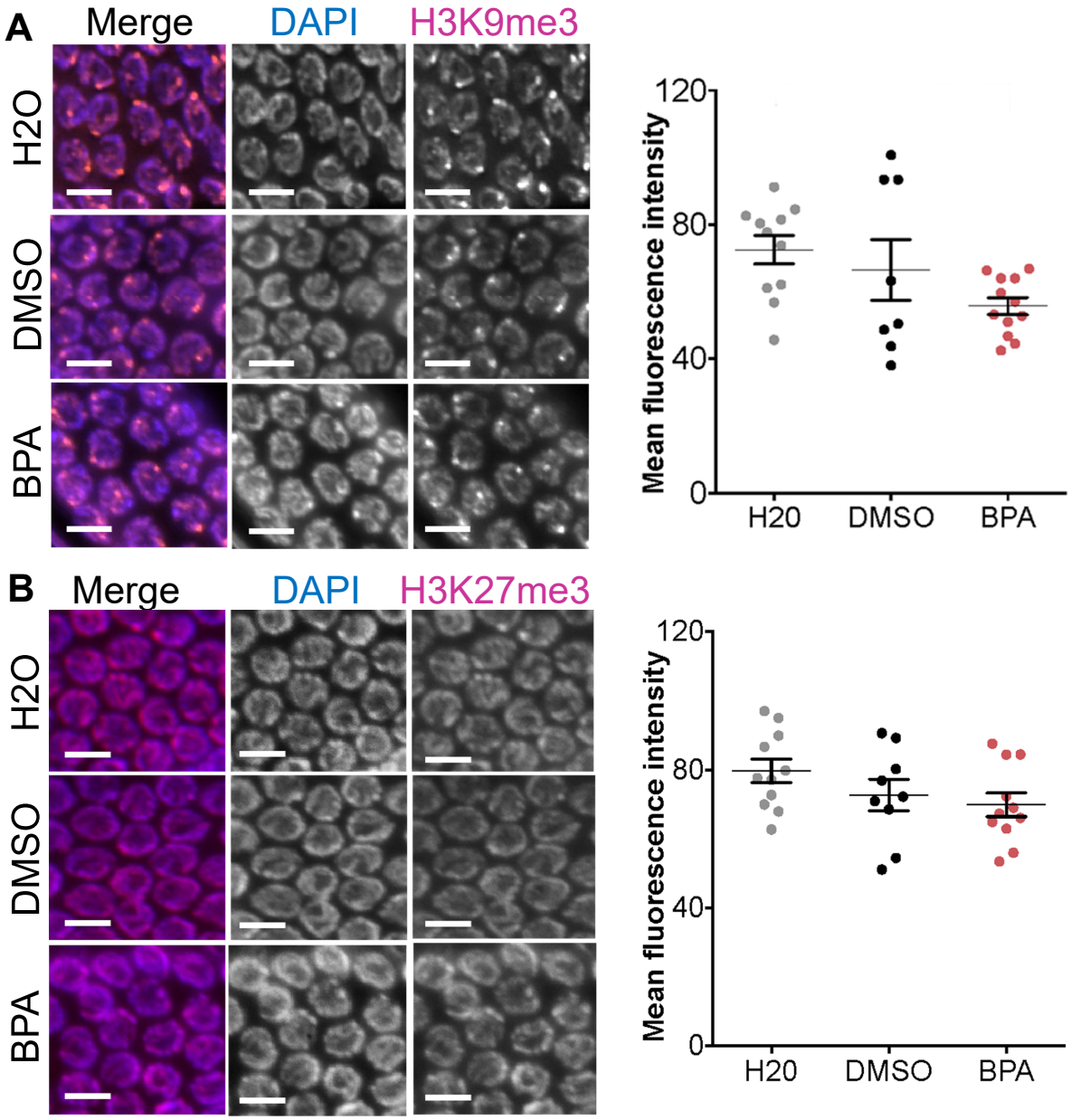

Figure S5: Ancestral BPA exposure does not decrease H3K9me3 and H3K27me3 levels in F7 germlines. Related to Figure 4. Immunofluorescence of mid-to-late pachytene F7 germline nuclei ancestrally exposed and stained for H3K9me3 (A) or H3K27me3 (B). DAPI is blue and the histone marks magenta in the merge. All images were selected representative of the mean values after quantification of all germline nuclei from that exposure group. N=10-12 worms, 10 nuclei quantified per worm. Two-way ANOVA with Sidak correction. All data are represented as mean +/- SEM.

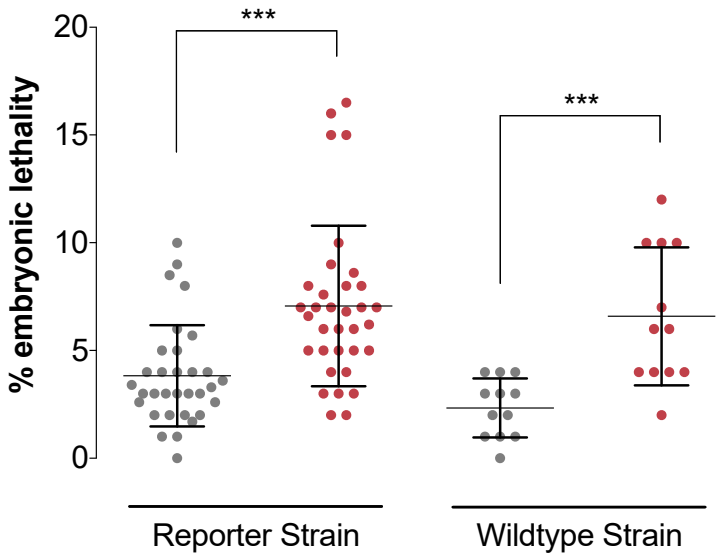

Figure S6: Variation in embryonic lethality phenotype based on genotype and variation in germline desilencing based on mode of inheritance. Related to Figure 6. Embryonic lethality in *pkIs1582* array-carrying NL2507 strain (labeled reporter) and wildtype (N2) *C. elegans* strains at the F3 generation following ancestral DMSO (grey circles) or BPA (red circles) exposure. N=12-30 worms, ***P≤0.001. All data are represented as mean +/- SEM.

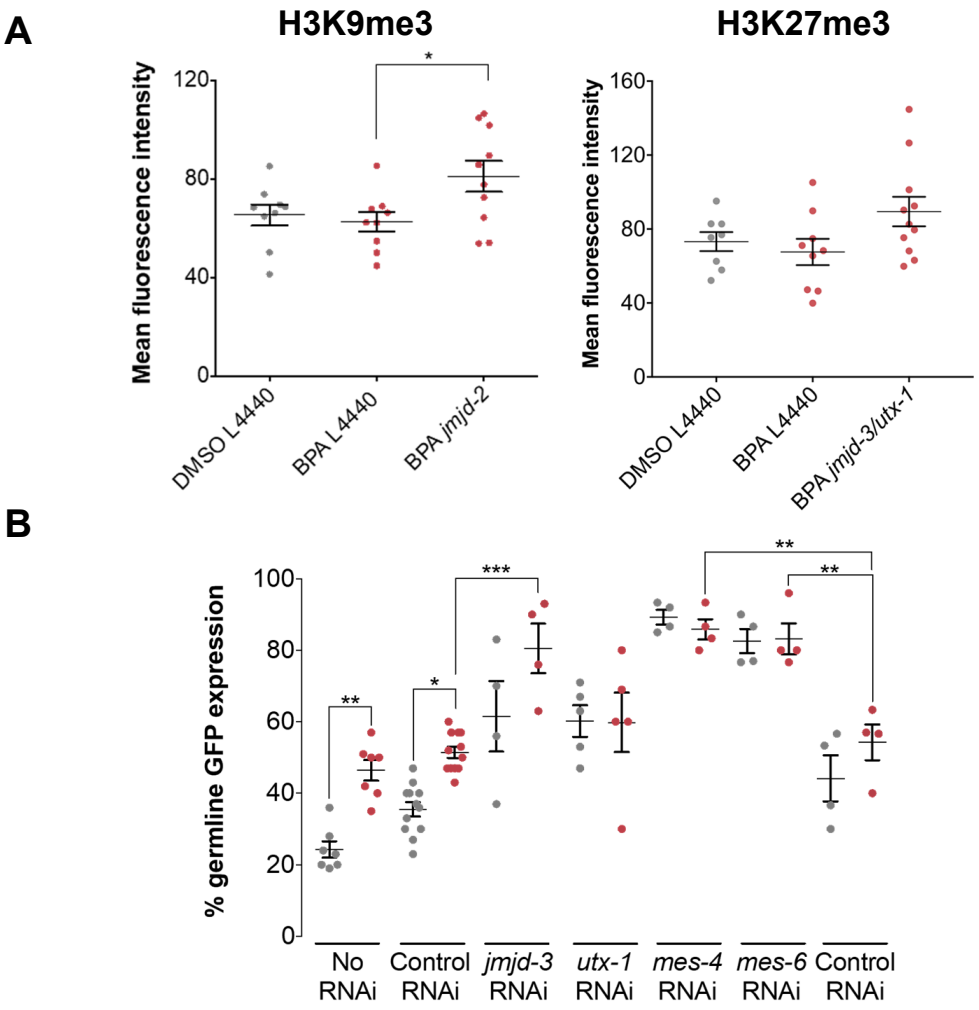

Figure S7: Changes in H3K9me3, H3K27me3, and array desilencing in the F3 generation following RNAi. Related to Figure 7. P0 nematodes were either exposed to DMSO (grey) or BPA (red) and the progeny of GFP-positive P0 worms was then exposed to RNAi. The subsequent F3 generation was then examined for H3K9me3 or H3K27me3 levels by immunofluorescence (A) or expression of the *pkIs1582* integrated array in the germline (B). *mes-4* and *mes-6* RNAi was performed at the F2 to F3 transition to circumvent their maternal sterility phenotype. (A) N=4 repeats, 8-11 gonad per treatment group, 10 nuclei per gonad, *P≤0.05. (B) N=4-7, 30 worms each *P≤0.05, **P≤0.01, ***P≤0.001. Two-way ANOVA. For the *mes* genes, only the comparisons between BPA groups are shown. All data are represented as mean +/- SEM.

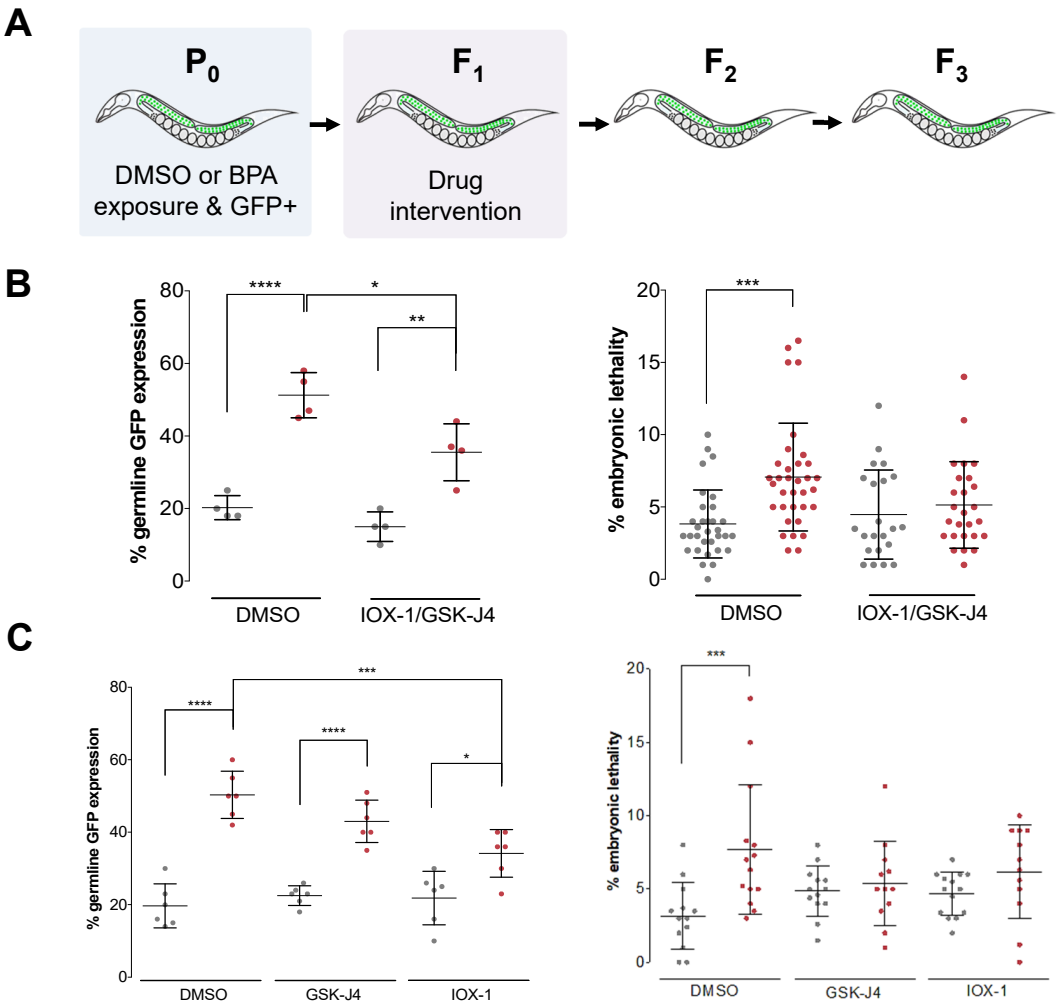

Figure S8: Rescue of F3 germline *pkIs1582* array desilencing and embryonic lethality phenotypes by inhibitor drug exposures. Related to Figure 7. A. Worms exposed to DMSO or BPA and GFP-positive at the P0 are subsequently exposed to DMSO, GSK-J4 and/or IOX-1 as F1s and assayed at the F3 generation. B. Co-treatment with IOX-1 (JMJD-2) and GSK-J4 (JMJD-3) demethylase inhibitors partially rescues the array desilencing and fully rescues BPA-induced embryonic lethality. N=4, 30 worms each desilencing assay and N=10 worms embryonic lethality assay. C. Rescue of BPA-induced transgenerational effects by single exposure at the F1 generation. Array desilencing: N=6, 25-30 worms each. Embryonic lethality: N=12-14,. Grey = DMSO exposed P0s. Red = BPA-exposed P0s. For all panels, * P≤0.05, **P≤0.01 ***P≤0.001, ****P≤0.0001, two-way ANOVA. All data are represented as mean +/- SEM.

Table S.1: RNA-Seq. Related to Figure 2

GeneNames	DAVID_IDs	feature	transcriptNames	FC (BPA/DMSO)	p-val	q-val
F11E6.7	WBGene00008710	transcript	TCONS_00034600	22.91871074	0.020499	0.999966
Y47G6A.14	WBGene00021640	transcript	TCONS_00002975	21.62575318	2.11E-12	2.19E-08
D1044.6	WBGene00017031	transcript	TCONS_00014441	20.56571706	0.0243	0.999966
F36A2.13	NA	transcript	TCONS_00004097	19.13054049	0.021667	0.999966
taf-5	WBGene00006386	transcript	TCONS_00001275	18.11671495	0.026784	0.999966
tag-256	NA	transcript	TCONS_00012700	17.25750344	0.014117	0.999966
pif-1	WBGene00004028	transcript	TCONS_00000085	17.13469793	0.024202	0.999966
F55F10.1	WBGene00018898	transcript	TCONS_00016610	15.39210301	0.023874	0.999966
faah-4	WBGene00013232	transcript	TCONS_00015694	14.52446262	1.60E-07	0.000554
F32B6.3	WBGene00009320	transcript	TCONS_00028295	14.3149513	0.007312	0.999966
sop-3	WBGene00004946	transcript	TCONS_00002859	12.12318748	0.020483	0.999966
syx-5	WBGene00006373	transcript	TCONS_00036844	9.623302077	0.031124	0.999966
C35D10.5	WBGene00016442	transcript	TCONS_00011891	8.979393591	0.026724	0.999966
ufd-2	WBGene00006734	transcript	TCONS_00006885	8.48064623	0.039101	0.999966
sgo-1	WBGene00016381	transcript	TCONS_00027853	8.425925624	0.037215	0.999966
T24H7.2	WBGene00020781	transcript	TCONS_00006424	7.988985762	0.005334	0.999966
Y77E11A.1	NA	transcript	TCONS_00016172	7.691582185	0.024462	0.999966
Y37E11B.5	WBGene00021377	transcript	TCONS_00025723	7.519790865	0.025241	0.999966
fce-2	WBGene00001406	transcript	TCONS_00038558	7.517657054	0.031577	0.999966
epg-4	WBGene00018150	transcript	TCONS_00012348	7.502932937	0.035637	0.999966
Y39B6A.42	WBGene00012700	transcript	TCONS_00042592	7.228606281	0.023899	0.999966
T05E7.3	WBGene00020259	transcript	TCONS_00000935	7.204869304	6.18E-05	0.080179
Y48G8AL.10	WBGene00021689	transcript	TCONS_00002690	7.188244464	0.011635	0.999966
D1044.6	WBGene00017031	transcript	TCONS_00014442	6.224987376	0.044101	0.999966
jmjd-1.2	WBGene00017920	transcript	TCONS_00016665	5.738988397	0.025741	0.999966
ztf-17	WBGene00011639	transcript	TCONS_00009733	5.485929283	0.020772	0.999966
H24K24.3	WBGene00019240	transcript	TCONS_00034779	5.468550758	0.038218	0.999966
W02D3.4	WBGene00020933	transcript	TCONS_00003644	5.396964159	0.032669	0.999966
F42A6.6	WBGene00018328	transcript	TCONS_00025679	5.355162599	0.008547	0.999966
sgo-1	WBGene00016381	transcript	TCONS_00027854	5.341636043	0.018525	0.999966
mpst-7	WBGene00011307	transcript	TCONS_00041423	5.100124078	0.038862	0.999966
F44E2.10	WBGene00018423	transcript	TCONS_00015134	4.938708809	0.037462	0.999966
C36A4.11	WBGene00044167	transcript	TCONS_00025807	4.928874268	1.96E-05	0.029118
uaf-2	WBGene00006698	transcript	TCONS_00034402	4.778134656	0.032316	0.999966
bath-28	WBGene00017461	transcript	TCONS_00008798	4.621857383	0.024052	0.999966
ctl-3	WBGene00013220	transcript	TCONS_00011003	4.559536582	0.010914	0.999966
scrm-4	WBGene00008681	transcript	TCONS_00004719	4.535401797	0.041272	0.999966
W03F8.4	WBGene00020994	transcript	TCONS_00016991	4.471245187	0.038569	0.999966
ucr-2.1	WBGene00012158	transcript	TCONS_00045144	4.4281965	0.009942	0.999966
Y48E1C.1	WBGene00013014	transcript	TCONS_00007914	4.411254194	0.023784	0.999966
sop-2	WBGene00004945	transcript	TCONS_00007750	4.409482026	0.002722	0.999966
B0432.8	WBGene00015189	transcript	TCONS_00008233	4.387580586	0.026096	0.999966
D1005.9	NA	transcript	TCONS_00000320	4.369925663	0.027122	0.999966
F52D2.12	WBGene00219451	transcript	TCONS_00043160	4.318076262	0.046221	0.999966

coq-5	WBGene00000765	transcript	TCONS_00014910	4.240980232	0.036412	0.999966
csnk-1	WBGene00013709	transcript	TCONS_00004458	4.119071132	0.000346	0.338368
Y39G10AR.7	NA	transcript	TCONS_00000273	3.888032354	0.026379	0.999966
met-2	WBGene00019883	transcript	TCONS_00012604	3.867788824	0.025808	0.999966
F44E2.10	WBGene00018423	transcript	TCONS_00015133	3.865045089	0.030498	0.999966
Y52B11A.2	NA	transcript	TCONS_00004602	3.75203157	0.034617	0.999966
F45H11.5	WBGene00009745	transcript	TCONS_00001771	3.472772193	0.047674	0.999966
F49C12.11	WBGene00009880	transcript	TCONS_00028159	3.421527165	0.048823	0.999966
C34B4.2	WBGene00007907	transcript	TCONS_00037196	3.287729156	0.023026	0.999966
tra-3	WBGene00006606	transcript	TCONS_00030400	3.16631588	0.031517	0.999966
.	NA	transcript	TCONS_00034628	3.088758845	0.012577	0.999966
Y50D4A.5	WBGene00021739	transcript	TCONS_00034812	2.974337832	0.010803	0.999966
tag-325	WBGene00008006	transcript	TCONS_00011868	2.832967555	0.040508	0.999966
F43G6.10	WBGene00009662	transcript	TCONS_00007651	2.792606925	0.003777	0.999966
F10C2.5	WBGene00008646	transcript	TCONS_00036930	2.770239069	0.044578	0.999966
epg-4	WBGene00018150	transcript	TCONS_00012359	2.766093442	0.03346	0.999966
C54E4.2	NA	transcript	TCONS_00016261	2.744160211	0.025764	0.999966
F22B3.4	NA	transcript	TCONS_00019293	2.737695156	0.022284	0.999966
mtm-3	WBGene00003476	transcript	TCONS_00014069	2.617072763	0.030481	0.999966
dnj-22	WBGene00001040	transcript	TCONS_00040207	2.387717391	0.04019	0.999966
nucb-1	WBGene00009674	transcript	TCONS_00044819	2.176969149	0.02779	0.999966
T08B2.5	WBGene00020346	transcript	TCONS_00000940	2.082998688	0.013864	0.999966
hpo-24	WBGene00011945	transcript	TCONS_00001692	2.075937495	0.035806	0.999966
T26C11.9	WBGene00194679	transcript	TCONS_00046352	1.95223635	0.007288	0.999966
fox-1	WBGene00001484	transcript	TCONS_00046461	1.922965694	0.032121	0.999966
F57C9.1	WBGene00019008	transcript	TCONS_00000679	1.845940481	0.024263	0.999966
T02G5.4	NA	transcript	TCONS_00006651	1.823718231	0.032603	0.999966
dpf-4	WBGene00001057	transcript	TCONS_00012118	1.815256008	0.025662	0.999966
pqn-59	WBGene00004143	transcript	TCONS_00002598	1.811470083	0.013732	0.999966
sir-2.4	WBGene00004803	transcript	TCONS_00000886	1.747926404	0.015264	0.999966
C35D10.1	WBGene00016439	transcript	TCONS_00011897	1.744733015	0.001331	0.812952
Y73B6BL.29	WBGene00022250	transcript	TCONS_00017983	1.715056004	0.002422	0.999966
aars-1	WBGene00000196	transcript	TCONS_00010515	1.710321348	0.046796	0.999966
set-26	WBGene00013106	transcript	TCONS_00033908	1.627965777	0.031279	0.999966
pgl-3	WBGene00003994	transcript	TCONS_00035342	1.62126183	0.009898	0.999966
.	NA	transcript	TCONS_00010782	1.620146382	0.031022	0.999966
C05D2.10	WBGene00015470	transcript	TCONS_00014452	1.592650276	0.023219	0.999966
Y43E12A.3	WBGene00012795	transcript	TCONS_00019199	1.589986933	0.003535	0.999966
egl-30	WBGene00001196	transcript	TCONS_00000216	1.542385467	0.02562	0.999966
C14A4.3	WBGene00007556	transcript	TCONS_00007379	1.522919077	0.015894	0.999966
CD4.8	WBGene00016993	transcript	TCONS_00039565	1.517044335	0.023906	0.999966
asd-1	WBGene00011279	transcript	TCONS_00011694	1.479331847	0.032117	0.999966
lin-37	WBGene00003022	transcript	TCONS_00014727	1.457347041	0.000824	0.570739
mtm-1	WBGene00003475	transcript	TCONS_00000737	1.43404089	0.047324	0.999966
B0272.3	WBGene00007129	transcript	TCONS_00044660	1.430161988	0.023535	0.999966

Y95D11A.3	WBGene00045434	transcript	TCONS_00001906	1.428964698	0.037743	0.999966
Y92H12BR.3	WBGene00022369	transcript	TCONS_00000160	1.399835725	0.035558	0.999966
F38H4.10	WBGene00009551	transcript	TCONS_00019401	1.396394372	0.00779	0.999966
F10D2.13	NA	transcript	TCONS_00039931	1.355791074	0.026141	0.999966
F10D2.15	NA	transcript	TCONS_00035808	1.341420193	0.026133	0.999966
W01A11.7	WBGene00020912	transcript	TCONS_00039763	1.32786249	0.042122	0.999966
Y45F10D.10	WBGene00012889	transcript	TCONS_00029400	1.319319993	0.032374	0.999966
chin-1	WBGene00015267	transcript	TCONS_00013700	1.317339541	0.016654	0.999966
usp-39	WBGene00017280	transcript	TCONS_00005623	1.315422527	0.034793	0.999966
swah-1	WBGene00007985	transcript	TCONS_00001592	1.310523019	0.004272	0.999966
ife-3	WBGene00002061	transcript	TCONS_00038656	1.293136003	0.038879	0.999966
met-2	WBGene00019883	transcript	TCONS_00012603	1.285540034	0.034932	0.999966
tol-1	WBGene00006593	transcript	TCONS_00000049	1.257417852	0.043807	0.999966
pes-9	WBGene00003982	transcript	TCONS_00041793	1.237161115	0.045108	0.999966
C13C4.4	WBGene00007548	transcript	TCONS_00041195	1.235446018	0.029972	0.999966
R151.8	WBGene00020111	transcript	TCONS_00014782	1.234246148	0.021395	0.999966
C50F4.16	WBGene00008238	transcript	TCONS_00040437	1.220034485	0.047208	0.999966
F53E4.2	WBGene00206516	transcript	TCONS_00037755	1.219397202	0.049769	0.999966
rop-1	WBGene00004405	transcript	TCONS_00040628	1.211875512	0.003898	0.999966
dhps-1	WBGene00012460	transcript	TCONS_00007693	1.191625486	0.0188	0.999966
hcp-1	WBGene00001829	transcript	TCONS_00035704	1.190692714	0.033482	0.999966
nape-2	WBGene00021370	transcript	TCONS_00025747	1.183164676	0.030967	0.999966
rnp-4	WBGene00004387	transcript	TCONS_00011747	1.172567201	0.048033	0.999966
F53F8.5	WBGene00010002	transcript	TCONS_00042840	1.164519548	0.031077	0.999966
ZK858.7	WBGene00014120	transcript	TCONS_00004182	1.159967717	0.018093	0.999966
Y43D4A.4	WBGene00012790	transcript	TCONS_00024769	1.155201963	0.013497	0.999966
rskd-1	WBGene00010096	transcript	TCONS_00041241	1.152642043	0.028376	0.999966
F01D4.5	WBGene00008488	transcript	TCONS_00028466	1.147625545	0.043988	0.999966
mms-19	WBGene00016060	transcript	TCONS_00035459	1.144227692	0.025713	0.999966
K07C5.2	WBGene00010625	transcript	TCONS_00036434	1.139850747	0.015099	0.999966
arf-1.2	WBGene00000182	transcript	TCONS_00012089	1.139338898	0.021533	0.999966
prp-21	WBGene00004188	transcript	TCONS_00005284	1.138573279	0.014038	0.999966
arrd-13	WBGene00011054	transcript	TCONS_00007949	1.136127057	0.008785	0.999966
Y43D4A.3	WBGene00012789	transcript	TCONS_00034040	1.135776908	0.015255	0.999966
gly-4	WBGene00001629	transcript	TCONS_00042715	1.127296623	0.013199	0.999966
ZK1307.9	WBGene00014250	transcript	TCONS_00007222	1.124847571	0.044766	0.999966
T20B12.1	NA	transcript	TCONS_00012405	1.114075053	0.001802	0.999966
K07G5.6	NA	transcript	TCONS_00003738	1.113802215	0.026018	0.999966
vnut-1	WBGene00010758	transcript	TCONS_00008072	1.113355816	0.034025	0.999966
deps-1	WBGene00022034	transcript	TCONS_00000054	1.10627448	0.040388	0.999966
eif-3.I	WBGene00001232	transcript	TCONS_00000295	1.091279722	0.049054	0.999966
F32B4.4	WBGene00009314	transcript	TCONS_00001975	1.08947315	0.02112	0.999966
cpt-2	WBGene00011122	transcript	TCONS_00019248	1.089137826	0.019819	0.999966
henn-1	WBGene00015349	transcript	TCONS_00012564	1.08909032	0.023997	0.999966
ppk-2	WBGene00004088	transcript	TCONS_00011391	1.08639034	0.043162	0.999966

C03C10.4	NA	transcript	TCONS_00014124	1.086205874	0.033953	0.999966
ZK546.5	WBGene00022762	transcript	TCONS_00006095	1.084629637	0.033367	0.999966
ZK856.8	NA	transcript	TCONS_00040600	1.083332679	0.041651	0.999966
haf-2	WBGene00001812	transcript	TCONS_00009621	1.081226915	0.020519	0.999966
thoc-2	WBGene00015813	transcript	TCONS_00012200	1.063021138	0.008136	0.999966
laat-1	WBGene00021546	transcript	TCONS_00008221	0.924758658	0.013392	0.999966
F56B3.2	WBGene00018928	transcript	TCONS_00025383	0.874564218	0.029909	0.999966
.	NA	transcript	TCONS_00045329	0.874536667	0.020491	0.999966
F54D11.3	WBGene00018813	transcript	TCONS_00039391	0.870205793	0.011504	0.999966
C06A5.2	WBGene00015500	transcript	TCONS_00000888	0.867890785	0.045766	0.999966
R02D3.3	WBGene00019821	transcript	TCONS_00025307	0.865761529	0.032531	0.999966
C06A5.3	WBGene00015501	transcript	TCONS_00000885	0.850733069	0.046492	0.999966
par-4	WBGene00003919	transcript	TCONS_00038219	0.849279991	0.032357	0.999966
T15B7.15	WBGene00020527	transcript	TCONS_00039852	0.829102465	0.005034	0.999966
F01F1.15	WBGene00017169	transcript	TCONS_00014502	0.815600584	0.02567	0.999966
R01B10.6	WBGene00019808	transcript	TCONS_00039673	0.80804297	0.016612	0.999966
Y40C5A.4	WBGene00021497	transcript	TCONS_00027734	0.8055999	0.031696	0.999966
kel-8	WBGene00020952	transcript	TCONS_00035055	0.804518187	0.013131	0.999966
clp-6	WBGene00000546	transcript	TCONS_00025474	0.796979102	0.005629	0.999966
oig-4	WBGene00043050	transcript	TCONS_00006779	0.792278748	0.03251	0.999966
gly-14	WBGene00001639	transcript	TCONS_00014000	0.784697604	0.040655	0.999966
tba-4	WBGene00006530	transcript	TCONS_00007437	0.783269993	0.022244	0.999966
H24K24.3	WBGene00019240	transcript	TCONS_00034780	0.778835377	0.033567	0.999966
kin-31	NA	transcript	TCONS_00012669	0.765730916	0.044035	0.999966
Y38F2AR.10	WBGene00021428	transcript	TCONS_00025560	0.76301085	0.04958	0.999966
C07A9.9	WBGene00007405	transcript	TCONS_00015313	0.753842179	0.034148	0.999966
C27F2.1	WBGene00016165	transcript	TCONS_00011926	0.746033626	0.006073	0.999966
.	NA	transcript	TCONS_00046325	0.742973457	0.004007	0.999966
C28D4.10	WBGene00007796	transcript	TCONS_00018914	0.741282489	0.041249	0.999966
F23H11.2	WBGene00017758	transcript	TCONS_00011255	0.739694572	0.041343	0.999966
ZC262.2	WBGene00022579	transcript	TCONS_00012593	0.73729853	0.035898	0.999966
cyn-2	WBGene00000878	transcript	TCONS_00013500	0.736146058	0.014026	0.999966
fzr-1	WBGene00001510	transcript	TCONS_00010122	0.730145636	0.036981	0.999966
ZK795.2	WBGene00014082	transcript	TCONS_00028949	0.727836902	0.03633	0.999966
rpoa-12	WBGene00007616	transcript	TCONS_00041744	0.726742317	0.020541	0.999966
immp-1	WBGene00007021	transcript	TCONS_00013248	0.718953015	0.027641	0.999966
mtrr-1	WBGene00006510	transcript	TCONS_00007152	0.715948735	0.009827	0.999966
C56G2.9	WBGene00016982	transcript	TCONS_00014591	0.714301942	0.036593	0.999966
fbxa-113	WBGene00013757	transcript	TCONS_00038529	0.703369558	0.012578	0.999966
knl-3	WBGene00020392	transcript	TCONS_00034894	0.699350789	0.007381	0.999966
Y39G10AR.32	WBGene00219275	transcript	TCONS_00002797	0.682186142	0.029242	0.999966
rab-39	WBGene00004286	transcript	TCONS_00010052	0.667743504	0.044449	0.999966
F40F9.14	NA	transcript	TCONS_00036326	0.664515698	0.007308	0.999966
nfi-1	WBGene00003592	transcript	TCONS_00006753	0.661512998	0.030067	0.999966
glh-4	WBGene00001601	transcript	TCONS_00000488	0.634619276	0.032161	0.999966

ztf-17	WBGene00011639	transcript	TCONS_00009732	0.621995643	0.01946	0.999966
E02H9.3	WBGene00017101	transcript	TCONS_00011444	0.616669207	0.038718	0.999966
nrd-1	WBGene00017004	transcript	TCONS_00003185	0.609619925	0.010994	0.999966
F13G3.6	WBGene00008766	transcript	TCONS_00003782	0.601508034	0.012804	0.999966
F48F7.6	WBGene00009851	transcript	TCONS_00045500	0.600462993	0.044095	0.999966
ncl-1	WBGene00003559	transcript	TCONS_00012462	0.594957679	0.017765	0.999966
nop-1	WBGene00017774	transcript	TCONS_00012134	0.572447032	0.039582	0.999966
Y52B11A.8	WBGene00013127	transcript	TCONS_00001912	0.566559844	0.005036	0.999966
D2096.12	WBGene00017079	transcript	TCONS_00018628	0.566495517	0.009628	0.999966
T10C6.7	WBGene00011689	transcript	TCONS_00042104	0.564635801	0.020073	0.999966
cec-10	WBGene00022831	transcript	TCONS_00000599	0.561754889	0.041896	0.999966
lst-6	WBGene00016889	transcript	TCONS_00009546	0.558756428	0.032953	0.999966
F25H8.1	WBGene00009131	transcript	TCONS_00028314	0.548196043	0.029995	0.999966
rps-29	WBGene00004498	transcript	TCONS_00011230	0.529290595	0.049658	0.999966
.	NA	transcript	TCONS_00011860	0.519827678	0.014317	0.999966
.	NA	transcript	TCONS_00040790	0.507744641	0.001001	0.650143
C41H7.4	WBGene00016574	transcript	TCONS_00005693	0.506534214	0.045959	0.999966
F53F10.3	WBGene00018765	transcript	TCONS_00000507	0.503856376	0.041637	0.999966
sqrd-1	WBGene00008538	transcript	TCONS_00020591	0.489451128	0.033976	0.999966
tag-325	WBGene00008006	transcript	TCONS_00011863	0.485491478	0.023754	0.999966
pin-2	WBGene00004030	transcript	TCONS_00019608	0.4695527	0.031608	0.999966
T07E3.3	WBGene00020314	transcript	TCONS_00012299	0.460328695	0.003467	0.999966
kal-1	WBGene00002181	transcript	TCONS_00005063	0.452834078	0.023441	0.999966
B0280.17	WBGene00044674	transcript	TCONS_00014745	0.45229781	0.045052	0.999966
D1054.1	WBGene00008370	transcript	TCONS_00040765	0.441249101	0.033316	0.999966
Y54G2A.19	WBGene00021884	transcript	TCONS_00025613	0.420066491	0.022999	0.999966
osta-3	WBGene00012182	transcript	TCONS_00008126	0.417432257	0.048016	0.999966
F21A10.2	NA	transcript	TCONS_00047939	0.396978229	0.046126	0.999966
ZK1127.3	WBGene00022850	transcript	TCONS_00006633	0.395824537	0.029205	0.999966
F56A6.4	NA	transcript	TCONS_00002626	0.392221773	0.013175	0.999966
T05H4.11	WBGene00020274	transcript	TCONS_00039743	0.387241922	0.046329	0.999966
rfp-1	WBGene00007008	transcript	TCONS_00012601	0.379588851	0.005634	0.999966
rfp-1	WBGene00007008	transcript	TCONS_00012600	0.370728287	0.004793	0.999966
K12D12.5	WBGene00010787	transcript	TCONS_00007657	0.366474977	0.036945	0.999966
lin-66	WBGene00001562	transcript	TCONS_00020157	0.34892521	0.031793	0.999966
21ur-2599	NA	transcript	TCONS_00021712	0.34880291	0.014735	0.999966
21ur-9510	NA	transcript	TCONS_00031104	0.347298354	0.014844	0.999966
C06A5.6	WBGene00015504	transcript	TCONS_00003473	0.340469106	0.002592	0.999966
ubc-12	WBGene00006707	transcript	TCONS_00002013	0.337138424	0.024218	0.999966
sop-3	WBGene00004946	transcript	TCONS_00002853	0.330892759	0.035119	0.999966
mib-1	WBGene00012933	transcript	TCONS_00015615	0.32882473	0.018226	0.999966
Y73B3A.3	NA	transcript	TCONS_00046119	0.322853511	0.030521	0.999966
F10E7.2	WBGene00017344	transcript	TCONS_00006665	0.3195963	0.04689	0.999966
D2005.4	WBGene00008399	transcript	TCONS_00001257	0.292242944	0.031216	0.999966
mtm-3	WBGene00003476	transcript	TCONS_00014064	0.285715248	0.038985	0.999966

F11A10.5	WBGene00008686	transcript	TCONS_00019464	0.276162192	0.014348	0.999966
dlst-1	WBGene00020950	transcript	TCONS_00039818	0.275751858	0.03353	0.999966
F52D2.12	WBGene00219451	transcript	TCONS_00043161	0.267729713	0.045361	0.999966
ucr-2.1	WBGene00012158	transcript	TCONS_00045143	0.267069649	0.000379	0.338368
adr-2	WBGene00000080	transcript	TCONS_00014784	0.26369516	0.023349	0.999966
C13F10.6	WBGene00015745	transcript	TCONS_00039951	0.249431115	0.039032	0.999966
zip-1	WBGene00006986	transcript	TCONS_00013306	0.24419306	0.000391	0.338368
F27B3.5	NA	transcript	TCONS_00014635	0.219705085	0.029906	0.999966
dnj-25	WBGene00001043	transcript	TCONS_00042847	0.217036217	0.028272	0.999966
R08D7.5	WBGene00011145	transcript	TCONS_00012727	0.201236113	0.025693	0.999966
selb-1	NA	transcript	TCONS_00002221	0.196565959	0.013954	0.999966
set-26	WBGene00013106	transcript	TCONS_00033909	0.195379591	0.026328	0.999966
B0205.6	WBGene00015021	transcript	TCONS_00001866	0.187884937	0.049898	0.999966
fut-3	WBGene00006402	transcript	TCONS_00009207	0.163474947	0.032707	0.999966
emc-5	WBGene00195248	transcript	TCONS_00007585	0.163066383	0.024427	0.999966
math-33	WBGene00010406	transcript	TCONS_00036629	0.161994309	0.035765	0.999966
dpf-4	WBGene00001057	transcript	TCONS_00012115	0.154170485	0.022565	0.999966
sdz-27	WBGene00011124	transcript	TCONS_00019251	0.132836757	0.025735	0.999966
zig-7	WBGene00006984	transcript	TCONS_00000668	0.126111675	0.017533	0.999966
ptc-1	WBGene00004208	transcript	TCONS_00006855	0.125948211	0.027702	0.999966
F42A6.6	WBGene00018328	transcript	TCONS_00025681	0.116357956	0.030007	0.999966
crn-3	WBGene00000796	transcript	TCONS_00007385	0.111815052	0.045284	0.999966
Y48G8AL.10	WBGene00021689	transcript	TCONS_00002691	0.097467723	0.024067	0.999966
Y45F10D.7	WBGene00012887	transcript	TCONS_00020036	0.094399161	0.028954	0.999966
arp-11	WBGene00016793	transcript	TCONS_00027876	0.089729687	0.01539	0.999966
Y47G6A.14	WBGene00021640	transcript	TCONS_00002974	0.087148884	0.000613	0.45509
scrm-4	WBGene00008681	transcript	TCONS_00004716	0.076845336	3.75E-06	0.009735
ctl-3	WBGene00013220	transcript	TCONS_00011007	0.071959993	1.77E-05	0.029118
F32B6.3	WBGene00009320	transcript	TCONS_00028296	0.064267428	0.022443	0.999966
R05D3.2	WBGene00019877	transcript	TCONS_00012605	0.062601546	0.026092	0.999966
ZK418.5	WBGene00022734	transcript	TCONS_00014729	0.062560955	0.000207	0.239352
F55F10.1	WBGene00018898	transcript	TCONS_00016611	0.061576426	0.024748	0.999966
faah-4	WBGene00013232	transcript	TCONS_00015695	0.057956971	6.46E-09	3.35E-05
C14C11.2	WBGene00015766	transcript	TCONS_00035491	0.057951613	0.045849	0.999966
arx-6	WBGene00000204	transcript	TCONS_00011898	0.053914916	7.58E-06	0.015754
M05D6.2	WBGene00010875	transcript	TCONS_00006972	0.048176434	0.000476	0.380518
T24H7.2	WBGene00020781	transcript	TCONS_00006429	0.045977222	0.024317	0.999966
acdh-3	WBGene00019433	transcript	TCONS_00003586	0.039078117	0.03097	0.999966
F36A2.13	NA	transcript	TCONS_00004098	0.037068928	0.024054	0.999966
sup-17	WBGene00006324	transcript	TCONS_00001442	0.034755212	0.025715	0.999966

Table S2: Differentially expressed reproduction genes. Related to Figure S3.

RNA-seq identification of 61 genes differentially expressed between BPA and DMSO and belonging to the GO term "reproduction" GO:0000003.

F55F10.1, NFI-1, FOX-1, IFE-3, ARF-1.2, SGO-1, Y47G6A.14, TBA-4, EIF-3.I, B0205.6, E02H9.3, USP-39, R151.8, CSNK-1, THOC-2, AARS-1, HCP-1, DEPS-1, SOP-2, SOP-3, FZR-1, MET-2, C14C11.2, B0280.17, NOP-1, DNJ-22, Y45F10D.7, SYX-5, SIR-2.4, RNP-4, RPS-29, C06A5.3, PTC-1, KEL-8, TRA-3, F32B6.3, DLST-1, Y95D11A.3, KAL-1, F23H11.2, T08B2.5, LIN-66, LIN-37, RFP-1, R02D3.3, Y43E12A.3, UBC-12, KNL-3, MTM-3, RPOA-12, ZK858.7, UAF-2, F53E4.2, EGL-30, F11A10.5, UFD-2, W03F8.4, PQN-59, ARP-11, PRP-21, GLH-4

Table S3: Broad peak counts. Related to Figure 2 and S3.

Count of all identified broad peaks by MACS2 broad peak function

	H3K9me3	H3K27me3
water	3,740	19,810
DMSO	4,951	21,741
BPA	4,888	19,019

Table S4: ChIP-seq GO analysis. Related to Figure 2.

GO analysis of genes associated with a loss of H3K27me3

GO biological process complete	Reference gene list	Uploaded gene list	Expected gene count	Upload fold enrichment	P-value	FDR
Cellular response to unfolded protein (GO:0034620)	77	9	1.9	4.74	2.25E-04	2.58E-02
Steroid hormone mediated signaling pathway (GO:0043401)	280	19	6.91	2.75	1.27E-04	1.84E-02
Intracellular transport (GO:0046907)	382	22	9.43	2.33	3.98E-04	4.21E-02
Regulation of transcription, DNA-templated (GO:0006355)	935	47	23.08	2.04	8.54E-06	2.04E-03
Ion transport (GO:0006811)	724	35	17.87	1.96	2.47E-04	2.77E-02
Transmembrane transport (GO:0055085)	855	41	21.1	1.94	8.12E-05	1.35E-02
Organelle organization (GO:0006996)	1,150	50	28.38	1.76	1.94E-04	2.32E-02
Cellular macromolecule metabolic process (GO:0044260)	2,565	93	63.3	1.47	1.81E-04	2.27E-02
Nitrogen compound metabolic process (GO:0006807)	3,679	131	90.8	1.44	1.05E-05	2.30E-03

Table S5: Histone PTM quantitation. Related to Figure 2 and Figure 4.

Histone PTM level change following DMSO or BPA exposure following Luminex based multiplex quantitation assay

	H3K9me1	H3K9me2	H3K9me3	H3K27me2	H3K27me3	H3K36me3
DMSO	0.44 (6.2E-5)	0.11 (1.2E-4)	0.25 (9E-3)	0.13 (9.5E-3)	0.28 (2E-3)	0.28 (9.1E-4)
BPA	0.31 (9.9E-4)	0.08 (5.5E-3)	0.19 (1.9E-3)	0.06 (3.5E-3)	0.20 (8.7E-3)	0.31 (5.3E-3)
% change	-30.37	-33.41	-24.71	-56.27	-29.07	+8.40

CHAPTER 4
Transgenerational germline dysfunction due to BPA exposure in *C. elegans*

Summary

BPA has been shown to alter the germline epigenome and cause reproductive dysfunction both directly and for multiple generations after the initial exposure (multigenerational and transgenerational) (1). Our aim is to further characterize the transgenerational mechanisms through which BPA elicits reproductive defects such as increased embryonic lethality and germline apoptosis. Previous findings have shown that BPA can affect the meiotic processes of synapsis and recombination in worms directly exposed (2)(3). Our work focuses on the transgenerational effects of BPA on meiotic recombination processes, specifically double strand break repair and homologous chromosome crossover dynamics.

Introduction

The process of meiosis generates haploid gametes from diploid precursors through a specialized cell division program. This program facilitates proper homologous pairing and recombination during prophase I, which are essential to ensure proper chromosome inheritance (4). Homologous pairing enables homologous chromosomes find each other and assume side-by-side alignment and is necessary for crossover (CO) (5). Recombination allows the exchange of genetic material between homologous chromosomes and is facilitated through these COs. Both pairing and recombination are tightly regulated to ensure proper execution of the meiotic process (4).

Environmental toxicant exposures can directly and indirectly affect the homeostasis of meiotic processes, and thus it is important to investigate their underlying effects. BPA has been shown to alter meiotic progression in mice, monkeys and *C. elegans* (3,6,7). Specifically, exposure to BPA resulted in impaired chromosome synapsis and disruption of meiotic double-strand break repair (DSBR) progression, which is correlated with increased sterility and embryonic lethality (2,3). Recent work in our lab observed an increase in embryonic lethality and germline

nuclei apoptosis from both direct and transgenerational BPA exposures (P0-F3)(1). We are therefore interested in investigating if these transgenerational BPA effects are mediated similarly to those observed from direct exposures. This chapter will examine BPA's effects on transgenerational reproductive dysfunction, with a focus on the meiotic recombination process.

Results

Transgenerational BPA exposure leads to increased aneuploidy

In our previous work we observed decreased fertility stemming from BPA exposure that lasted until the F3 generation. Specifically, we saw an increase in embryonic lethality in BPA groups (F1 and F3) when compared to DMSO and water controls. Embryonic lethality is reflective of the viability of a worms' progeny and often a proxy for germline dysfunction. It can be induced by the production of gametes and embryos with an abnormal number of chromosomes (termed aneuploidy). In order to assess direct and transgenerational effects of BPA on chromosome segregation, we utilized a GFP transgenic Pxol-1::GFP containing strain (TY2441) that reports the induction of aneuploidy in early embryos (8). Specifically, GFP is expressed in embryonic cells that inherit one X-chromosome instead of the two it normally would. Previously, the strain has been utilized to report errors in chromosome segregation that result from germline disruption and can be both visualized and quantified using fluorescence microscopy (9,10). We utilized this strain with the established exposure protocol and assessed the F1 (direct) and F3 (transgenerational) worm generations for the presence of GFP positive embryos. At F1, BPA had a significant induction of aneuploidy in adult worm embryos when compared to both DMSO and water controls (Figure 1B, F1: H20 0.63±0.31, DMSO 2.04±0.57, BPA 8.27±1.71, **P<0.01), while at F3, we observed that BPA induced an increase in aneuploidy, but only trended toward significance when compared to DMSO (Figure 1C, F3: H20 0.25±0.25, DMSO 1.25±1.25, BPA 6.70±2.33). Results

display the induction of aneuploidy caused by BPA may be correlated with the transgenerational embryonic lethality previously observed.

Transgenerational impact of BPA on DSB initiation

In addition to the effects on embryonic lethality observed from transgenerational BPA exposure, another effect indicative of germline dysfunction is induction of germline apoptosis. Apoptosis in the germline is a checkpoint response to terminal chromosome damage, therefore we need to investigate what responses are being triggered to induce these effects resulting in cell culling. Previous results showed us that the BPA's effects on fertility mediated through disruption of meiotic recombination processes (2,3). SPO-11 is a conserved enzyme that begins the recombination process by introducing DSBs (11). SPO-11's activity is tightly regulated, ensuring that breaks occur in a structural context where they can be repaired in an efficient matter but also to optimize number, timing, and distribution of DSBs (4). This optimization is a major determinant of CO patterns, and thus we can assess how BPA affects recombination from break formation all the way to crossover resolution directly and transgenerationally. We can focus on recombination dynamics utilizing mutant worms homozygous for the *spo-11* deletion, as they display an array of phenotypes indicating errors of meiotic chromosome segregation, but specifically, they lack *spo-11* dependent apoptosis (11–13). We exposed a *spo-11* balanced strain (AV157) to BPA at P0, then maintained the population until F3 to assess the presence of apoptotic nuclei. The AV157 strain carries a lethal balancer that allows us to select for *spo-11* homozygotes. A third of the population is *spo-11* homozygotes, another third will be heterozygotes (which we will use as a control), and the last third will not survive. After exposures, we maintain the heterozygote population until F2 then select the homozygous offspring (F3), grow to adulthood and assess induction of apoptosis. In worms transgenerationally exposed to BPA, apoptosis induction was not rescued and was significantly higher than in the controls, very similar to our own heterozygous

controls (Figure 2: H20 2.97±0.25, DMSO 4.35±0.38, BPA 5.6±0.52, *P<0.05, ***P<0.001). These results indicate that BPA may be either inducing double strand breaks itself and/or apoptosis, transgenerationally.

DNA strand exchange protein RAD-51 is transgenerationally impacted by BPA during early pachytene

To further assess BPA's effects on germline dysfunction causing induction of apoptosis, we can focus on another important protein for DSB and DSB repair dynamics. RAD-51 is a recombinase protein that promotes homology search and strand invasion into homologous chromosomes as an effort to repair DSBs introduced by SPO-11(11). Our assessment looked further into this phenomenon by assessing transgenerational effects of BPA on RAD-51 turn-over rates. We found an elevation of RAD-51 foci in the early and mid-pachytene regions of our adult *C. elegans* germlines. In F1 (directly exposed worms) RAD-51 levels remained indistinguishable from controls, with exception of early pachytene zone (EPZ, Figure 3A), while RAD-51 levels in BPA F3 worms are elevated during both early and mid-pachytene (EPZ, MPZ, Figure 3B) but resolve by late pachytene. Our findings indicate a different mechanism by which BPA can induce additional double strand breaks to be repaired.

BPA affects crossover sites during late pachytene, directly and transgenerationally

DSBs induced by SPO-11 begin the meiotic recombination process, and these can result in the formation of crossovers as means of repair. Homeostasis in meiotic machinery ensures a CO event per chromosome, six in *C. elegans*, and is known as CO assurance (4). In *C. elegans,* COSA-1 (cyclin-like protein) is required for CO formation and predicted to function in CO designation (14). Six COSA-1 foci are evident in late pachytene germ-cell nuclei, designating the 6 obligate CO's in each chromosome (Figure 4A).

We assessed COSA-1 foci in a COSA-1::GFP tagged *C. elegans* strain (AV604) directly and transgenerationally exposed to BPA (15). Results display a difference in distribution of foci per germ cell nuclei in the adult germline of BPA exposed worms both directly and transgenerationally (Fig 1B, COSA-1 F1: DMSO vs BPA $p<0.001$, F3: DMSO vs BPA $p<000.1$, N=250 nuclei in 18-25 worms per group, Chi-square test). To validate, we also assessed a ZHP-3::GFP strain (UV7), as the ZHP-3 protein is a cytological marker for CO formation, as it localizes to sites of crossover recombination in late pachytene and diplotene(16). Similarly, ZHP-3 indicated a difference in distribution in F1 and F3 BPA exposed worms (Figure 1C ZHP-3 F1: DMSO vs. BPA $p=0.1$, F3: DMSO vs. BPA $p<0.01$, N= 170 nuclei, 7-10 worms per group, Chi square test). This variation suggests that meiotic recombination is affected by altering homologous crossover dynamics.

Conclusions and future directions

Our research on potential mechanisms behind BPA's transgenerational effects on reproductive dysfunction show a glimpse of a larger picture involving many players within the meiotic process. Our first assessment on mechanisms mediating elevated embryonic lethality both directly and at the F3 generation, showed effects could be mediated through chromosome mis-segregation as we saw higher incidence of aneuploidy in embryos (Figure 1). Interestingly, we examined diakinesis oocytes in all of the exposure groups and failed to see any change from the normal 6 bivalents per nucleus (data now shown). With the increased fold induction of aneuploidy seen at F1 and F3 generations, it is surprising that diakinesis occurs normally (given results indicating crossover disruption, Figure 4). Going forward, we propose to take a closer look at diakinesis chromosomes where there may be synaptonemal complex/chiasma damage present that is not readily visualized. Previous studies have revealed that at AIR-2 localizes on the short arms of paired homologous chromosomes, replacing synaptonemal complex proteins, and

promotes the separation of homologs at the end of meiosis (4). By monitoring its presence in the appropriate location of the short arms of chromosomes during diakinesis, by utilizing a GFP-tagged strain labeling AIR-2 or antibody, we can look beyond the presence of six bivalents but also at the underlying proteins enabling these chromosomes to proceed past the end of meiotic prophase I (17).

Our results also indicate DSBR pathway is altered, as F3 worms transgenerationally exposed to BPA display a DSB-independent apoptotic response (Figure 2). PCH-2, a protein phosphatase (AAA-ATPASE) important in the synapsis checkpoint as it is required for induction of apoptosis when synapsis fails, can tell us if we're looking at effects that are inducing spo-11-independent apoptosis at the transgenerational level. We can use a pch-2 mutant and expose it to BPA, and assess if apoptosis is still present, indicating the dependency of a synapsis checkpoint. Additionally, we can also asses if the cell death we are witnessing is indeed apoptosis or necrosis, or a combination of both. Necrosis is cell death caused by an external factor, while apoptosis constitutes programmed cell death. Utilizing a GFP-tagged strain, for CED-1 that labels engulfed apoptotic nuclei, we can validate the results we observed with acridine orange. Conversely, we can also utilize a ced-3 or ced-4 loss of function mutant to ablate cell programmed apoptosis (18) and assess any left-over presence of cell death (presumably necrosis). This can allow us to explore the nature of the induction of cell death we observe in the F3 generation.

Our assessment of strand invasion protein RAD-51 turnover rate added to the narrative of BPA's transgenerational defects through DSBR, as rates of RAD-51 foci were elevated during early and mid-pachytene (Figure 3). We also observed transgenerational effects on CO dynamics, as CO proteins COSA-1 and ZHP-3, were disrupted in the F3 generation (Figure 4). We observe resolution of DSBs, as levels of RAD-51 are indistinguishable between exposure groups during late pachytene, yet there is disruption of CO well into late pachytene. One way to assess these results is to focus on ATL-1, a homolog of ATR and kinase that enables detection of DSBs. Once

activated by unrepaired DSBs, ATL-1 (ATR) can delay meiotic progression (recombination checkpoint) or can alternatively provide an opportunity to cull cells unable to complete DSBR through apoptosis (reviewed in (19)). In a *C. elegans* mutant lacking ATL-1, meiotic DSBs can be repaired, but crossover formation is defective due to chromosome mis-segregation (20,21). If ATL-1 is being targeted by transgenerational BPA exposure, this would explain the increase in DSBs (RAD-51 increase) during early pachytene, and disruption of COs in late pachytene.

Together, our findings begin to tell a narrative of a potential mechanism by which BPA is inducing transgenerational reproductive dysfunction. We see effects on DSBR, but we must still investigate the larger meiosis picture, as apoptosis and embryonic lethality can induced prior to DSB initiation of recombination, during synapsis and pairing processes. Moving forward It will also be critical to take into account our previous findings indicating the importance of epigenetic machinery in advancing these transgenerational defects (1). Assessment of the influence of epigenetic marks on both chromatin structure and the proteins facilitating meiotic progression will connect the importance of histone demethylase activity on transgenerational reproductive dysfunction.

Experimental Procedures

Culture conditions and strains

Standard methods of culturing and handling of *C. elegans* were followed (22). Worms were maintained on nematode growth medium (NGM) plates streaked with OP50 E. coli. Strains used in this chapter were obtained from the *C. elegans* Genetics Center (CGC) and others include the following: AV604 (meIs8[unc-199(+)pie-1promoter::gfp::cosa-1] II; unc-119(ed3) III), UV7 (unc-119(ed3)III; jfls 2 jfls 2 (mi16, pie-promoter::GFP::zhp-3+unc-119(+)). AV157 (spo-11 (me44)/nT1 [unc-?(n754) let-? qls50] (IV;V)), TY2441 (yls34 (Pxol-1::GFP+rol-6 (pRF4)),

Chemical exposure protocol

The exposure was performed as described in Lundby et al., 2016 (see Appendix). BPA was obtained from Sigma Aldrich and dissolved in DMSO to a stock concentration of 100mM. Worms were synchronized by bleaching an adult population of either strain, plating the eggs and allowing the population to reach L4 larval stage (50-52 hours). Worms were then exposed for 48 hours, and After 48 hours, then allowed to recover on NGM plates for 1-2 hours (mixed population) and recovered there.

Chromosome missegregation/aneuploidy assay

TY2441 (Pxol-1::GFP) worms are synchronized and collected 16-20 hours post-L4 at F1 and F3 generations after direct exposures. Worms were scored for GFP positive embryo expression using a Nikon H600L microscope at 40X magnification.

Apoptosis assay

Apoptosis assay was performed by Acridine Orange staining on synchronized adult AV157

(spo-11) hermaphrodites collected at 20-24 hours post-L4 as previously described (Allard and Colaiacovo, 2011; Chen et al., 2016).

Rad-51 Immunofluorescence

Immunofluorescence images were collected at 0.5 μm z intervals with an Eclipse Ni-E microscope (Nikon) and a cooled CCD camera (model CoolSNAP HQ, Photometrics) controlled by the NIS Elements AR system (Nikon). The images presented and quantified are projections approximately halfway through 3D data stacks of *C. elegans* gonads, which encompass entire nuclei. RAD-51 quantification from mitotic zone to late pachytene zone germ cell nuclei was performed with Image J software. F3 worms were staged at L4 and gonad dissection and immunofluorescence was performed 20-24hrs post-L4 as previously described (Chen et al., 2016). Primary antibody was used at the following dilution: rabbit α-RAD-51 1:10,000. Secondary antibody was used at the following dilutions: Cy3 α-rabbit, 1:700; (Jackson ImmunoResearch).

RAD-51 time-course analysis

RAD-51 foci in germline nuclei of age-matched (20-24 hours post-L4) hermaphrodites were quantified as described in (Allard and Colaiacovo, 2010) with the following modification: the germline was divided by stages of meiotic prophase I and only the nuclei in the middle of each stage were scored.

GFP-tagged worm strain analysis

Worms were selected at L4 stage and placed overnight at 25°C. They were then collected at 20-24 hours post-L4 stage and dissected in 10μl of M9. Excess liquid was removed, and 10μl of Hoechst 33342 (10mg/mL) was added at a concentration of 1μg/ml. Slides are covered, and

allowed to settle for 5-10min, then imaged on an Eclipse Ni-E microscope (Nikon) and a cooled CCD camera (model CoolSNAP HQ, Photometrics) controlled by the NIS Elements AR system (Nikon). After image collection, late-pachytene COSA-1 and ZHP-3 foci were quantified with Image J software.

Statistical Analyses

Unless indicated otherwise, an unpaired t-test assuming unequal variance with Welch's correction was applied. For multi-group comparisons, a one-way ANOVA with Sidak correction or two-way ANOVA was used. For crossover foci distribution analysis, Chi-square test was applied.

References

1. Camacho J, Truong L, Kurt Z, Chen Y-W, Morselli M, Gutierrez G, et al. The Memory of Environmental Chemical Exposure in C. elegans Is Dependent on the Jumonji Demethylases jmjd-2 and jmjd-3/utx-1. Cell Reports. 2018 May;23(8):2392–404.

2. Chen Y, Shu L, Qiu Z, Lee DY, Settle SJ, Que Hee S, et al. Exposure to the BPA-Substitute Bisphenol S Causes Unique Alterations of Germline Function. Cohen PE, editor. PLOS Genetics. 2016 Jul 29;12(7):e1006223.

3. Allard P, Colaiacovo MP. Bisphenol A impairs the double-strand break repair machinery in the germline and causes chromosome abnormalities. Proceedings of the National Academy of Sciences. 2010 Nov 23;107(47):20405–10.

4. Hillers KJ. Meiosis. WormBook. 2017 May 4;1–43.

5. MacQueen AJ, Villeneuve AM. Nuclear reorganization and homologous chromosome pairing during meiotic prophase require C. elegans chk-2. Genes Dev. 2001 Jul 1;15(13):1674–87.

6. Susiarjo M, Hassold TJ, Freeman E, Hunt PA. Bisphenol A Exposure In Utero Disrupts Early Oogenesis in the Mouse. PLoS Genetics. 2007;3(1):e5.

7. Hunt PA, Lawson C, Gieske M, Murdoch B, Smith H, Marre A, et al. Bisphenol A alters early oogenesis and follicle formation in the fetal ovary of the rhesus monkey. Proceedings of the National Academy of Sciences. 2012 Oct 23;109(43):17525–30.

8. Kelly KO, Dernburg AF, Stanfield GM, Villeneuve AM. Caenorhabditis elegans msh-5 Is Required for Both Normal and Radiation-Induced Meiotic Crossing Over but Not for Completion of Meiosis. Genetics. 2000 Oct 1;156(2):617–30.

9. Daniela A P, Jasmine S, Yichang C, Patrick A. Reproductive toxicity and meiotic dysfunction following exposure to the pesticides Maneb, Diazinon and Fenarimol †Electronic supplementary information (ESI) available. See DOI: 10.1039/c4tx00141a Click here for additional data file. Click here for additional data file. Click here for additional data file. Toxicol Res (Camb). 2015 May 27;4(3):645–54.

10. Allard Patrick, Kleinstreuer Nicole C., Knudsen Thomas B., Colaiácovo Monica P. A C. elegans Screening Platform for the Rapid Assessment of Chemical Disruption of Germline Function. Environmental Health Perspectives. 2013 Jun 1;121(6):717–24.

11. Dernburg AF, McDonald K, Moulder G, Barstead R, Dresser M, Villeneuve AM. Meiotic Recombination in C. elegans Initiates by a Conserved Mechanism and Is Dispensable for Homologous Chromosome Synapsis. Cell. 1998 Aug;94(3):387–98.

12. Westphal T, Reuter G. Recombinogenic effects of suppressors of position-effect variegation in Drosophila. Genetics. 2002;160(2):609–21.

13. Phillips CM, McDonald KL, Dernburg AF. Cytological Analysis of Meiosis in Caenorhabditis elegans. In: Keeney S, editor. Meiosis: Volume 2, Cytological Methods [Internet]. Totowa, NJ: Humana Press; 2009 [cited 2019 Feb 11]. p. 171–95. (Methods in Molecular Biology). Available from: https://doi.org/10.1007/978-1-60761-103-5_11

14. Yokoo R, Zawadzki KA, Nabeshima K, Drake M, Arur S, Villeneuve AM. COSA-1 Reveals Robust Homeostasis and Separable Licensing and Reinforcement Steps Governing Meiotic Crossovers. Cell. 2012 Mar;149(1):75–87.

15. Lundby Z, Camacho J, Allard P. Fast Functional Germline and Epigenetic Assays in the Nematode Caenorhabditis elegans. In: Zhu H, Xia M, editors. High-Throughput Screening Assays in Toxicology [Internet]. New York, NY: Springer New York; 2016 [cited 2018 Aug 24]. p. 99–107. Available from: http://link.springer.com/10.1007/978-1-4939-6346-1_11

16. Bhalla N, Wynne DJ, Jantsch V, Dernburg AF. ZHP-3 Acts at Crossovers to Couple Meiotic Recombination with Synaptonemal Complex Disassembly and Bivalent Formation in C. elegans. PLoS Genet [Internet]. 2008 Oct 24 [cited 2019 Feb 15];4(10). Available from: https://www.ncbi.nlm.nih.gov/pmc/articles/PMC2567099/

17. Nadarajan S, Mohideen F, Tzur YB, Ferrandiz N, Crawley O, Montoya A, et al. The MAP kinase pathway coordinates crossover designation with disassembly of synaptonemal complex proteins during meiosis [Internet]. eLife. 2016 [cited 2019 Feb 14]. Available from: https://elifesciences.org/articles/12039

18. Ellis HM, Horvitz HR. Genetic control of programmed cell death in the nematode C. elegans. Cell. 1986 Mar 28;44(6):817–29.

19. MacQueen AJ, Hochwagen A. Checkpoint mechanisms: the puppet masters of meiotic prophase. Trends in Cell Biology. 2011 Jul 1;21(7):393–400.

20. Jaramillo-Lambert A, Harigaya Y, Vitt J, Villeneuve A, Engebrecht J. Meiotic Errors Activate Checkpoints that Improve Gamete Quality without Triggering Apoptosis in Male Germ Cells. Current Biology. 2010 Dec 7;20(23):2078–89.

21. Garcia-Muse T, Boulton SJ. Distinct modes of ATR activation after replication stress and DNA double-strand breaks in Caenorhabditis elegans. The EMBO Journal. 2005 Dec 21;24(24):4345–55.

22. Stiernagle T. Maintenance of C. elegans. WormBook [Internet]. 2006 [cited 2019 Jan 30]; Available from: http://www.wormbook.org/chapters/www_strainmaintain/strainmaintain.html

Figure Legends

Figure 1. Transgenerational BPA exposure perturbs chromosome segregation and induces aneuploidy

A: 10X images of TY2441 (Pxol-1::GFP) worms, DIC (left) and FITC (right). Red arrows point to embryos, negative in DMSO (top right) and positive in BPA (bottom right). Scale 100μm. Adult worms at F1 (B) and F3 (C) generation after P0 BPA exposure. The number of GFP+ embryos per worm was recorded and expressed as the fold ratio over H20 control. N=30 worms per group, 4 replicates per treatment group. Tests are based on One-way ANOVA. *P<0.05, **P<0.01.

Figure 2. BPA's transgenerational effects on double strand breaks

Number of apoptotic nuclei per gonadal arms of F3 worms. N=3 repeats, 20 worms each. , *P<0.05, **P<0.01, ***P<0.001, one-way ANOVA.

Figure 3. BPA exposure has influence on RAD-51 kinetics during early phases of pachytene

Quantitation of RAD-51 foci per germline nuclei of controls (0.1% H20 and 0.1% DMSO) and BPA (100μM), at F1 (A), and F3 (B) generations after exposure. The average number of RAD-51 foci per nucleus with SEM (y axis) in each prophase 1 meiotic stage (x axis). N=4 worms per group, three repeats per treatment group. Tests are based on One-way ANOVA, **P<0.01, ***P<0.001. Scale 10μm.

Figure 4. Transgenerational BPA exposure affects meiotic crossover dynamics

A: Late pachytene region of AV604 worm germline, with nuclei displaying 6 COSA-1 foci (merge of GFP and DAPI, left) DAPI middle, GFP right. Late pachytene progression from left to right. Exposures: DAPI 200ms, FITC 800 ms. Scale 10μm. B: Frequency distribution bar graphs of late

pachytene nuclei containing COSA-1 foci, ranging from 3-8, for water, DMSO, and BPA in F1 and F3 generations. N=250 nuclei in 18-25 worms per group, Chi-square test, ***P<0.001. C: Frequency distribution bar graphs of late pachytene nuclei containing ZHP-3 foci, ranging from 4-10, for water, DMSO, and BPA in F1 and F3 generations. N= 170 nuclei, 7-10 worms per group, Chi square test, **P<0.01, ***P<0.001.

Figure 1

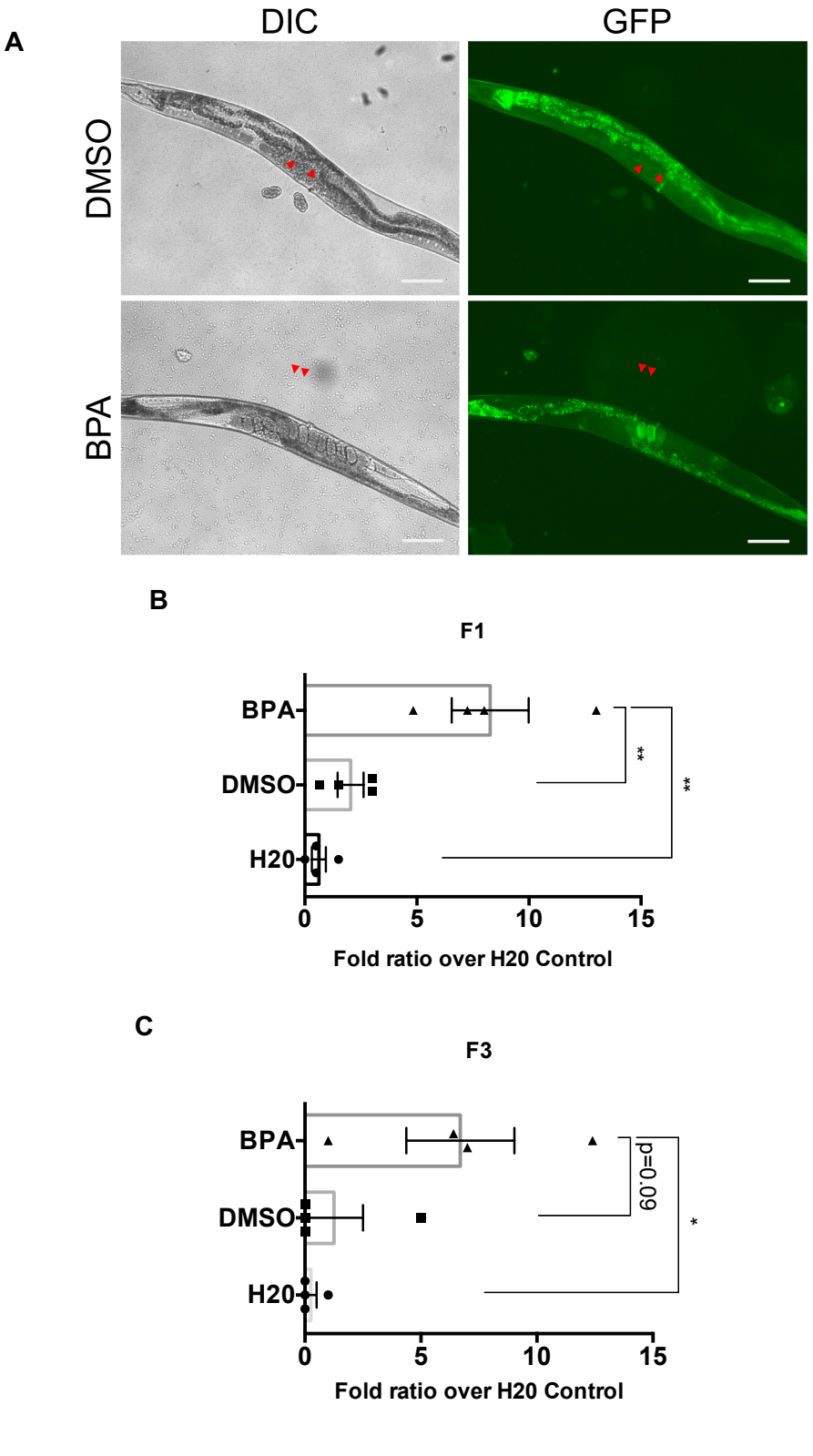
A
DIC
GFP
DMSO
BPA
B
F1
BPA
DMSO
H20
**
**
0
5
10
15
Fold ratio over H20 Control
C
F3
BPA
DMSO
H20
p=0.09
*
0
5
10
15
Fold ratio over H20 Control

Figure 2.

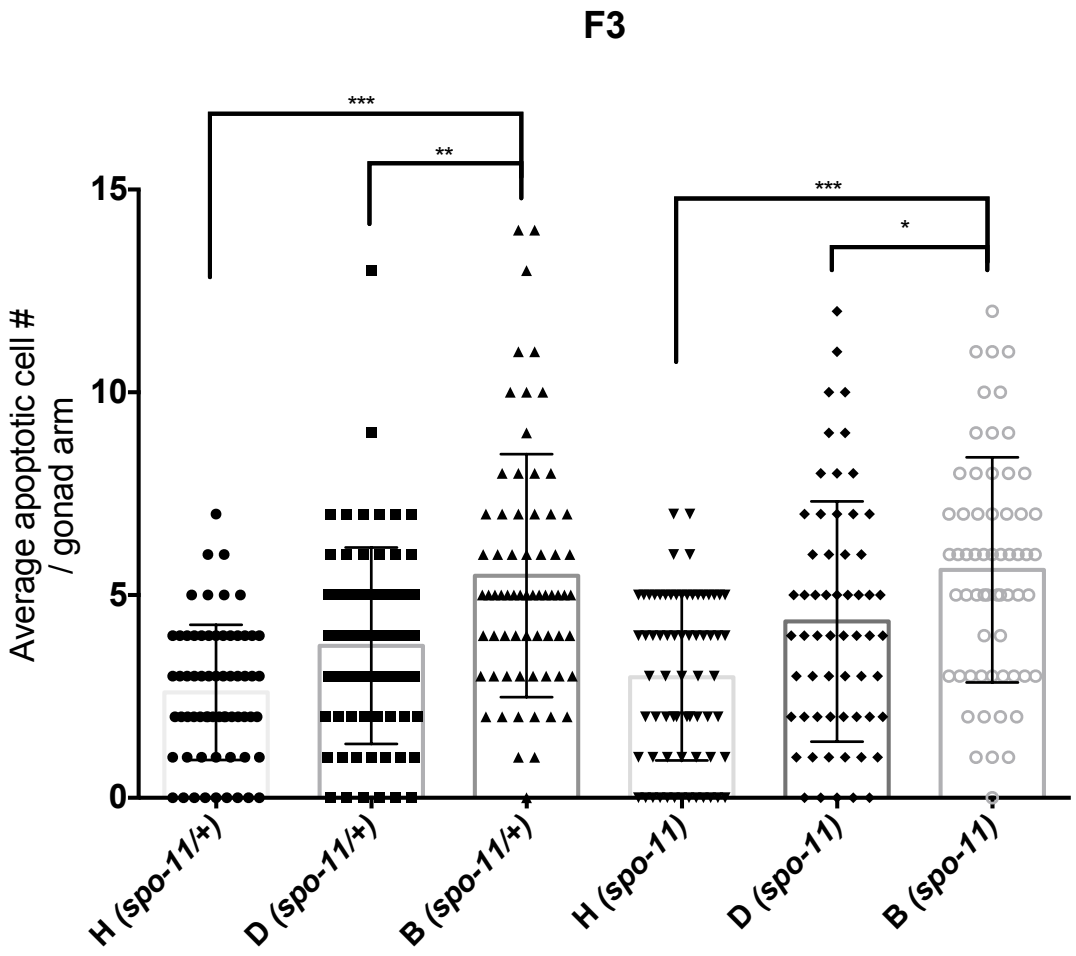
F3
***
**
***
*
15
10
5
0
Average apoptotic cell # / gonad arm
H (spo-11/+)
D (spo-11/+)
B (spo-11/+)
H (spo-11)
D (spo-11)
B (spo-11)

Figure 3

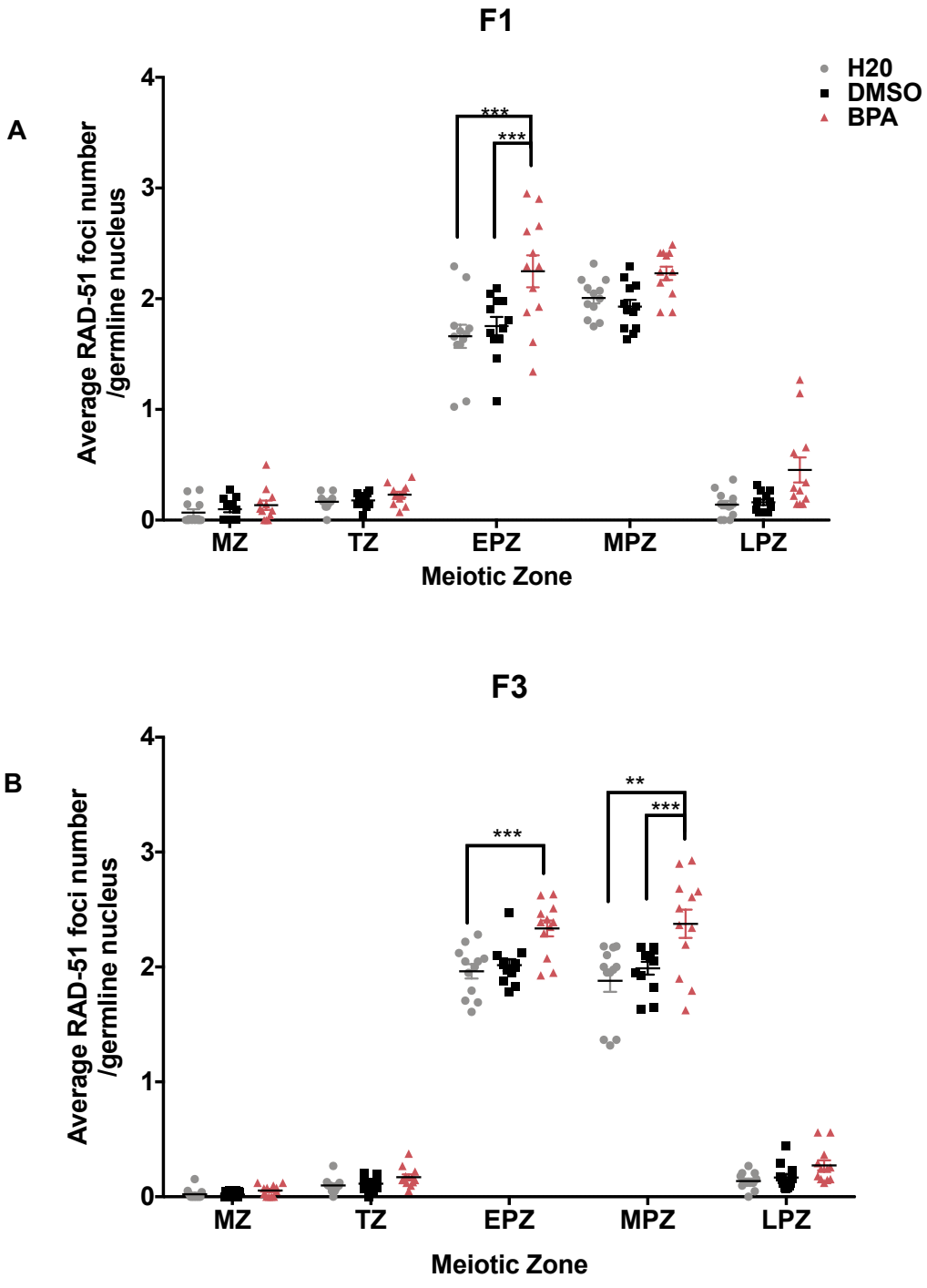
A
F1
H20
DMSO
BPA
Average RAD-51 foci number /germline nucleus
0
1
2
3
4
***
***
MZ
TZ
EPZ
MPZ
LPZ
Meiotic Zone
B
F3
Average RAD-51 foci number /germline nucleus
0
1
2
3
4
***
**
***
MZ
TZ
EPZ
MPZ
LPZ
Meiotic Zone

Figure 4.

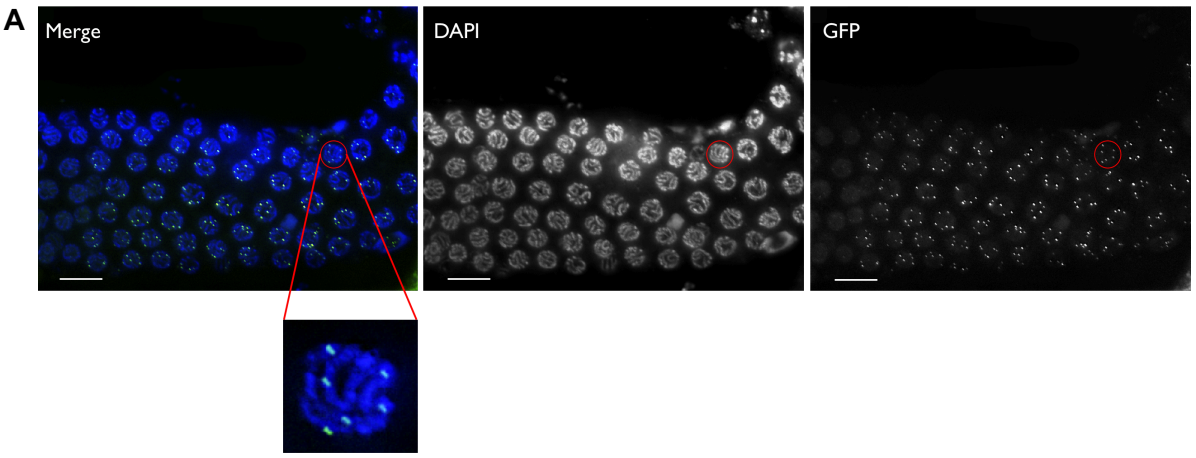
A
Merge
DAPI
GFP

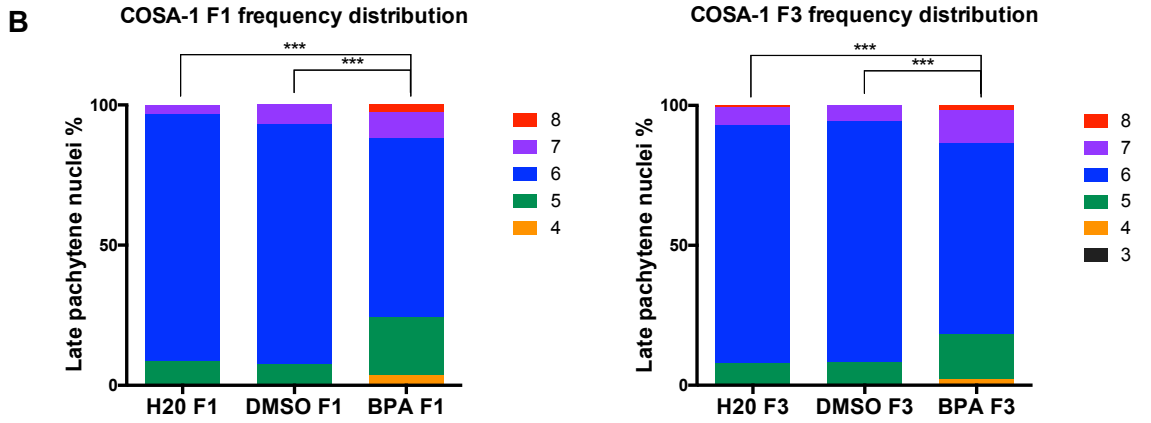
B
COSA-1 F1 frequency distribution
***
***
Late pachytene nuclei %
100
50
0
H20 F1
DMSO F1
BPA F1
8
7
6
5
4
COSA-1 F3 frequency distribution
***
***
Late pachytene nuclei %
100
50
0
H20 F3
DMSO F3
BPA F3
8
7
6
5
4
3

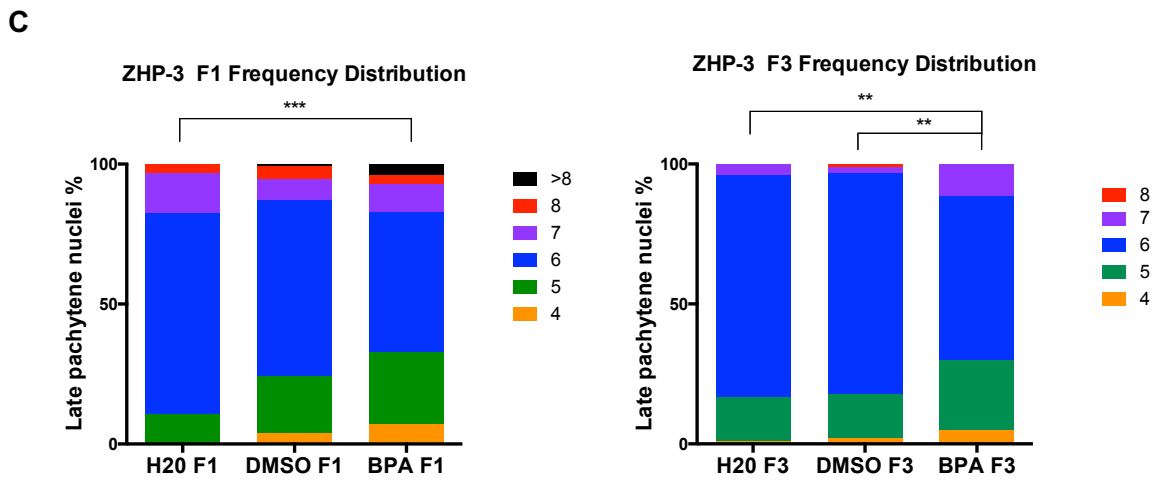
C
ZHP-3 F1 Frequency Distribution
***
Late pachytene nuclei %
100
50
0
H20 F1
DMSO F1
BPA F1
>8
8
7
6
5
4
ZHP-3 F3 Frequency Distribution
**
**
Late pachytene nuclei %
100
50
0
H20 F3
DMSO F3
BPA F3
8
7
6
5
4

CHAPTER 5

Summary and Discussion

Note: Part of Chapter 5 was published as a commentary article in Epigenetic Insights titled "**"Histone Modifications: Epigenetic Mediators of Environmental Exposure Memory."**

The elicitation and inheritance of phenotypes from environmental cues has been researched and debated for decades (1). There is now ample evidence that the epigenome is a key mediator of biologic response and adaptation of organisms to a wide array of natural environmental changes such as starvation (2), diet (3-5), temperature (6-7), and hyperosmotic stress (8). However, whether these changes could be passed down to future generations and whether non-natural, i.e., man-made, cues could also elicit a transgenerational response largely remain to be clarified, especially from a mechanistic standpoint.

Since the identification of a transgenerational impact of exposure to the pesticide Vinclozolin (9-10), followed by similar findings with Bisphenol A (BPA) and phthalates (11), DNA methylation has been proposed to be a central mediator of effect transmission since the various phenotypes observed in later generations beyond where a direct exposure could have occurred were correlated with an alteration of DNA methylation patterns. These findings also indicated a prominent role for germ cells since these marks could only be transferred to later generations via the germline. However, the extensive epigenetic reprogramming of primordial germ cells during early embryogenesis, where most CpG methylation is erased (12), has been seen as a challenge in explaining how DNA methylation alone could be the mechanism of inheritance. Thus, these studies left a gap in our mechanistic understanding of environmental epigenetic inheritance and did not explore the involvement of other epigenetic marks beside DNA methylation.

Our work (13) sought to clarify the mechanisms of transgenerational effects of man-made environmental chemicals, while focusing on epigenetic marks other than DNA methylation. This was made possible utilizing the *Caenorhabditis elegans* model, which lacks definitive 5mC DNA methylation, but shares a remarkable degree of conservation of histone modifications and of the machinery that regulates them. In *C. elegans*, core histones share 80% identical amino acid sequence when compared with human histones (14). Additionally, some of the post-translational modifications of the *C elegans* H3 (CeHIS3) and *C. elegans* H4 (CeHIS4) proteins have been

shown to be identical to those in human H3 and H4 proteins (15-17). Because of sequence conservation, it is hypothesized that *C. elegans* have direct orthologues of all the mammalian modification enzymes (18). *C. elegans* can therefore provide further information to fill the existent gap in knowledge regarding environmental exposures and inherited effects. In our work, we decided to focus on exposure to BPA, a well-known plastic manufacturing chemical and endocrine disruptor. Previous studies showed that its exposure is linked to epigenetic alterations such as decreased DNA methylation in mice (19), decreased DNA methylation in preadolescent girls (20), as well as reduced concentration of H3K9me3 in mouse germinal vesicle oocytes (21). These studies indicated BPA's ability to affect the epigenome in a variety of ways, and our research therefore aimed to clearly identify BPA's short- and long-term generational effects and the mechanisms behind them.

In sum, we uncovered a transgenerational effect on reproduction stemming from exposure to BPA that was mediated in part by: deregulation of repressive histone modifications (13), and disruption of the meiotic process in the germline (Chapter 4). To come to this conclusion, we first used a strain carrying a highly repetitive GFP transgene that is epigenetically silenced in the germline in a fashion that is reminiscent of the silencing of endogenous heterochromatin in the germline. Our assessment focused on the ability of BPA to disrupt the silenced state of the transgene in the germline that we could monitor and measure over several generations (Figure 1). Results indicated a significantly higher repetitive array de-silencing effect in the germline after BPA exposure that endured for five generations. To further investigate the impact of ancestral BPA exposure on the germline, we performed RNA-seq analysis on germline tissue, which identified 264 transcripts that were significantly upregulated or downregulated in F3 germlines ancestrally exposed to BPA compared with dimethyl sulfoxide (DMSO). Gene ontology analyses of functional categories represented highlighted reproduction as a representative functional category, indicating a profound transgenerational impact of ancestral BPA exposure on the germline transcriptome, and ultimately

germline function.

In addition to RNA-seq, we also performed ChIP-seq analysis in whole worms, which showed that the repressive marks H3K9me3 and H3K27me3 predominantly occupy the gene body of silenced genes and that H3K27me3 is significantly reduced in the gene body of BPA ancestrally exposed worms compared with the control groups. Comparing distribution of repressive marks along the chromosome axes showed reduction of both marks from the distal chromosomal regions, largely heterochromatic, and a slight enrichment in the chromosome centers when comparing BPA to DMSO. Noting these differences in the epigenome occur transgenerationally, our focus shifted back to the germline where the changes must occur in order to be inherited. Pachytene germline nuclei imaged by immunofluorescence showed a significant ~25% reduction in global H3K9me3 and H3K27me3 between DMSO and BPA. This transgenerational impact on repressive marks in the germline was not solely confined to the repetitive array but was also detectable on the autosomes and the X-chromosome.

Since F3 germlines showed a strong alteration of their chromatin and transcriptome, we investigated whether these were associated with transgenerational reproductive defects. We indeed measured an increase in embryonic lethality in worms ancestrally exposed to BPA when compared with DMSO control. Additionally, we measured germline health by monitoring induction of germline apoptosis and observed a significant increase in apoptotic germline nuclei in F3 worms ancestrally exposed to BPA. This indicated that ancestral BPA exposure elicits a clear transgenerational reproductive dysfunction effect. Current preliminary work on BPA's transgenerational effects on fertility has indicated a potential mechanism driven by disruption of the homeostasis of meiotic processes. Double strand break repair mechanisms, critical for meiotic recombination, are disrupted directly and transgenerationally by BPA exposures (Chapter 4), but future studies must address the importance of meiosis overall, including homologous pairing, synapsis, recombination events, and checkpoint activation.

We also tested the causal relationship between the reduction in H3K9me3 and H3K27me3 germline levels and BPA-induced transgenerational outcomes. We believed that the dependence of these marks might involve the activity of enzymes that regulate them. This was supported by our own aforementioned RNA-seq data in which seven differentially expressed chromatin factors were identified. Since BPA appeared to reduce repressive marks, we focused on histone demethylases targeting H3K9me3 and H3K27me3 to attempt to rescue BPA's transgenerational effects. Using a feeding RNAi strategy targeting *jmjd-2* (H3K9me3/H3K36me3 KDM, (22-23)) *jmjd-3/utx-1* (H3K27me3 KDM (24)), we were able to modulate and rescue BPA's transgenerational effects. The downregulation of *jmjd-2* or *jmjd-3/utx-1* through RNAi at the F1 to F2 transition increased the levels of H3K9me3 and H3K27me3 in the F3 germlines. The RNAi treatment also led to a rescue of BPA-induced reproductive dysfunction in the F3. To validate these results, we also performed drug rescue experiments using KDM4/JMJD-2 inhibitor IOX-1, which has been shown to elevate H3K9me3 levels in vitro and in cell culture settings (25-27), and the potent selective Jumonji JMJD-3/UTX-1 H3K27 demethylase inhibitor GSK-J4 (28). Using the chemicals individually or in combination to inhibit both demethylases significantly decreased the germline array desilencing and embryonic lethality effects. These two distinct methods of rescuing BPA's transgenerational effects indicate that the activity of either JMJD2 or JMJD3/UTX1 is required for inheritance of BPA-induced reproductive effects. Our approach is what distinguishes our study from others. We did not use mutants where the initial response to the environmental cue would be abrogated. Instead, we used RNAi or drug exposure in such a way that the worms could respond appropriately to the cue first but then were prevented from transferring that information to the following generations. Therefore, our study is unique in its ability to discriminate between altered response and altered inheritance of effect.

Together, these results demonstrate the key role of repressive histone modifications, namely, H3K9me3 and H3K27me3, in the inheritance of reproductive dysfunctions induced by a

well-defined environmental exposure. These findings shine a light on how artificial environmental exposures can be biologically integrated and transgenerationally inherited. Our work highlights the importance of comprehensively examining our chemical environmental for its potential effects on our germline epigenome, which can in turn allow us to find interventional means to prevent transmission of effects to future generations. Although our work begins to answer questions in the field of environmental exposure effects on future generations, currently there is not a single epigenetic mark that can be considered responsible for the transfer of environmental exposure effects from one generation to the next, and H3K4me3, H3K9me3, and H3K27me3 have all been implicated in that process (29). This could be due to potential redundancy or crosstalk between specific marks although we cannot exclude the possibility that specific exposures may use distinct epigenetic mechanisms for their inheritance. Recent studies have highlighted the challenge of identifying a unifying mechanism of inheritance, if it indeed exists. For example, other *C. elegans* studies showed that starvation can cause transgenerational effects mediated through the generation of small RNAs that target genes important for nutrition (30). Interestingly, histone modifications were also functionally connected to transgenerational effects and small RNA transfer. Indeed, in met-2 *C. elegans* mutants, which are defective in H3K9 methyltransferase, there is a progressive reduction in fertility that unfolds over 10 to 30 generations (31). The argonaute factor hdre-1, associated with small RNAs, is required for the progressive sterility phenotype in the met-2 mutant. Thus, the authors proposed a model where MET-2 functions to suppress the transgenerational transfer of small RNAs via the regulation of H3K9me3, as a model of inheritance. Together, these recent studies show the importance of epigenetic mechanisms other than DNA methylation as vehicles for transgenerational effects and highlight the need to comprehensively examine distinct exposures and epigenetic mechanisms to improve our understanding of environmental memory.

Finally, our work as well as that of others point to another important question. For phenotypes that are present in the soma of later generations, how is the information, likely epigenetically encoded as demonstrated by our efforts, transferred from germ cells across developmental and differentiation stages to affect adult cell types, altering their cellular programs and function.

Such a complex question is also best addressed in *C. elegans* where the location and timing of each cellular differentiation event are well described. Thus, while there is still much work to do, our current studies are helping to create guidelines based on model organisms and standardized approaches that will in turn allow us to understand the underlying intricate mechanisms of environmental exposure effects unraveling across generations.

References

1. Burbank L. The training of the human plant. The Century Magazine. May 1907, 1907:127–137.

2. Ravelli GP, Stein ZA, Susser MW. Obesity in young men after famine exposure in utero and early infancy. N Engl J Med. 1976;295:349–353.

3. Lambrot R, Xu C, Saint-Phar S, et al. Low paternal dietary folate alters the mouse sperm epigenome and is associated with negative pregnancy outcomes.Nat Commun. 2013;4:2889.

4. Ng S-F, Lin RCY, Laybutt DR, Barres R, Owens JA, Morris MJ. Chronic highfat diet in fathers programs β-cell dysfunction in female rat offspring. Nature.2010;467:963–966.

5. Carone BR, Fauquier L, Habib N, et al. Paternally induced transgenerational environmental reprogramming of metabolic gene expression in mammals. Cell. 2010;143:1084–1096.

6. Andrés F, Coupland G. The genetic basis of flowering responses to seasonal cues. Nat Rev Genet. 2012;13:627–639.

7. Song J, Angel A, Howard M, Dean C. Vernalization: a cold-induced epigenetic switch. J Cell Sci. 2012;125:3723–3731.

8. Seong KH, Li D, Shimizu H, Nakamura R, Ishii S. Inheritance of stress induced, ATF-2-dependent epigenetic change. Cell. 2011;145:1049–1061.

9. Anway MD, Cupp AS, Uzumcu M, Skinner MK. Epigenetic transgenerational actions of endocrine disruptors and male fertility. Science. 2005;308:1466–1469.

10. Anway MD, Leathers C, Skinner MK. Endocrine disruptor vinclozolin induced epigenetic transgenerational adult-onset disease. Endocrinology. 2006;147:5515–5523.

11. Manikkam M, Tracey R, Guerrero-Bosagna C, Skinner MK. Plastics derived endocrine disruptors (BPA, DEHP and DBP) induce epigenetic transgenerational inheritance of obesity, reproductive disease and sperm epimutations. PLoS ONE. 2013;8:e55387.

12. Tang WWC, Kobayashi T, Irie N, Dietmann S, Surani MA. Specification and epigenetic programming of the human germ line. Nat Rev Genet. 2016;17:585–600.

13. Camacho J, Truong L, Kurt Z, et al. The memory of environmental chemical exposure in C. elegans is dependent on the Jumonji demethylases jmjd-2 and jmjd-3/utx-1. Cell Rep. 2018;23:2392–2404.

14. Vanfleteren JR, Bun SMV, Delcambe LL, Beeumen JJV. Multiple forms of histone H2B from the nematode Caenorhabditis elegans. Biochem J.1986;235:769–773.

15. Vanfleteren JR, Bun SMV, Beeumen JJV. The primary structure of histone H2A from the nematode Caenorhabditis elegans. Biochem J. 1987;243:297–300.

16. Vanfleteren JR, Van Bun SM, Van Beeumen JJ. The primary structure of histone H3 from the nematode Caenorhabditis elegans. FEBS Lett. 1987;211:59–63.

17. Vanfleteren JR, Van Bun SM, Van Beeumen JJ. The primary structure of histone H4 from the nematode Caenorhabditis elegans. Comp Biochem Physiol. 1987;87:847–849.

18. Cui M, Han M. Roles of chromatin factors in C. elegans development. In: The C. elegans Research Community, ed. WormBook; May 2007:1-16.

19. Dolinoy DC, Huang D, Jirtle RL. Maternal nutrient supplementation counteracts bisphenol A-induced DNA hypomethylation in early development. Proc Natl Acad Sci USA. 2007;104:13056–13061.

20. Kim JH, Rozek LS, Soliman AS, et al. Bisphenol A-associated epigenomic changes in prepubescent girls: a cross-sectional study in Gharbiah, Egypt. Environ Health. 2013;12:33.

21. Trapphoff T, Heiligentag M, Hajj NE, Haaf T, Eichenlaub-Ritter U. Chronic exposure to a low concentration of bisphenol A during follicle culture affects the epigenetic status of germinal vesicles and metaphase II oocytes. Fertil Steril. 2013;100:1758. e1–1767.e1.

22. Greer EL, Beese -Sims SE, Brookes E, et al. A histone methylation network regulates transgenerational epigenetic memory in C. Elegans. Cell Rep. 2014;7:113–126.

23. Whetstine JR, Nottke A, Lan F, et al. Reversal of histone lysine trimethylation by the JMJD2 family of histone demethylases. Cell. 2006;125:467–481.

24. Agger K, Cloos PAC, Christensen J, et al. UTX and JMJD3 are histone H3K27 demethylases involved in HOX gene regulation and development. Nature. 2007;449:731–734.

25. King ONF, Li XS, Sakurai M, et al. Quantitative high-throughput screening identifies 8-hydroxyquinolines as cell-active histone demethylase inhibitors. PLoS ONE. 2010;5:e15535.

26. Hu Q, Chen J, Zhang J, Xu C, Yang S, Jiang H. IOX1, a JMJD2A inhibitor, suppresses the proliferation and migration of vascular smooth muscle cells induced by angiotensin II by regulating the expression of cell cycle-related proteins. Int J Mol Med. 2016;37:189–196.

27. Schiller R, Scozzafava G, Tumber A, et al. A cell-permeable ester derivative of the JmjC histone demethylase inhibitor IOX1. ChemMedChem. 2014;9:566–571.

28. Kruidenier L, Chung C, Cheng Z, et al. A selective Jumonji H3K27 demethylase inhibitor modulates the proinflammatory macrophage response. Nature. 2012;488:404–408.

29. Weinhouse C, Truong L, Meyer JN, Allard P. Caenorhabditis elegans as an emerging model system in environmental epigenetics. Environ Mol Mutagen. 2018;59:7560–7575.

30. Rechavi O, Houri-Ze'evi L, Anava S, Goh WSS, Kerk SY, Hannon GJ, Hobert O. Starvation-induced transgenerational inheritance of small RNAs in C. Elegans. Cell. 2014;158:2277–2287.

31. Lev I, Seroussi U, Gingold H, Bril R, Anava S, Rechavi O. MET-2-dependent H3K9 methylation suppresses transgenerational small RNA inheritance. Curr Biol. 2017;27:81138–8

Figure 1.

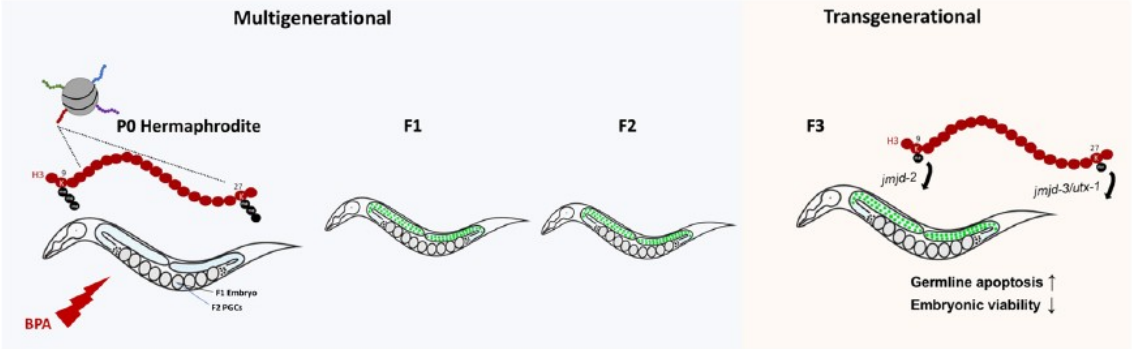

BPA exposures in *C. elegans* reduces the levels of the repressive histone marks H3K9me3 and H3K27me3, regulated by the demethylases jmjd-2 and jmjd-3/utx-1, respectively. This disruption causes a de-silencing effect and reproductive dysfunction observed from the P0 generation until the F4. The F3 generation represents the first generation where there was no direct contact with the environmental toxicant (BPA).

Appendix

Chapter 11

Fast Functional Germline and Epigenetic Assays in the Nematode *Caenorhabditis elegans*

Zachary Lundby, Jessica Camacho, and Patrick Allard

Abstract

Germ cells are unique in their ability to transfer traits and genetic information from one generation to the next. The proper development and integrity of their genome are therefore of utmost importance for the health of organisms and survival of species. Many features of mammalian germ cells, including their long development span and difficulty of access, present challenges for their study in the context of toxicity assays. In light of these barriers, the model system *Caenorhabditis elegans* shows great potential given its ease of manipulation and genetic tractability which can be easily adapted for high-throughput analysis. In this chapter, we discuss the advantages of examining germ cell processes in *C. elegans*, and describe three functional germline assays for the examination of chemical impact on germline maintenance and function including assays probing germ cell differentiation, germline apoptosis, and germline epigenetic regulation.

Key words *C. elegans*, Germline, Meiosis, Toxicity, Apoptosis

1 Introduction

The nematode *Caenorhabditis elegans* is arguably one of the most valuable contemporary genetic model organisms. Discoveries in the free-living roundworm include the identification of the apoptotic cascade, RNA interference, and microRNAs to only name a few [1]. *C. elegans* was first isolated and described by Emile Maupas from Algerian soil in the early 1900s but it was not until the 1940s that the organism was studied in a laboratory setting by Victor Nigon and Ellsworth Dougherty [2]. Soon after, Sydney Brenner focused its attention on the nematode, rightly arguing that its ease of maintenance and tractability would enlighten the fields of genetics and developmental biology [3]. It is precisely these features, as well as many others described below, that make *C. elegans* a powerful model system not only for the aforementioned fields but also for the field of toxicology [4].

C. elegans worms are easily and cheaply grown and maintained in the laboratory setting. The most common method of *C. elegans*

Hao Zhu and Menghang Xia (eds.), *High-Throughput Screening Assays in Toxicology*, Methods in Molecular Biology, vol. 1473, DOI 10.1007/978-1-4939-6346-1_11, © Springer Science+Business Media New York 2016

culture is on regular plastic petri dishes filled with nematode growth medium (NGM) [5]. The agar media is then covered in a layer of bacteria, most commonly OP50 or HB101 strains, which will serve as food source for the lifetime of the worms. Alternatively, the worms can also be grown in liquid media composed of a salt buffer and bacteria. Either growth media allows for scalability and versatility in worm culture depending on the desired application. Worms can be grown in flasks, tubes, or plates of all sizes including 96-well and 384-well plates, a useful format for high-throughput screening [6, 7].

In these media, and under normal temperature conditions (15–25 °C), the worms will develop as embryos, hatch, and then proceed through four larval stages to reach adulthood in 3–4 days. Once the worms are adult, they will lay between 200 and 300 embryos for another 4 days after which the worms will cease to reproduce. Importantly, the worms are self-fertilizing hermaphrodites. They make sperm as they transition from their last larval stage (L4) into adulthood at which point, their germline will only produce oocytes. As these oocytes pass through the spermatheca, located next to the uterus, they are fertilized and initiate embryonic development within the confines of the uterus before being laid into the media (Fig. 1) [8].

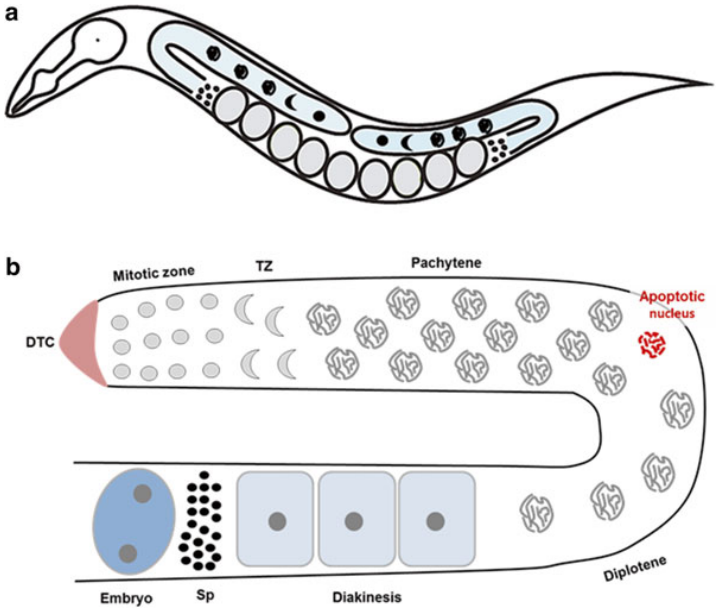

Fig. 1 Worm and germline morphological features. (**a**) *Caenorhabditis elegans* nematodes are round worms displaying two gonadal arms (*lightly shaded in blue*) that open into one common uterus where embryos develop before being deposited into the media through the vulva. (**b**) Schematized representation of one gonadal arm. The distal tip cell emits a Notch ligand that maintains germ cells in mitosis. Once far enough away from the ligand, the germ cells will enter and progress through the different phases of prophase I of meiosis. Apoptotic nuclei, an outcome of defective meiotic recombination or synapsis, are visible in late pachytene. TZ = Transition zone (leptotene and zygotene). *Sp* = spermatheca

In the assays described in this chapter (Fig. 2), several other features of *C. elegans* are mobilized. In particular, assessment of toxicity is simplified by the transparency of the worm's cuticle, allowing for the observation of many endpoints without dissection of the worm itself. This is particularly useful for the monitoring of germ cell differentiation in the gonad of *C. elegans*. In the nematode, germline nuclei differentiate continuously from the distal mitotic zone, through transition zone (leptotene and zygotene of prophase I), pachytene, diplotene, and diakinesis of prophase I. Each stage of meiotic differentiation harbors specific nuclear morphology which can be appreciated without the need for dissection by simple fixation of whole worms and staining by DAPI [9]. Thus, the kinetics of meiotic differentiation as well as germline nuclear loss can be quickly monitored in *C. elegans* following exposure.

The other two assays rely on the number of genetic strains that are available in *C. elegans* available from the *Caenorhabditis* Genetics Center (CGC). We are making use of two specific strains: the first carries a transgene coding for CED-1::GFP which surrounds engulfed apoptotic nuclei. The expression of CED-1::GFP therefore easily labels apoptotic nuclei in the germline of *C. elegans* [10]. This assay is particularly informative as germline apoptosis is a hallmark of defective processes of meiotic differentiation including defective chromosomal synapsis and meiotic recombination. Induction of germline apoptosis is therefore used as a proxy for defective germline function [11–13].

Similarly, the third assay relies on a GFP-based reporter which is specifically silenced in the germline of *C. elegans* but not in its somatic tissues [14–17]. Furthermore, this silencing is controlled through epigenetic means involving the recruitment of repressive histone modifications and the loss of active marks [16, 17]. We describe here the application of this reporter approach for the screening of chemicals with epigenetic dysregulation effects.

2 Materials

1. M9 (stored at ambient temperature).
   3 g KH2PO$_4$, 6 g Na2HPO$_4$, 5 g NaCl, 1 mL 1 M MgSO$_4$, H$_2$O to 1 L.
2. NMG media plates.
   3 g NaCl, 2.5 g Bactopeptone, 20 g Sigma Agar, add H$_2$O to 1 L, 1 mL 5 mg/mL cholesterol, 1 mL 1 M CaCl$_2$, 1 mL 1 M MgSO$_4$, autoclave for 40 min, 25 mL 1 M pH6 KH$_2$PO$_4$.
3. Positively charged slides.
4. Cover slips.
5. 1.5 mL Microcentrifuge tubes.

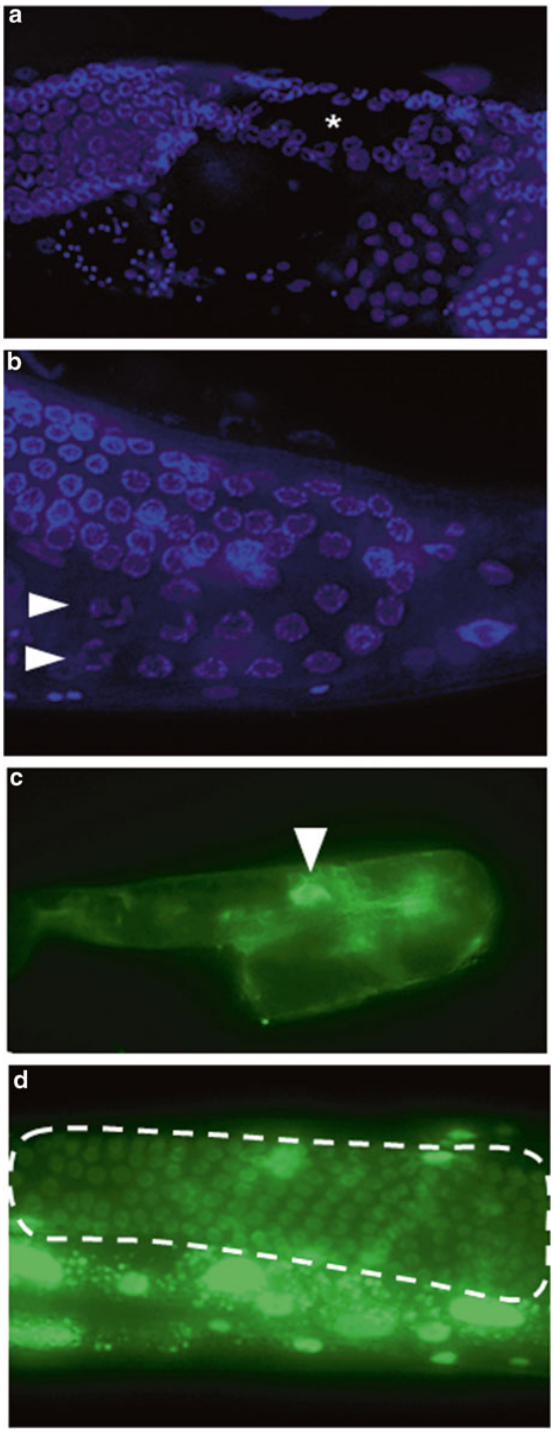

Fig. 2 Several tools to examine germline toxicity. (**a**) Example of DAPI staining of the worm germline showing a large gap. (**b**) Example of defective germline morphology with two rows of diplotene-stage nuclei instead of the normal sole row of nuclei. (**c**) Use of the CED-1::GFP apoptotic reporter showing an apoptotic nucleus within the germline. (**d**) Epigenetic assay. The worm shown here was exposed for 48 h to the HDAC inhibitor valproic acid at 100 μM. Dashed line surrounds the germline nuclei expressing GFP from the normally epigenetically repressed let-858::gfp transgene

6. Fluorescence microscope.
7. Positive controls (stored at −20 °C unless otherwise noted).
   (a) BPA—CAS 80-05-7.
   (b) Vinclozolin—CAS 50471-44-8.
   (c) Sodium butyrate—CAS 156-54-7.
8. Dimethyl sulfoxide—CAS 67-68-5 (stored at ambient temperature).
9. 15 mL Conical vials.
10. Glass Pasteur pipette.
11. Pipette 1000, 10, 1 μL.
12. Worm pick.
13. NL2507 worms (CGC).
14. Ced-1::GFP worms (CGC).
15. Wild-type worms.
16. 60 mm vented plates.
17. OP50 bacteria.
18. Immersion oil.
19. DAPI stain (Sigma-Aldrich).
20. Carnoy's solution.
21. Kimwipes.
22. Nail polish.

Note that this is but a brief summary of the steps for each of our methods of analysis. For more detailed information, please visit Parodi DA, Damoiseaux R, Allard P(2015) Comprehensive assessment of germline chemical toxicity using the nematode *Caenorhabditis elegans*. Journal of visualized experiments: JoVE 96 available in PubMed #25741987.

3 Methods

3.1 Procedure for Caenorhabditis elegans Growth and Exposure

This procedure focuses on establishing a viable population of worms that can be used in any of the experiments listed later in this chapter. Following this procedure, one will possess chemically exposed worms at the proper larval stage to immediately begin the epigenetic, DAPI, or apoptotic analysis.

1. Dilute all chemicals of interest to 100 mM with DMSO directly in stock bottle and transfer to 1.5 mL microcentrifuge tubes.
2. Store at −20 °C.
3. Synchronize worms by bleaching and plate worms until they reach L4 stage.

4. Label three 15 mL conical vials one through three.
5. Fill tubes 1 and 2 with 7 mL of M9.
6. Wash 3–4 plates of worms using 1 mL of M9.
7. Dispense on each plate twice to collect worms and add them to the first conical vial.
8. Allow L4 worms to settle to the bottom of the first conical vial.
9. During this process, start on the following:
   (a) Thaw out chemical stocks by placing them in the fume hood.
   (b) Add 50 µL of OP50 bacteria to the third conical vial per each exposure group.
   (c) Add 500 µL of M9 to the third conical vial per each exposure group.
10. Once the L4 worms have settled, extract them with a glass Pasteur pipette and add them to the second conical vial.
11. After they have settled once more, transfer them to the third and final conical vial using the glass Pasteur pipette once more.
12. Count the worms from the third conical vial.
13. Count 5 µL worth of worms on a cover slip and multiply by 100.
14. This figure should not exceed 400 worms.
15. Label the 1.5 mL tubes with the appropriate markings to designate the chemicals that will be used.
16. Add 500 µL of the solution from the third conical vial to each of the 1.5 mL microcentrifuge tubes.
17. Transfer the 1.5 mL tubes to the fume hood.
18. Add 0.5 µL of chemical of interest to each tube to reach a final concentration of 100 µM.
19. Dispense 0.5 µL of DMSO (0.1 % final) directly from the stock bottle as the negative control into the appropriately marked 1.5 mL microcentrifuge tube.
20. Dispense 0.5 µL of any of the aforementioned positive controls into the appropriately marked 1.5 mL tubes.
21. Vortex each of the 1.5 mL tubes upon completion to ensure complete distribution.
22. Place the 1.5 mL tubes in a rotator for 24 h at 20 °C.
23. Note that rotation is necessary for proper growth.
24. At the end of 24 h, remove the 1.5 mL tubes from the rotator for 5 min to aerate.
25. Add an additional 50 µL of OP50 bacteria to each tube.
26. Place back in rotator for another 24 h.
27. At the end of the final 24 h, label petri dishes corresponding to each of the chemicals used.

28. Retrieve the 1.5 mL tubes and allow the worms to settle to the bottom.
29. Extract the worm pellet and plate on the proper petri dishes.
30. Allow the worms to settle for 1–2 h on the petri dishes at 20 °C.

Note that after this step each of the different types of analysis diverges. Be aware that a 24 h exposure does not require any of the steps after **step 24**.

3.2 DAPI Analysis

Chemical disruption can result in morphological errors in the germline of the worm that may manifest itself in a variety of ways [18, 19]. The goal of this type of analysis is to discover what, if any, morphological errors have occurred.

1. After placing N2 worms in 10 μL of M9 on positively charged slide, use a Kimwipe to absorb as much of the M9 liquid as possible while being careful not to extract the worms as well.
2. Add Carnoy's solution dropwise until the worms have been completely dehydrated.
3. Rehydrate the worms with a humidifying apparatus by suspending the slide between two objects with water underneath.
4. Add M9 directly to the dehydrated worms and cover the apparatus for 1 h.
5. At the end of the hour, absorb the M9 once more with Kimwipes.
6. Add a single drop of DAPI stain and distribute it evenly with a worm pick.
7. Add a cover slip over the solution and seal the edges with nail polish.
8. Store at 0 °C when not being examined.
9. Place slide under Nikon H600L microscope and identify worms at 10× with bright-field illumination.
10. Add immersion oil after the worms have been identified.
11. Switch to the software package and while retaining focus on the worm of interest, rotate to the 100× objective lens.
12. Additional magnification may be necessary to see the germline clearly; our lab recommends 400x using the "4×" option on the software package.
13. The nuclei in the germline will be plainly visible. Gaps in nuclei, uneven distribution of nuclei, extension of the mitotic or transition zones, and other gross errors in morphology are all evidence of toxicity. Areas of apoptosis $n > 5$ are "major" errors while areas of apoptosis $n < 5$ are "minor" errors.

3.3 Apoptotic Analysis

The goal of this type of analysis is to look specifically for cell death in the germline of the worm. Apoptotic cells are marked by the surrounding expression of the engulfment marker CED-1::GFP transgene which will be visible through the microscope [10]. While apoptosis is a process that occurs even in a healthy organism, a number of apoptotic nuclei exceeding the baseline can be used as an indicator of toxicity of the chemical in question.

1. Select for the CED-1::GFP worms with the best wild-type movement.
2. Following the same steps as the "epigenetic screen," examine the germline looking specifically for expression that appears as bright circles or a network of circles.
3. Distribute worms evenly across the liquid and add a cover slip for analysis.
4. Using the Nikon H600L microscope, identify worms at 10x under bright-field illumination.
5. Switch to FITC illumination and deactivate the standard microscope light source.
6. Nuclei positive for apoptosis will be surrounded by a GFP-positive ring (*see* Fig. 2).

3.4 Epigenetic Analysis

The goal of this type of analysis is to uncover changes in epigenetic expression, specifically epigenetic desilencing, resulting from chemical exposure. Such desilencing is revealed by the de-repression of a repetitive GFP transgene via the removal of repressive histone marks and the addition of activating histone marks [16, 17]. Furthermore, de-repression of the germline in the P0 generation has the possibility of being transmitted to successive generations.

1. Select NL2507 worms with the best rolling phenotype from the aforementioned petri dishes and add to 10 μL of M9 placed directly in the middle of a positively charged slide.
2. Distribute worms evenly across the liquid and add a cover slip for analysis.
3. Using the Nikon H600L microscope, identify worms at 10x under bright-field illumination.
4. Switch to FITC illumination and deactivate the standard microscope light source.
5. It may also be helpful to work in a darkroom for better identification.
6. Somatic cells will automatically fluoresce but the germline is the area of interest.
7. Redirect the image from the microscope lens to the software program.
8. If nothing is visible in the germline, it is negative for expression.

9. If individual nuclei are visible, it is positive for expression.
10. Expression should be plainly evident without magnifying further or adjusting the contrast. Please see attached images as a reference (Fig. 2).

4 Conclusion

The complementary of the three assays described above allows to obtain a broad picture of toxicity elicited by chemical exposure in *C. elegans*. Mechanistic follow-ups are needed to examine the germline pathways perturbed by the exposure. This can be easily performed by examining the resistance or sensitivity of mutants involved in germline processes. The use of the nematode as a reproductive model therefore offers the possibility to quickly reveal mechanisms of toxicity that may have taken much longer in other species.

References

1. Macrae R (2014) On the shoulders of worms. Trends Genet 30(11):475–475
2. de Chadarevian S (1998) Of worms and programmes: Caenorhabditis elegans and the study of development. Stud Hist Phil Biol Biomed Sci 29(1):81–105
3. Brenner S (2009) In the beginning was the worm …. Genetics 182(2):413–415
4. Leung MC, Williams PL, Benedetto A, Au C, Helmcke KJ, Aschner M, Meyer JN (2008) Caenorhabditis elegans: an emerging model in biomedical and environmental toxicology. Toxicol Sci 106(1):5–28
5. Brenner S (1974) The genetics of Caenorhabditis elegans. Genetics 77(1):71–94
6. Parodi DA, Damoiseaux R, Allard P (2015) Comprehensive assessment of germline chemical toxicity using the nematode Caenorhabditis elegans. J Vis Exp 96
7. Boyd WA, McBride SJ, Rice JR, Snyder DW, Freedman JH (2010) A high-throughput method for assessing chemical toxicity using a Caenorhabditis elegans reproduction assay. Toxicol Appl Pharmacol 245(2):153–159
8. Greenstein D (2005) Control of oocyte meiotic maturation and fertilization. WormBook 1-12
9. Colaiacovo MP (2006) The many facets of SC function during C. elegans meiosis. Chromosoma 115(3):195–211
10. Zhou Z, Hartwieg E, Horvitz HR (2001) CED-1 is a transmembrane receptor that mediates cell corpse engulfment in C. elegans. Cell 104(1):43–56
11. Bhalla N, Dernburg AF (2005) A conserved checkpoint monitors meiotic chromosome synapsis in Caenorhabditis elegans. Science 310(5754):1683–1686
12. Gartner A, Boag PR, Blackwell TK (2008) Germline survival and apoptosis. WormBook 1-20
13. Gartner A, MacQueen AJ, Villeneuve AM (2004) Methods for analyzing checkpoint responses in Caenorhabditis elegans. Methods Mol Biol 280:257–274, doi: 1-59259-788-2:257
14. Kelly WG (2014) Transgenerational epigenetics in the germline cycle of Caenorhabditis elegans. Epigenetics Chromatin 7(1):6
15. Li T, Kelly WG (2011) A role for Set1/MLL-related components in epigenetic regulation of the Caenorhabditis elegans germ line. PLoS Genet 7(3), e1001349
16. Schaner CE, Kelly WG (2006) Germline chromatin. WormBook 1–14
17. Kelly WG, Xu S, Montgomery MK, Fire A (1997) Distinct requirements for somatic and germline expression of a generally expressed Caernorhabditis elegans gene. Genetics 146(1): 227–238
18. Allard P, Kleinstreuer NC, Knudsen TB, Colaiacovo MP (2013) A C. elegans screening platform for the rapid assessment of chemical disruption of germline function. Environ Health Perspect 121(6):717–724
19. Parodi DA, Sjarif J, Chen Y, Allard P (2015) Reproductive toxicity and meiotic dysfunction following exposure to the pesticides Maneb, Diazinon and Fenarimol. Toxicol Res 4(3):645–654

Histone Modifications: Epigenetic Mediators of Environmental Exposure Memory

Epigenetics Insights
Volume 11: 1–3

DOI: 10.1177/2516865718803641

Jessica Camacho[1] and Patrick Allard[1,2]

[1]Molecular Toxicology Interdepartmental Program, University of California, Los Angeles, Los Angeles, CA, USA. [2]Institute for Society and Genetics, University of California, Los Angeles, Los Angeles, CA, USA.

ABSTRACT: How organisms retain a memory of ancestral environmental exposure is a phenomenon that is still poorly understood. Recently published work by our group and others, regarding environmentally induced transgenerational effects, have identified an array of mechanisms, with a particular focus on histone modifications, that shed some light on the underlying epigenetic processes driving long-term generational effects.

KEYWORDS: *C. elegans*, transgenerational inheritance, reproductive function, Bisphenol A, histone demethylase

RECEIVED: August 28, 2018. **ACCEPTED:** September 3, 2018.

TYPE: Commentary

FUNDING: The author(s) disclosed receipt of the following financial support for the research, authorship and/or publication of this article: JC received support from NIH/NIEHS T32 ES015457 Training in Molecular Toxicology, the North American Graduate Fellowship, the NSF AGEP Competitive Edge, the NSF Graduate Research Fellowship, and the Eugene-Cota Robles Fellowship. PA is supported by NIH/NIEHS R01 ES02748701 and the Burroughs Wellcome Foundation.

DECLARATION OF CONFLICTING INTERESTS: The author(s) declared no potential conflicts of interest with respect to the research, authorship, and/or publication of this article.

CORRESPONDING AUTHOR: Patrick Allard, Institute for Society and Genetics, University of California, Los Angeles, 3360 Life Science Building, Los Angeles, CA 90095, USA. Email: pallard@ucla.edu

COMMENT ON: Camacho J, Truong L, Kurt Z, Chen YW, Morselli M, Gutierrez G, Pellegrini M, Yang X, Allard P. The memory of environmental chemical exposure in *C. elegans* is dependent on the Jumonji demethylases jmjd-2 and jmjd-3/utx-1. *Cell Rep*. 2018;23:2392-2404. doi:10.1016/j.celrep.2018.04.078. PubMed PMID: 29791850; PubMed Central PMCID: PMC6003705. https://www.ncbi.nlm.nih.gov/pmc/articles/PMC6003705/

The elicitation and inheritance of phenotypes from environmental cues has been researched and debated for decades.[1] There is now ample evidence that the epigenome is a key mediator of biologic response and adaptation of organisms to a wide array of natural environmental changes such as starvation,[2] diet,[3–5] temperature,[6,7] and hyperosmotic stress.[8] However, whether these changes could be passed down to future generations and whether non-natural, i.e., man-made, cues could also elicit a transgenerational response largely remain to be clarified, especially from a mechanistic standpoint.

Since the identification of a transgenerational impact of exposure to the pesticide Vinclozolin,[9,10] followed by similar findings with Bisphenol A (BPA) and phthalates,[11] DNA methylation has been proposed to be a central mediator of effect transmission since the various phenotypes observed in later generations beyond where a direct exposure could have occurred were correlated with an alteration of DNA methylation patterns. These findings also indicated a prominent role for germ cells since these marks could only be transferred to later generations via the germline. However, the extensive epigenetic reprogramming of primordial germ cells during early embryogenesis, where most CpG methylation is erased,[12] has been seen as a challenge in explaining how DNA methylation alone could be the mechanism of inheritance. Thus, these studies left a gap in our mechanistic understanding of environmental epigenetic inheritance and did not explore the involvement of other epigenetic marks beside DNA methylation.

Our work[13] sought to clarify the mechanisms of transgenerational effects of man-made environmental chemicals, while focusing on epigenetic marks other than DNA methylation. This was made possible utilizing the *Caenorhabditis elegans* model, which lacks definitive 5 mC DNA methylation, but shares a remarkable degree of conservation of histone modifications and of the machinery that regulates them. In *C. elegans*, core histones share 80% identical amino acid sequence when compared with human histones.[14] Additionally, some of the post-translational modifications of the *C. elegans* H3 (CeHIS3) and *C. elegans* H4 (CeHIS4) proteins have been shown to be identical to those in human H3 and H4 proteins.[15–17] Because of sequence conservation, it is hypothesized that *C. elegans* have direct orthologues of all the mammalian modification enzymes.[18] *C. elegans* can therefore provide further information to fill the existent gap in knowledge regarding environmental exposures and inherited effects. In our work, we decided to focus on exposure to BPA, a well-known plastic manufacturing chemical and endocrine disruptor. Previous studies showed that its exposure is linked to epigenetic alterations such as decreased DNA methylation in mice,[19] decreased DNA methylation in preadolescent girls,[20] as well as reduced concentration of H3K9me3 in mouse germinal vesicle oocytes.[21] These studies indicated BPA's ability to affect the epigenome in a variety of ways, and our research therefore aimed to clearly identify BPA's short- and long-term generational effects and the mechanisms behind them.

In sum, we uncovered a transgenerational effect on reproduction stemming from exposure to BPA that was mediated in part by a deregulation of repressive histone modifications.[13] To come to this conclusion, we first used a strain carrying a highly repetitive GFP transgene that is epigenetically silenced in the germline in a fashion that is reminiscent of the silencing of endogenous heterochromatin in the germline. Our assessment focused on the ability of BPA to disrupt the silenced state of the transgene in the germline that we could monitor and measure over several generations (see Figure 1). Results indicated a significantly higher repetitive array de-silencing effect in the germline after BPA exposure that

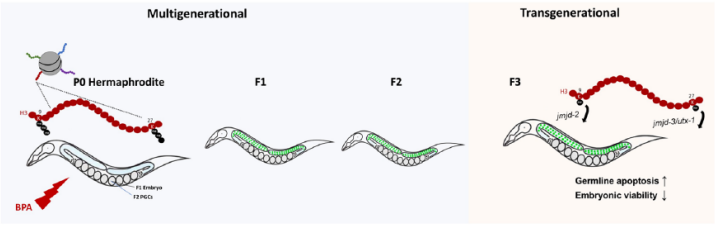

Figure 1. BPA exposures in *C. elegans* reduces the levels of the repressive histone marks H3K9me3 and H3K27me3, regulated by the demethylases *jmjd-2* and *jmjd-3/utx-1*, respectively. This disruption causes a de-silencing effect and reproductive dysfunction observed from the P0 generation until the F4. The F3 generation represents the first generation where there was no direct contact with the environmental toxicant (BPA).

endured for five generations. To further investigate the impact of ancestral BPA exposure on the germline, we performed RNA-seq analysis on germline tissue, which identified 264 transcripts that were significantly upregulated or downregulated in F3 germlines ancestrally exposed to BPA compared with dimethyl sulfoxide (DMSO). Gene ontology analyses of functional categories represented highlighted reproduction as a representative functional category, indicating a profound transgenerational impact of ancestral BPA exposure on the germline transcriptome, and ultimately germline function.

In addition to RNA-seq, we also performed ChIP-seq analysis in whole worms, which showed that the repressive marks H3K9me3 and H3K27me3 predominantly occupy the gene body of silenced genes and that H3K27me3 is significantly reduced in the gene body of BPA ancestrally exposed worms compared with the control groups. Comparing distribution of repressive marks along the chromosome axes showed reduction of both marks from the distal chromosomal regions, largely heterochromatic, and a slight enrichment in the chromosome centers when comparing BPA to DMSO. Noting these differences in the epigenome occur transgenerationally, our focus shifted back to the germline where the changes must occur in order to be inherited. Pachytene germline nuclei imaged by immunofluorescence showed a significant ~25% reduction in global H3K9me3 and H3K27me3 between DMSO and BPA. This transgenerational impact on repressive marks in the germline was not solely confined to the repetitive array but was also detectable on the autosomes and the X-chromosome. Since F3 germlines showed a strong alteration of their chromatin and transcriptome, we investigated whether these were associated with transgenerational reproductive defects. We indeed measured an increase in embryonic lethality in worms ancestrally exposed to BPA when compared with DMSO control. Additionally, we measured germline health by monitoring induction of germline apoptosis and observed a significant increase in apoptotic germline nuclei in F3 worms ancestrally exposed to BPA. This indicated that ancestral BPA exposure elicits a clear transgenerational reproductive dysfunction effect.

Finally, getting to mechanisms, we tested the causal relationship between the reduction in H3K9me3 and H3K27me3 germline levels and BPA-induced transgenerational outcomes. We believed that the dependence of these marks might involve the activity of enzymes that regulate them. This was supported by our own aforementioned RNA-seq data in which seven differentially expressed chromatin factors were identified. Since BPA appeared to reduce repressive marks, we focused on histone demethylases targeting H3K9me3 and H3K27me3 to attempt to rescue BPA's transgenerational effects. Using a feeding RNAi strategy targeting *jmjd-2* (H3K9me3/H3K36me3 KDM)[22,23] or *jmjd-3/utx-1* (H3K27me3 KDM),[24] we were able to modulate and rescue BPA's transgenerational effects. The downregulation of *jmjd-2* or *jmjd-3/utx-1* through RNAi at the F1 to F2 transition increased the levels of H3K9me3 and H3K27me3 in the F3 germlines. The RNAi treatment also led to a rescue of BPA-induced reproductive dysfunction in the F3. To validate these results, we also performed drug rescue experiments using KDM4/JMJD-2 inhibitor IOX-1, which has been shown to elevate H3K9me3 levels *in vitro* and in cell culture settings,[25–27] and the potent selective Jumonji JMJD-3/UTX-1 H3K27 demethylase inhibitor GSK-J4.[28] Using the chemicals individually or in combination to inhibit both demethylases significantly decreased the germline array desilencing and embryonic lethality effects. These two distinct methods of rescuing BPA's transgenerational effects indicate that the activity of either JMJD2 or JMJD3/UTX1 is required for inheritance of BPA-induced reproductive effects. Our approach is what distinguishes our study from others. We did not use mutants where the initial response to the environmental cue would be abrogated. Instead, we used RNAi or drug exposure in such a way that the worms could respond appropriately to the cue first but then were prevented from transferring that information to the following generations. Therefore, our study is unique in its ability to discriminate between altered response and altered inheritance of effect.

Together, these results demonstrate the key role of repressive histone modifications, namely, H3K9me3 and H3K27me3, in the inheritance of reproductive dysfunctions induced by a well-defined environmental exposure. These findings shine a light on how artificial environmental exposures can be biologically integrated and transgenerationally inherited. Our work highlights the importance of comprehensively examining our chemical environmental for its potential effects on our germline

epigenome, which can in turn allow us to find interventional means to prevent transmission of effects to future generations.

Although our work begins to answer questions in the field of environmental exposure effects on future generations, currently there is not a single epigenetic mark that can be considered responsible for the transfer of environmental exposure effects from one generation to the next, and H3K4me3, H3K9me3, and H3K27me3 have all been implicated in that process.[29] This could be due to potential redundancy or crosstalk between specific marks although we cannot exclude the possibility that specific exposures may use distinct epigenetic mechanisms for their inheritance. Recent studies have highlighted the challenge of identifying a unifying mechanism of inheritance, if it indeed exists. For example, other *C. elegans* studies showed that starvation can cause transgenerational effects mediated through the generation of small RNAs that target genes important for nutrition.[30] Interestingly, histone modifications were also functionally connected to transgenerational effects and small RNA transfer. Indeed, in *met-2 C. elegans* mutants, which are defective in H3K9 methyltransferase, there is a progressive reduction in fertility that unfolds over 10 to 30 generations.[31] The argonaute factor *hdre-1*, associated with small RNAs, is required for the progressive sterility phenotype in the *met-2* mutant. Thus, the authors proposed a model where MET-2 functions to suppress the transgenerational transfer of small RNAs via the regulation of H3K9me3, as a model of inheritance. Together, these recent studies show the importance of epigenetic mechanisms other than DNA methylation as vehicles for transgenerational effects and highlight the need to comprehensively examine distinct exposures and epigenetic mechanisms to improve our understanding of environmental memory.

Finally, our work as well as that of others point to another important question. For phenotypes that are present in the soma of later generations, how is the information, likely epigenetically encoded as demonstrated by our efforts, transferred from germ cells across developmental and differentiation stages to affect adult cell types, altering their cellular programs and function. Such a complex question is also best addressed in *C. elegans* where the location and timing of each cellular differentiation event are well described. Thus, while there is still much work to do, our current studies are helping to create guidelines based on model organisms and standardized approaches that will in turn allow us to understand the underlying intricate mechanisms of environmental exposure effects unraveling across generations.

Author Contributions

JC and PA wrote the manuscript.

REFERENCES

1. Burbank L. The training of the human plant. *The Century Magazine*. May 1907, 1907:127–137.
2. Ravelli GP, Stein ZA, Susser MW. Obesity in young men after famine exposure in utero and early infancy. *N Engl J Med*. 1976;295:349–353.
3. Lambrot R, Xu C, Saint-Phar S, et al. Low paternal dietary folate alters the mouse sperm epigenome and is associated with negative pregnancy outcomes. *Nat Commun*. 2013;4:2889.
4. Ng S-F, Lin RCY, Laybutt DR, Barres R, Owens JA, Morris MJ. Chronic high-fat diet in fathers programs β-cell dysfunction in female rat offspring. *Nature*. 2010;467:963–966.
5. Carone BR, Fauquier L, Habib N, et al. Paternally induced transgenerational environmental reprogramming of metabolic gene expression in mammals. *Cell*. 2010;143:1084–1096.
6. Andrés F, Coupland G. The genetic basis of flowering responses to seasonal cues. *Nat Rev Genet*. 2012;13:627–639.
7. Song J, Angel A, Howard M, Dean C. Vernalization: a cold-induced epigenetic switch. *J Cell Sci*. 2012;125:3723–3731.
8. Seong KH, Li D, Shimizu H, Nakamura R, Ishii S. Inheritance of stress-induced, ATF-2-dependent epigenetic change. *Cell*. 2011;145:1049–1061.
9. Anway MD, Cupp AS, Uzumcu M, Skinner MK. Epigenetic transgenerational actions of endocrine disruptors and male fertility. *Science*. 2005;308:1466–1469.
10. Anway MD, Leathers C, Skinner MK. Endocrine disruptor vinclozolin induced epigenetic transgenerational adult-onset disease. *Endocrinology*. 2006;147:5515–5523.
11. Manikkam M, Tracey R, Guerrero-Bosagna C, Skinner MK. Plastics derived endocrine disruptors (BPA, DEHP and DBP) induce epigenetic transgenerational inheritance of obesity, reproductive disease and sperm epimutations. *PLoS ONE*. 2013;8:e55387.
12. Tang WWC, Kobayashi T, Irie N, Dietmann S, Surani MA. Specification and epigenetic programming of the human germ line. *Nat Rev Genet*. 2016;17:585–600.
13. Camacho J, Truong L, Kurt Z, et al. The memory of environmental chemical exposure in *C. elegans* is dependent on the Jumonji demethylases jmjd-2 and jmjd-3/utx-1. *Cell Rep*. 2018;23:2392–2404.
14. Vanfleteren JR, Bun SMV, Delcambe LL, Beeumen JJV. Multiple forms of histone H2B from the nematode *Caenorhabditis elegans*. *Biochem J*. 1986;235:769–773.
15. Vanfleteren JR, Bun SMV, Beeumen JJV. The primary structure of histone H2A from the nematode *Caenorhabditis elegans*. *Biochem J*. 1987;243:297–300.
16. Vanfleteren JR, Van Bun SM, Van Beeumen JJ. The primary structure of histone H3 from the nematode *Caenorhabditis elegans*. *FEBS Lett*. 1987;211:59–63.
17. Vanfleteren JR, Van Bun SM, Van Beeumen JJ. The primary structure of histone H4 from the nematode *Caenorhabditis elegans*. *Comp Biochem Physiol*. 1987;87:847–849.
18. Cui M, Han M. Roles of chromatin factors in *C. elegans* development. In: The C. elegans Research Community, ed. *WormBook*; May 2007:1-16. Available at: https://www.ncbi.nlm.nih.gov/pubmed/?term=Roles+of+chromatin+factors+in+C.+elegans+development.
19. Dolinoy DC, Huang D, Jirtle RL. Maternal nutrient supplementation counteracts bisphenol A-induced DNA hypomethylation in early development. *Proc Natl Acad Sci USA*. 2007;104:13056–13061.
20. Kim JH, Rozek LS, Soliman AS, et al. Bisphenol A-associated epigenomic changes in prepubescent girls: a cross-sectional study in Gharbiah, Egypt. *Environ Health*. 2013;12:33.
21. Trapphoff T, Heiligentag M, Hajj NE, Haaf T, Eichenlaub-Ritter U. Chronic exposure to a low concentration of bisphenol A during follicle culture affects the epigenetic status of germinal vesicles and metaphase II oocytes. *Fertil Steril*. 2013;100:1758.e1–1767.e1.
22. Greer EL, Beese -Sims SE, Brookes E, et al. A histone methylation network regulates transgenerational epigenetic memory in *C. Elegans*. *Cell Rep*. 2014;7:113–126.
23. Whetstine JR, Nottke A, Lan F, et al. Reversal of histone lysine trimethylation by the JMJD2 family of histone demethylases. *Cell*. 2006;125:467–481.
24. Agger K, Cloos PAC, Christensen J, et al. UTX and JMJD3 are histone H3K27 demethylases involved in HOX gene regulation and development. *Nature*. 2007;449:731–734.
25. King ONF, Li XS, Sakurai M, et al. Quantitative high-throughput screening identifies 8-hydroxyquinolines as cell-active histone demethylase inhibitors. *PLoS ONE*. 2010;5:e15535.
26. Hu Q,, Chen J, Zhang J, Xu C, Yang S, Jiang H. IOX1, a JMJD2A inhibitor, suppresses the proliferation and migration of vascular smooth muscle cells induced by angiotensin II by regulating the expression of cell cycle-related proteins. *Int J Mol Med*. 2016;37:189–196.
27. Schiller R, Scozzafava G, Tumber A, et al. A cell-permeable ester derivative of the JmjC histone demethylase inhibitor IOX1. *ChemMedChem*. 2014;9:566–571.
28. Kruidenier L, Chung C, Cheng Z, et al. A selective Jumonji H3K27 demethylase inhibitor modulates the proinflammatory macrophage response. *Nature*. 2012;488:404–408.
29. Weinhouse C, Truong L, Meyer JN, Allard P. *Caenorhabditis elegans* as an emerging model system in environmental epigenetics. *Environ Mol Mutagen*. 2018;59:7560–7575.
30. Rechavi O, Houri-Ze'evi L, Anava S, Goh WSS, Kerk SY, Hannon GJ, Hobert O. Starvation-induced transgenerational inheritance of small RNAs in C. *Elegans*. *Cell*. 2014;158:2277–2287.
31. Lev I, Seroussi U, Gingold H, Bril R, Anava S, Rechavi O. MET-2-dependent H3K9 methylation suppresses transgenerational small RNA inheritance. *Curr Biol*. 2017;27:81138–81147.